University of Alberta

The Pleistocene Ironshore Formation, Grand Cayman: Diagenetic Response to Sea Level Change

by

Rong Li

A thesis submitted to the Faculty of Graduate Studies and Research
in partial fulfillment of the requirements for the degree of

Doctor of Philosophy

Department of Earth and Atmospheric Sciences

Spring 2014
Edmonton, Alberta

ABSTRACT

The Ironshore Formation, a Pleistocene limestone succession found on Grand Cayman, is formed of six unconformity-bounded units (A to F) that developed in response to transgressive-regressive cycles. Highstands led to deposition whereas lowstands led to diagenetic change in the earlier deposited limestones. Analysis of the diagenetic features in the matrices and corals from each unit shows that the diagenetic styles of individual samples cannot be linked to specific unconformities. Instead, both intrinsic (e.g., skeletal microstructure, porosity and permeability of substrate) and extrinsic (e.g., sea level position, climate, exposure time) factors controlled development of the heterogeneous diagenetic patterns. The fact that the matrices of the limestones have undergone more meteoric diagenetic alteration than the corals can probably be ascribed to the higher permeabilities of the matrices that allowed larger volumes of water to flow through them. Maximum diagenesis took place during the lowstands that followed the deposition of units C and D, which can be attributed to the long-lasting lowstands that were accompanied by a wet climate with high rainfall. Interpretation of the diagenesis displayed in the Ironshore Formation highlights the fact that the diagenetic fabrics in a carbonate succession do not necessarily follow a systematic pattern that can be linked to the transgressive-regressive cycles that governed its formation.

The laminar and non-laminar calcretes developed on Unit D of the Ironshore Formation on Grand Cayman display various diagenetic features that reflect the interactions between substrate, soil cover, climate, and biological influences that dictated their development. The $\delta^{13}C$ values of the laminar calcretes record a change from C_3 dominated vegetation that grew in a cool, wet climate to a C_3/C_4 mixed plant vegetation that grew in a drier, hotter climate. The

similarities between Cayman calcareous crusts and those found in Florida suggest that such crusts are related to regional climate conditions and may therefore facilitate regional stratigraphic correlation.

ACKNOWLEDGEMENT

I would not have been able to complete my PhD without the support of many people throughout this dissertation. First and foremost, I would like to express my deep gratitude to my supervisor Dr. Brian Jones for taking me to work on this project. Two-and-a-half year research work under the guidance of Dr. Jones has taught me many valuable lessons including the importance of digging into data, the significance of proper editing, and most importantly, what I have always found to be the most difficult, the necessity to evaluate my own work more critically. Many thanks to Dr. Jones for being such an excellent, professional, knowledgeable, and patient supervisor. Without his help, my dissertation would never have taken flight.

I would also like to thank Dr. Karlis Muehlenbachs for generously providing his laboratory for the stable isotope analysis; Mark Labbe and Martin Von Dollen for preparing the thin sections; Diane Caird for running the XRD samples; and George Braybrook and De-Ann Rollings for taking the SEM photomicrographs used in this study.

I am grateful to the Natural Sciences and Engineering Research Council of Canada, which funded this research (Grant A6090 to Jones); Hendrik van Genderen (Water Authority of Cayman Islands), who helped in collection of some of the samples. I am also grateful to the Chinese Scholarship Council for providing financial support during my four years study in University of Alberta.

I am delighted to share the lab with the members of the Carbonate Research Group: Hongwen Zhao, Josh Thomas, Alexandra Der, Megan Black, Ting Liang, and Min Ren. It has been a real pleasure of having the opportunity to work with all of them.

Finally, thanks go to my family for their love, patience, constant support,

and encouragement throughout the years. Dad and Mom, thank you so much for everything you have done for me and for being so proud of me no matter what. I would not be where I am today without you.

TABLE OF CONTENTS

LIST OF TABLES

LIST OF FIGURES

CHAPTER 1: INTRODUCTION

1. Introduction

The Pleistocene epoch, which lasted from 2.6 million to 11,700 years ago, was characterized by repeated glaciations that triggered numerous changes in sea level changes. Sediments were deposited during the highstands whereas denudation took place during the lowstands. Over the last 500 kyr, there was up to 159 m in sea level oscillations with lowstands as much as 139 ± 11 m below present sea level and highstands up to 20 m above present sea level (Rohling et al., 1998). Even during each highstand over the last 800 kyr, sea level is thought to have varied by about 10 m (Pirazzoli et al., 1991). Siddal et al. (2007) showed that the variability of sea level during the last four interglacial periods differed not only in height, but also in timing relative to northern summer insolation peaks. For example, Marine Isotope Stage (MIS) 9 had a single maximum highstand position that was maintained for less than 10 kyr, MIS 7 had several peaks, whereas the highstand during MIS 11 persisted with little variation for at least 30 kyr (Siddal et al., 2007). The asymmetrical and saw-toothed shape of Pleistocene sea level curve (Fig. 1-1) indicates abrupt sea level changes with glacial expansions that were terminated by rapid warming.

The high cyclicity of sea level fluctuations in Pleistocene has been attributed to orbital forcing (Mesolella et al., 1969; Imbrie et al., 1984) that drove the global climate and ice volume changes and hence dictated eustatic sea level changes. The magnitude of the sea level variations, as depicted on the SPECMAP timescale for the last 800 kyr, has been estimated largely from the oxygen isotope ratios that have been derived from foraminifera extracted from deep-sea sediments (Martinson et al., 1987; Siddall et al., 2007, their Figure 7.1). The oxygen isotope records from these fossil planktonic foraminifera were used

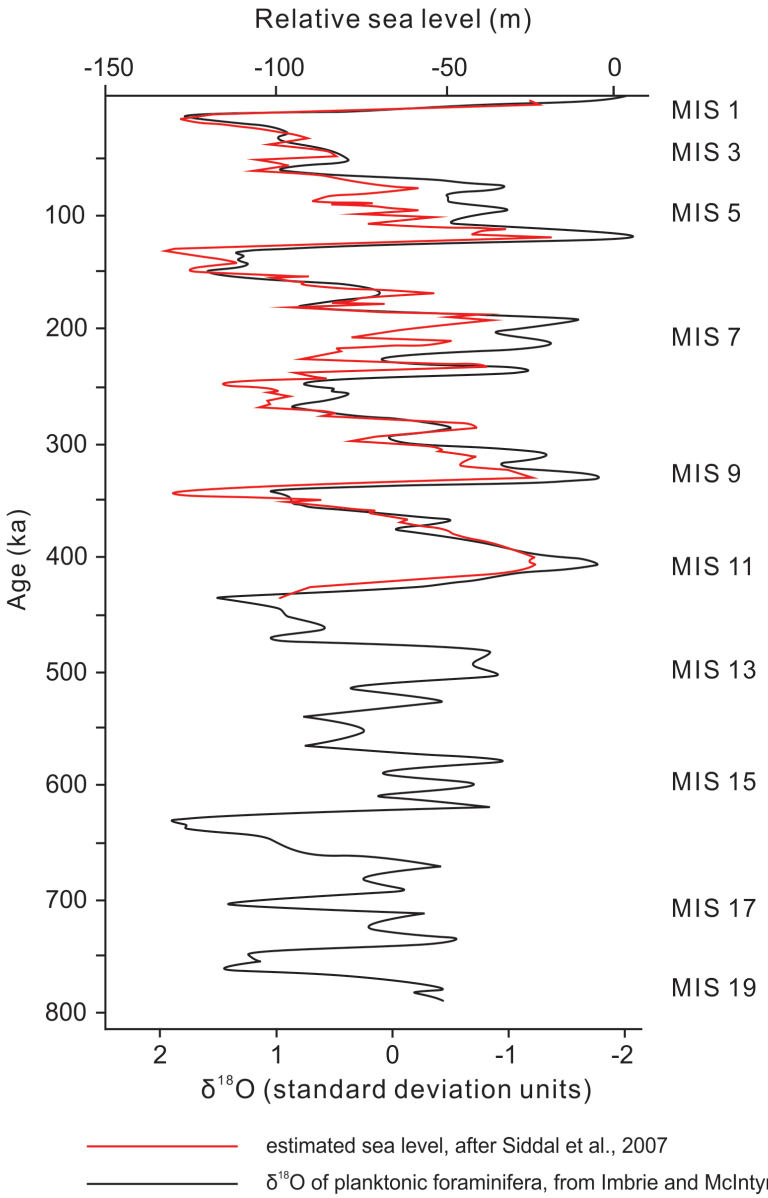

Fig. 1-1. Continuous sea-level estimates on the SPECMAP (SPECtral MApping Project) timescale from Siddal et al. (2007), compared with the planktonic normalized O^{18} record (Imbrie and McIntyre, 2006) from the equatorial Atlantic Ocean.

to divide the Pleistocene and Holocene into Marine Isotope Stages (MIS) 1 to 19 with each stage being 10 to 60 kyr long and numbered from the top downwards (Imbrie and McIntyre, 2006). Under this scheme, the even numbers represent glacial intervals and their associated sea level lowstands and the odd numbers represent the interglacial intervals with their associated sea level highstands (Fig.

1-1). Discontinuous records of sea-level positions have also been derived from depositional and erosional features throughout the world (Siddall et al., 2007). The common wave notches associated with the 125 ka old reefs in Caribbean islands, for example, show that sea level during the Last Interglacial period was about 6 m above present sea level. Numerous studies have focused on the deposits associated with each of the Pleistocene highstands (Mesolella, 1967; Matthews, 1973; Shackleton and Matthews, 1977; Blanchon and Eisenhauer, 2001).

Pleistocene limestones found throughout the Caribbean Sea, the Atlantic Ocean (e.g., Bahamas, Bermuda, Florida Keys, Barbados, Haiti, Jamaica), and the Pacific Ocean (e.g., Atauro Island, Sumba Islands, Papua New Guinea) have been widely studied in an effort to understand how depositional environments evolved in response to glacioeustatic sea-level change. In general, the Pleistocene carbonate successions on these islands consist of numerous marine/eolian units that formed during interglacial periods dating back to MIS 7 or earlier (Table 1-1). On the Bahama Islands, for example, the Pleistocene limestones of the Owl's Hole Formation (MIS 7 or earlier stages) and Grotto Beach Formation (MIS 5e) are formed largely of eolianites (Carew and Mylroie, 1995). On Bermuda, the Pleistocene succession includes deposits associated with oxygen isotope stages 5a, 7, 9, 11, and earlier stages that are formed mainly of bioclastic grainstones that accumulated on coastal beaches and as eolian dunes (Vacher et al., 1995). In south Florida and the Florida Keys, the Pleistocene succession that includes the Key Largo Limestone, the Miami Limestone, and the Fort Thompson Formation (Harrison and Coniglio, 1985; Multer et al., 2002), is divided into five time-stratigraphic units (Q1 to Q5 in ascending order; Perkins, 1977) that formed in association with MIS 5, 7, 9, 11, and an earlier stage (Hickey et al., 2010). Coral reef terraces on Barbados (Broecker et al., 1968; Mesolella et al., 1969; Bender et

Table 1-1. The Pleistocene successions of islands from Caribbean Sea, Atlantic Ocean, and Pacific Ocean and the stratigraphic correlation with marine oxygen isotope stage (MIS)

Location	**Pleistocene stratigraphy and correlated MIS**	**Reference**
The Bahama Islands	Grotto beach Fm (MIS 5e) Owl's hole Fm (MIS 7 or earlier stages)	Carew and Mylroie, 1995
Bermuda	Southampton/Rocky Bay Fm (MIS 5a) Belmont Fm (MIS 7) Town Hill Fm upper member (MIS 9) Town Hill Fm lower member (MIS 11) Walsingham Fm (earlier stage)	Vacher et al., 1995
South Florida; Florida Keys	Q5 (MIS 5) Q4b (MIS 7) Q4a (MIS 9) Q3 (MIS 11?) Q2, Q1 (earlier stage)	Perkins, 1977 Hickey et al., 2010
Barbados	Barbados I (MIS 5a) Barbados II (MIS 5c) Barbados III (MIS 5e) Older Barbados terraces (MIS 7, 9, 11, 13, 15, 17, 19)	Broecker et al., 1968 Mesolella et al., 1969 Bender et al., 1973; 1979
Jamaica	Falmouth Fm/Port Morant Fm (MIS 5e) Older Pleistocene units	Land, 1970 Mitchell et al., 2001
Haiti	Mole (MIS 5a) Saint (MIS 5c) Nicolas (MIS 5e)	Dodge et al., 1983
Huon Peninsula, Papua New Guinea	Reef complex II Reef complex IIIb Reef complex IV Reef complex V (MIS 5a) Reef complex VI (MIS 5c) Reef complex VII (MIS 5e) Older reef complexes	Bloom et al., 1974 Chappell, 1974 Chappell and Shackleton, 1986
Sumba Island, Indonesia	Terrace I (MIS 5) Terrace II (MIS 5, 7, 9) Terrace III (MIS 9, 11, 13) Terrace IV (MIS 15, 17) Terrace V (MIS 19, 21, 23,25) Terrace VI (MIS 27, 29)	Pirazzoli et al., 1991

Atauro Island	Terrace I (MIS 5) Terrace II (MIS 7) Terrace III (MIS 9) Terrace IV (MIS 11) Terrace V (MIS 13) Terrace VI (MIS 15)	Chappell and Veeh, 1978

al., 1973, 1979), Jamaica (Land, 1970; Mitchell et al., 2001), and Haiti (Dodge, 1983) have also been correlated with oxygen isotope substages 5a, 5c, and 5e. Similarly, in the Pacific Ocean, sequences of coral-reef terraces correlate with highstands that correspond to oxygen isotope records. The reef successions on the Huon Peninsula, Papua New Guinea, for example, have been extensively studied (Chappell, 1974; Bloom et al., 1974) and widely used to trace activity during the interglacial periods (Pirazzoli et al., 1991). There, reef complexes V, VI, and VII are known to correlate with MIS 5a, 5c, 5e, respectively (Chappell and Shackleton, 1986). On Atauro Island, the ages of reef terraces correlate quite well with periods of major glacio-eustatic rise over the last 700 ka as derived from the oxygen isotope record from the Pacific cores (Chappell and Veeh, 1978). On Sumba Island, the major reef terraces also can be corresponded to specific interglacial stages, with the oldest formed about 1 million years ago (Pirazzoli et al., 1991). In the Pleistocene successions where different depositional units can be correlated with known glacio-eustatic highstands, various geochemical proxies such as the Sr/Ca ratio, rare earth elements, and $\delta^{18}O$ obtained from fossil coral skeletons have been used to decode paleo-oceangraphic conditions.

During sea level lowstands, shallow water carbonate sediments formed during the previous highstands come under the influence of meteoric water and may undergo significant diagenetic changes. Thus, the mineralogy and geochemical proxies that are commonly used for assessing paleoclimate and paleo-ocenaographic conditions can be radically altered (e.g., Bar-Matthews et

al., 1993; McGregor and Gagan, 2003; Webb et al., 2009). Numerous studies of Pleistocene carbonates found on isolated oceanic islands throughout the Caribbean Sea, the Atlantic Ocean, and the Pacific Ocean have examined various aspects of diagenesis, including cementation (Matthews, 1967; Schroeder, 1973; Saller and Moore, 1991; Vollbrecht and Meischner, 1996), neomorphism (Buchbinder and Friedman, 1980; Martin et al., 1986; Rehman, 1992; Rehman et al., 1994), dissolution (Matthews, 1967), dolomitization (Land and Epstein, 1970), and calichification (James, 1972; Harrison, 1977; Harrison and Steinen, 1978). Less attention, however, has been paid to understanding superimposed diagenetic patterns in carbonate successions that may result from repeated phases of exposure that occur in concert with repeated and frequent lowstand phases (Braithwaite and Montaggioni, 2009; Braithwaite and Camoin, 2011). Nevertheless, the Pleistocene deposits found on isolated islands characterized by multiple depositional-erosional cycles provide an excellent opportunity for examining the diagenetic patterns of Pleistocene carbonate successions whereby the diagenetic changes can be correlated with known age ranges. From a theoretical perspective, therefore, it should be possible to correlate diagenetic changes with time and specific lowstands.

The Pleistocene Ironshore Formation on Grand Cayman, which includes six unconformity-bounded depositional units, provides an excellent opportunity for assessing diagenetic changes because (1) the stratigraphy is well established, (2) the ages of the units are known, (3) samples are readily available, and (4) the constituent limestones have been modified by many different diagenetic processes. Based on a detailed examination of the mineralogy, diagenetic fabrics, and stable isotope geochemistry of the limestone matrices, the corals, and the calcareous crusts, this thesis determines if the older units in the Ironshore Formation have undergone more diagenetic change than the younger units and

if the different styles of diagenesis can be related to specific lowstands. This study differs from other diagenetic studies on Pleistocene carbonate successions by (1) systematically examining the stratigraphic and geographic evolution of diagenesis in response to the transgressive-regressive cycles that occurred throughout the Pleistocene, (2) comparing the diagenetic responses of corals and their coeval matrices relative to the repeated transgressive-regressive cycles, and (3) examining the physical and chemical processes involved in the development of non-laminar and laminar calcretes that have formed on the surfaces of the exposed Pleistocene limestones. Critically, this study documents the diagenetic response of the Pleistocene carbonate succession to multiple episodes of sea level changes and recurring episodes of meteoric diagenesis that came into play during the periods of sea level lowstands.

2. Study area and methods

2.1. Study area

The Cayman Islands, located south of Cuba and northwest of Jamaica, comprise Grand Cayman, Little Cayman, and Cayman Brac (Fig. 1-2A). Grand Cayman, the largest of the three islands, is about 35 km long and 6-14 km wide with an area of 197 km^2 (Fig. 1-2B). Although the highest part of the island is 18 m above sea level, most of Grand Cayman is less than 3 m above sea level. Each of the Cayman Islands is a high point on the Cayman Ridge, which forms the southern boundary of North American Plate and the northern margin of the Cayman Trench (Fig. 1-2C). The Cayman Ridge is a submarine mountain range that extends from the Sierra Maestra Mountains of southeastern Cuba to the Misteriosa Bank (MB) near Belize and the Gulf of Honduras. The Cayman Trench and associated left lateral Oriente Transform Fault were generated by the eastward movement of the Caribbean Plate relative to the North American Plate (Perfit and

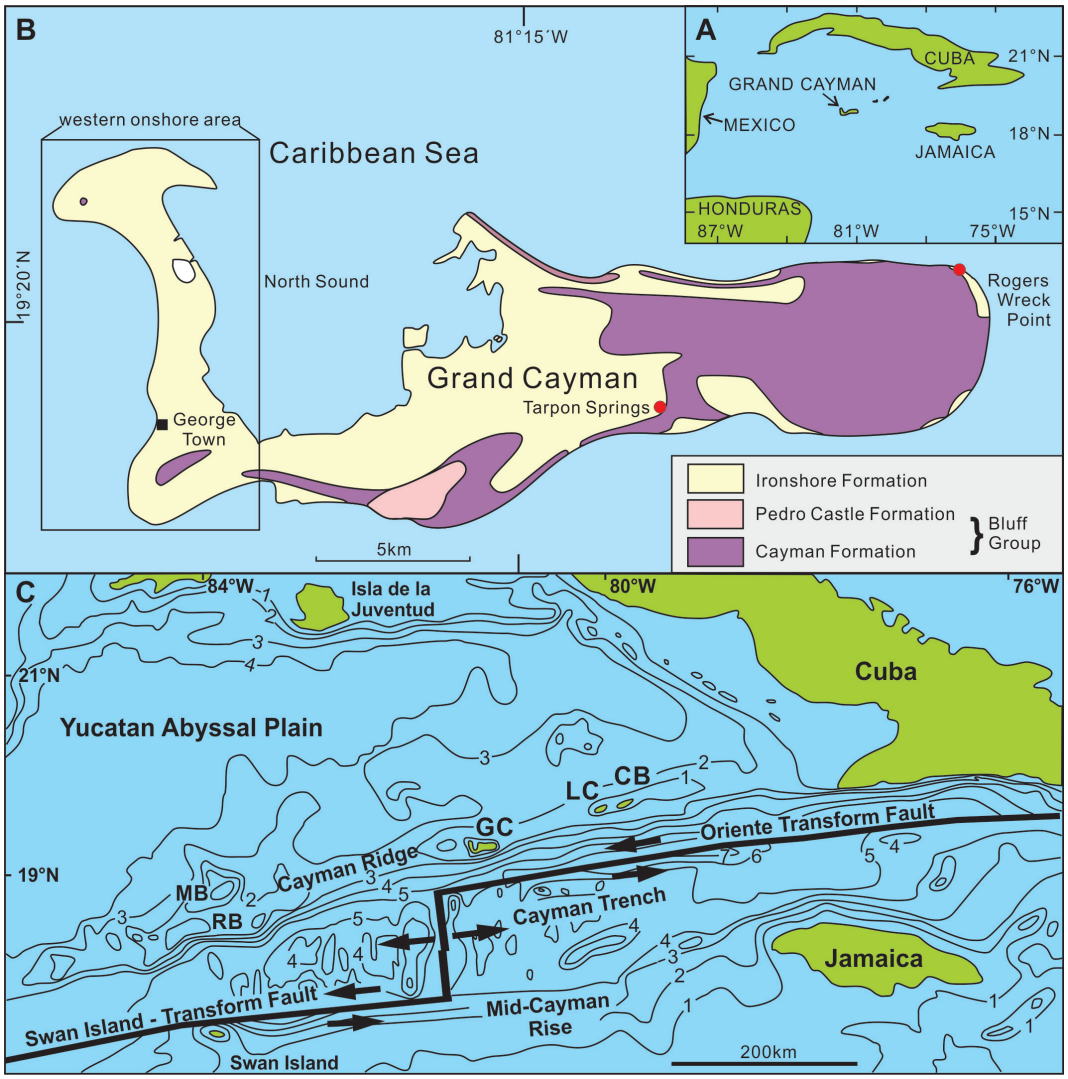

Fig. 1-2. (A) Location of Grand Cayman. (B) Geological map of Grand Cayman (modified from Jones, 1994) showing locations of George Town, western onshore area, Tarpon Springs, and Rogers Wreck Point. (3) Tectonic and bathymetric setting of the Cayman Islands on the Cayman Ridge (modified from Jones, 1994 and based on maps from Perfit and Heezen, 1978; MacDonald and Holcombe, 1978).

Heezen, 1978). Grand Cayman is located to the northeast of the Mid-Cayman spreading centre. Although the Cayman Islands are located in a tectonically active area, available evidence (such as the +6 m elevation of the wave-cut notch formed during the Sangamon highstand) indicates that the Pleistocene strata of Grand Cayman do not appear to have undergone any vertical movement over the last 125

ka (Emery, 1981; Jones, 1994; Jones and Hunter, 1990).

Matley (1926) named the Tertiary and Pleistocene strata of the Cayman Islands as the Bluff Limestone and Ironshore Formation, respectively. Jones et al. (1994) revised this stratigraphy by elevating the Bluff Limestone to group status to include the unconformity-bounded Brac Formation, Cayman Formation, and Pedro Castle Formation, in ascending order. The limestones and dolostones of the Bluff Group, which form the core of each of the Cayman Islands, are unconformably overlain by the Pleistocene Ironshore Formation (Fig. 1-2B) (Matley, 1926). By extensive examination of the lithologies, biota, and U/Th radiometric ages of the Pleistocene limestones on Grand Cayman, the Ironshore Formation (Fig. 1-3), which is up to 19 m thick, has been divided into six unconformity-bounded units, units A to F in ascending order (Vézina, 1997; Vézina et al., 1999; Coyne, 2003; Coyne et al., 2007).

A

Age** (ka)	Unit	Lithology	Biota	Sea level elevation* (m)
84	F	Cross-bedded ooid grainstones; coral floatstone; *Halimeda* floatstone	Head corals, branching corals, *Halimeda*	+3.0 to +5.0
104	E	Coral floatstones	Head corals	+2.0 to +5.0
131	D	Grainstones	Head corals, branching corals	+2.5 to +6.0
229	C	Rudstones, packstones, grainstones,bafflestone	Head corals, branching corals	-2.5 to +1.0
346	B	Packstones, grainstones, minor wackstones	Head corals, branching corals	-3.0 to +0.5
>400	A	Grainstones	Head corals, branching corals	-9.0 to -5.5

* The elevation is relative to present-day sea-level.

** Represent average ages, from(Vézina, 1997; Vézina et al., 1999; Coyne, 2003; Coyne et al., 2007).

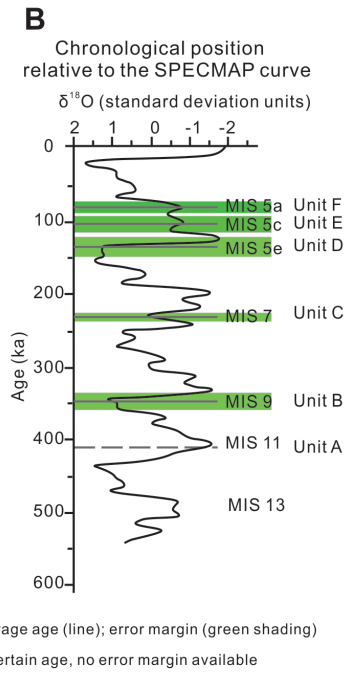

Fig. 1-3. (A) Internal stratigraphy of Ironshore Formation. Ages and sea-levels (relative to modern sea level) from Vézina et al. (1999) and Coyne et al. (2007). (B) Positions of units A to F in Ironshore Formation relative to sea level curve of Siddall et al. (2007).

Th/U dating of aragonitic corals and conches indicates that Unit A formed at >400 ka, Unit B ~346 ka, Unit C 226−232 ka, Unit D 121−147 ka, Unit E 95−110 ka, and Unit F 74−87 ka (Vézina, 1997; Vézina et al., 1999; Coyne, 2003; Coyne et al., 2007). Units A to F correlate with Marine Isotope Stages (MIS) 11, 9, 7, 5e, 5c, and 5a, respectively (Vézina, 1997; Vézina et al., 1999; Coyne, 2003; Coyne et al., 2007). Interpretation of the stratigraphy and sedimentology indicates that each of these units developed under different sea level positions. Compared to present day sea level, those sea levels have been estimated as follows: unit A, -9.0 to -5.5 m; unit B, -3.0 to +0.5 m; unit C, -2.5 to +1.0 m; unit D, +2.5 to +6.0 m, unit E, +2.0 to +5.0 m; and unit F, +3.0 to +5.0 m (Vézina, 1997; Vézina et al., 1999; Coyne, 2003; Coyne et al., 2007).

2.2. Methods

The samples used in this study came from (1) Rogers Wreck Point (RWP), (2) offshore George Town (GT), (3) the western onshore area (WA), and (4) Tarpon Springs (TS). Samples from Rogers Wreck Point came from outcrops and cores obtained from wells RWP#3, #6, #7, #8, #10, #11, #14, and #15 (Fig. 1-4A). These wells provide an excellent cross-section through the Ironshore Formation, which developed as an onlapping succession on an erosional beach that had been cut into the underlying Cayman Formation (Fig. 1-4B). The George Town samples came from two cores, BJC#1 (10.8 m long) and BJC#3 (15.2 m long), obtained from wells drilled offshore from George Town with their tops being 26.6 m and 25.8 m below present sea level, respectively (Fig. 1-4C, 1-4D). These cores were used because core recovery was good and they collectively include Units A to F. Samples from the western onshore area came from scattered outcrops and quarries (BL, JP, MH1, MH2, MH3, MH4, MH5, LSC1, LSCB, PBQA, PBQ, SB, SC, VDM1, VDM2, VDM4) on the western part of Grand

Cayman (Fig. 1-4E, 1-4F). Samples from Tarpon Springs were collected by Dr. Brian Jones. This comprehensive collection of samples, which is representative of all of the fossils and lithologies found in the Ironshore Formation, form the basis of this study.

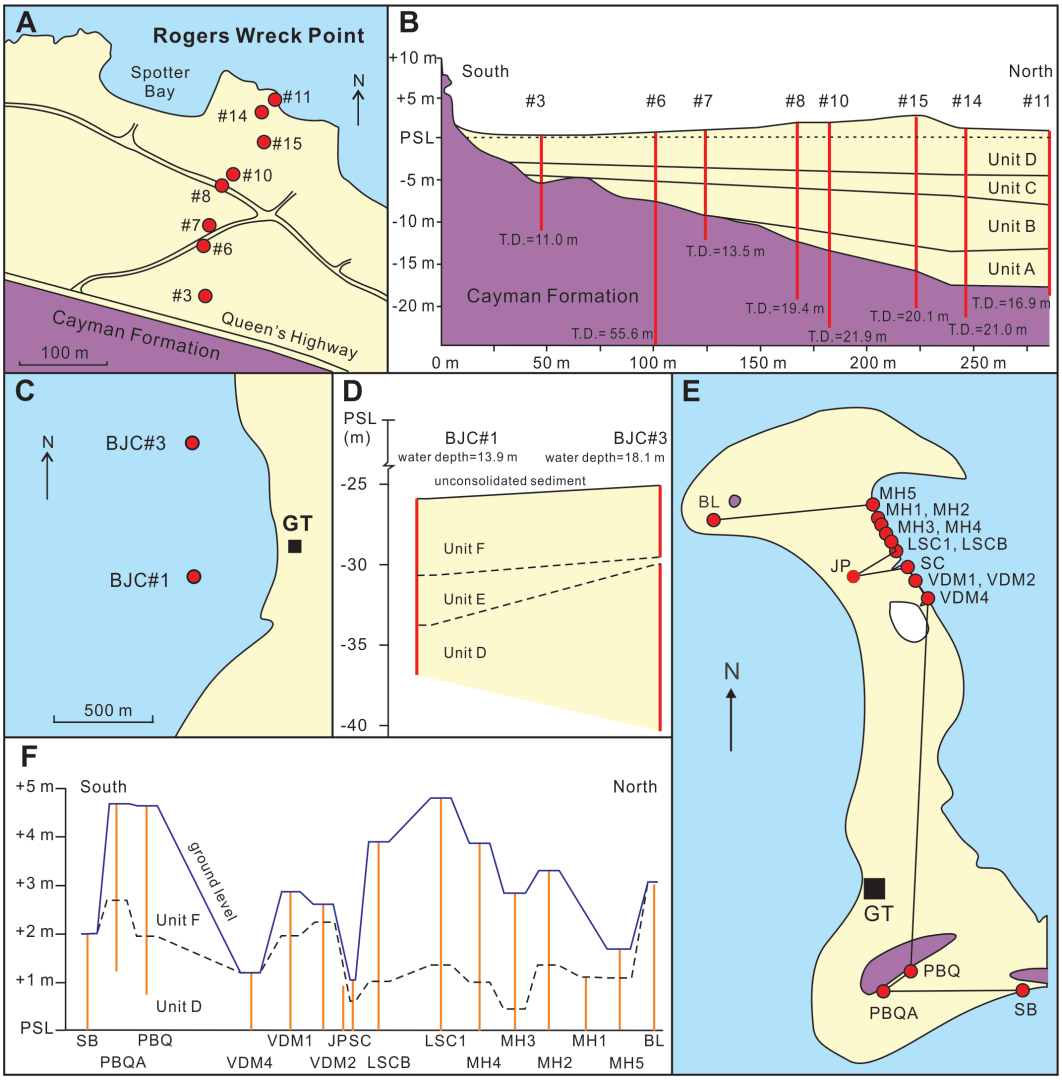

Fig. 1-4. (A) Location of sampled cores in Rogers Wreck Point area (modified from Vézina, 1997; Vézina et al., 1999). (B) Correlation of units A, B, C, and D in the Ironshore Formation in the eight studied cores from Rogers Wreck Point area (modified from Vézina, 1997). T.D. represent the termination depth of wells. (C) Location of cores through Ironshore Formation offshore from George Town (GT) (modified from Coyne, 2003; Coyne et al., 2007). (D) Correlation of units D, E, and F between BJC#1 and BJC#3

from offshore George Town (modified from Coyne, 2003). (E) Location of outcrops and quarries where the Ironshore Formation was sampled. (F) Correlation of units D and F on western part of Grand Cayman (modified from Coyne et al., 2007).

For comparison purposes, the corals and the matrices of the limestones were analyzed separately. The proportion of each type of skeletal grain in the matrices was determined by point counting of 50 thin sections (200 points per section) using the method outlined by Pruss and Clemente (2011). Identifications of the skeletal grains were verified by comparison with images in Scholle and Ulmer-Scholle (2003). Visual charts for estimating abundances of constituents in the thin section (Scholle and Ulmer-Scholle, 2003, their figure on page xii) were used to assess the proportion of skeletal grains, micrite matrix, and cements found between the corals.

The mineralogy of each sample was determined by X-ray diffraction (XRD) analysis. Each powder sample, weighing ~1 g, was analyzed on a Rigaku Ultima IV Powder XRD system that was run at 38 kV and 38 mA using a Ultima IV X-ray generator with a Co tube. All scans were run from 5° to 90° 2θ at a speed of 2°θ/min. The aragonite and calcite weight percentages were calculated from the intensities of the d_{110}, d_{021}, and d_{104} peaks using an aragonite-calcite calibration curve that had been derived from the analyses of artificial samples with known calcite:aragonite ratios. The values obtained using this method are accurate to ±2 wt%.

The diagenetic fabrics and microstructures in the limestones were initially determined from thin sections that had each been impregnated with blue epoxy with thin section photomicrographs being captured using a Polaroid DMC digital camera mounted on a Leica petrographic microscope. Scanning electron microscopy was used to determine the microscale attributes of the limestones. For this purpose, small fractured rock samples (~1 cm^3) were mounted on SEM

stubs with conductive glue and then sputter coated with gold. These samples were examined on a JEOL 6301 FE scanning electron microscope (SEM) and SEM photomicrographs were obtained using an accelerating voltage of 5 kV. The elemental content of selected spots in these samples were determined by using the energy dispersive X-ray (EDX) analyzer that is attached to the SEM (operated at an accelerating voltage of 20 kV).

Stable oxygen and carbon isotopic compositions were determined for the corals, matrices, and calcareous crusts. Powder samples, weighting 10-18 mg, were dissolved in H_3PO_4 at 25°C in a constant temperature water bath for 60 minutes following the protocol outlined by McCrea (1950). The evolved gases were analyzed on a Finnigan MAT 251 mass spectrometer. The isotope values are calibrated relative to the Vienna Peedee Belemnite using the NBS 19 ($\delta^{18}O$ = -2.20‰, $\delta^{13}C$ = +1.95‰) and NBS 18 ($\delta^{18}O$ = -23.00‰, $\delta^{13}C$ = -5.00‰) standards. The accuracy is better than 0.2‰ for $\delta^{13}C$, and better than 0.6‰ for $\delta^{18}O$.

3. Previous research on Ironshore Formation

3.1. Sedimentological framework

"Ironshore" is a local term used by the Caymanians for the low rocky shorelines formed by the calcareous rocks of the coastal platform (Matley, 1926; Brunt et al., 1973). Matley named the Ironshore Formation in 1926 and described the formation as "…white and cream-colored consolidated coral-sand and marl, with abundant coral-heads, and coralliferous limestone…". Typically, the friable limestones of this formation are capped by a hard crust that is, in turn, overlain by a layer of decalcified red or brown earth (Matley, 1926). The occurrence of the Ironshore Formation on Grand Cayman was mapped by Matley (1926) who noted that the formation "…occupies most of the periphery as a low coastal

terrace, which never rises to a greater height than 12 or 15 feet above the sea, and generally terminates abruptly inland against raised marine cliffs of the Bluff Limestone". Although Matley (1926) noted the presence of numerous corals and molluscs in the Ironshore Formation, he did not identify these fossils. Later studies by Rehder (1962), Woodroffe (1980), Cerridwen (1989), Jones and Hunter (1990), Cerridwen and Jones (1991), Hunter (1994), and Hunter and Jones (1996) provided detailed information on these diverse fossil assemblages. Based on the similarities in appearance and composition between Ironshore Formation and the Jamaican Falmouth Formation, Matley (1926) suggested that the Ironshore Formation was Pleistocene in age. Woodroffe et al. (1983) used U-series dating of *in situ* corals from the upper part of the Ironshore Formation to show that it was 124,000 years old.

Brunt et al. (1973) were the first to provide an overview of the depositional conditions under which the limestones of Ironshore Formation were deposited. They divided the Ironshore Formation into the (1) reef facies dominated by *Acropora* and *Porites* in growth position, (2) back-reef facies with massive corals, (3) lagoonal facies of marl with a diverse molluscan fauna, (4) a shoal facies of cross-bedded oolitic sands, and (5) a subaerial beach ridge facies. The paleogeographic framework of Grand Cayman ~125 ka was established by Jones and Hunter (1990), Hunter (1994), and Hunter and Jones (1996) based on rock type, sedimentary structures, fossils, and trace fossils. Jones and Hunter (1990) pointed out that (1) much of the Ironshore Formation was deposited in a large lagoon (called the Ironshore Lagoon) that covered the central and western part of Grand Cayman, and (2) the lagoonal sediments are overlain by limestones that were deposited in a high-energy, prograding beach-like environment. A detailed investigation of the Ironshore Formation facies by Shourie (1993) also revealed a shallowing-upward sequence.

Most research on the Ironshore Formation has focused on surface exposures of the Ironshore Formation, largely because obtaining cores from the formation is generally impossible as the limestones usually disintegrate during drilling. Thus, it has generally been impossible to obtain subsurface samples from the western and central parts of Grand Cayman. The lack of such samples meant that it was extremely difficult to establish the internal stratigraphy of Ironshore Formation. Drilling in Rogers Wreck Point area on the northeastern part of Grand Cayman in 1992 and 1993, however, produced cores from 15 wells. These cores provided the framework for resolving the internal stratigraphy of the Ironshore Formation. Those core showed that the Ironshore Formation in Rogers Wreck Point area is composed of rudstones, grainstones, and packstone-wackestone-mudstones that were deposited on a moderately high-energy, narrow shelf (Vézina, 1997; Vézina et al., 1999). The shelf had been produced by marine erosion that remove the Pedro Castle Formation and cut into the underlying Cayman Formation. The recognition of four unconformity-bounded packages in these cores led to the naming of units A to D (Vézina, 1997; Vézina et al., 1999). This depositional setting contrasted sharply with the quiet-water, lagoonal setting of the Ironshore Formation (Jones and Hunter, 1990) that existed on the western and central parts of Grand Cayman. Later, Coyne (2003) and Coyne et al. (2007) used data from the western onshore and offshore areas to show that that the Ironshore Formation includes two previously unrecognized younger units (units E and F). Cores from offshore George Town, contain units D to F that are formed of head coral floatstone, branching coral floatstone, mixed coral floatstone, *Halimeda* float/rudstone, and skeletal grain/pack/wackestone. These facies were deposited in deep marine environments below fairweather wave base (Coyne, 2003). The surface exposures of Ironshore Formation on the western part of Grand Cayman, which are formed of skeletal packstone/grainstone,

coral floatstone/rudstone, and ooid grainstones, belong to units D and F that are separated from each other by an erosional surface (Coyne, 2003; Coyne et al., 2007). It remains unclear if unit F was deposited in tidal channel (Jones and Pemberton, 1989) or under hurricane condition (Coyne, 2003; Coyne et al., 2007).

The ages of units A to F in the Ironshore Formation were established by Th/U dating of aragonitic corals and molluscs collected from the different units (Vézina,1997; Vézina et al., 1999; Coyne, 2003; Coyne et al., 2007). Collectively, the six units in the Ironshore Formation are a record of successive transgressive and regressive cycles that affected Grand Cayman during the Pleistocene.

3.2. Diagenesis

Only a few studies have focused on the diagenesis of the limestones found in the Ironshore Formation (Jones and Pemberton, 1988; Jones and Squair, 1989; Jones, 1990; Rehman, 1992; Rehman et al., 1994).

Jones and Pemberton (1988) examined the *Lithophaga* bivalve borings evident in many coral heads and argued that the borings played a major role in the evolution of diagenetic fabrics in the corals. Rehman (1992) and Rehman et al. (1994) examined the sponge borings in *Strombus gigas* and suggested that the sponge borings promoted aragonite-to-calcite inversion by providing conduits by which the reactive diagenetic fluids could penetrate the dense molluscan skeletons. As determined by staining and XRD analysis, Reham (1992) noticed that many corals in the Ironshore Formation are still formed of aragonite, whereas others had been diagenetically altered to calcite to varying degrees. By studying the aragonite-to-calcite alteration of corals (*Siderastrea sidereal* and *Montastrea annularis*), Rehman (1992) suggested that the replacement of aragonite by calcite was controlled by skeletal structure and the distribution and amount of porosity.

Jones (1990) also examined the diagenetic modification of tunicate spicules in Ironshore Formation and suggested that the syntaxial overgrowth on the spicules probably developed soon after deposition of the sediments while they were still in a marine setting.

Matley (1926) noted that the limestones of Ironshore Formation have a case-hardened crust that produces a metallic clink when struck (Brunt et al., 1973). Rigby and Roberts (1976) and Woodroffe (1980) suggested that the laminated or non-laminated surficial crust, overlying the Pleistocene bedrock and underlying the Holocene sediments, is probably of subaerial origin because of their similarity to the crusts found on the Florida Keys and described by Multer and Hoffmeister (1968). Jones and Squair (1989) studied the peloids in plant rootlets that penetrated the oolitic limestones of the Pleistocene Ironshore on Grand Cayman and concluded that the peloids, which are morphologically identical to the peloids found in many caliche units, probably originated as fecal pellets produced by mites. Later, subsurface cores from the northeast coast of Grand Cayman revealed four caliches (i.e. calcareous crust) at distinct unconformity surfaces throughout the Ironshore Formation (Vézina, 1997; Vézina et al., 1999), suggesting repeated subaerial exposures during the deposition of Pleistocene strata.

4. Objectives

The diagenesis of the Pleistocene Ironshore Formation on Grand Cayman has received little attention, especially when compared to the extensive work that has been done on Pleistocene carbonate successions from isolated oceanic islands throughout the Caribbean Sea, the Atlantic Ocean, and the Pacific Ocean. Complete understanding of the diagenetic history of the Pleistocene succession of Ironshore Formation requires systematic examination of diagenesis in each unit.

In addition, unconformities in the Ironshore Formation on Grand Cayman are commonly highlighted by terra rossa or calcareous crusts (Vézina, 1997; Vézina et al., 1999), but their petrographic and geochemical properties have never been fully assessed.

By examining the diagenetic changes in each unconformity-bounded unit of the Pleistocene Ironshore Formation, this thesis aims to (1) determine the diagenetic patterns in the limestones from units A to F, (2) determine the factors that controlled the diagenetic features found in the scleractinian corals, (3) ascertain whether or not diagenetic features can be linked with specific unconformities (sea level lowstands), and (4) delineate the factors that conrtolled the formation of non-laminar and laminar calcretes which can serve as regional subaerial unconformity marker.

This thesis on the Pleistocene Ironshore Formation is "paper based". Collectively, these papers examine the diagenetic features evident in the Ironshore Formation and their possible association with the unconformities that separate the different units. These papers are incorporated into this thesis as Chapters 2, 3, and 4.

Chapter 2 — This study examines the stratigraphic and geographic variations of mineralogy, fabrics, and stable isotope geochemistry of the limestones in the Pleistocene Ironshore Formation. In particular, it compares the diagenetic features of the corals with their associated matrices. The results demonstrate that the Ironshore Formation is characterized by heterogeneous diagenetic fabrics that reflects the complex interplay between many different intrinsic and extrinsic factors.

Published as: Li, R., Jones, B., 2013. Heterogeneous diagenetic patterns in the Pleistocene Ironshore Formation of Grand Cayman, British West Indies. Sedimentary Geology 294, 251-265.

Chapter 3 — This study examines the temporal and spatial variance in the diagenesis of the corals in the Ironshore Formation by documenting the stratigraphic and geographic variance in the diagenetic fabrics of the corals and their stable oxygen and carbon signatures. This paper focuses on the roles that intrinsic factors, extrinsic factors, and sea-level oscillations played in the diagenetic evolution of the corals.

Published as: Li, R., Jones, B., 2013. Temporal and spatial variations in the diagenetic fabrics and stable isotopes of Pleistocene corals from the Ironshore Formation of Grand Cayman, British West Indies. Sedimentary Geology 286-287, 58-72.

Chapter 4 — This paper examines the non-laminar calcrete and laminar calcrete found on limestones in the Pleistocene Ironshore Formation. Laminar calcrete developed on ooid grainstone and skeletal limestones from Morgan's Harbour and Tarpon Springs, which are partially to totally covered with vegetation, are characterized by calcified root structures, whereas the non-laminar calcretes developed on skeletal limestones from Rogers Wreck Point with rare vegetation cover are characterized by peloids and micrites. The results demonstrate that calcareous crusts develop in response to interactions between substrate, soil cover, climate, and biological influences that are operative during lowstand regimes. The Cayman calcareous crusts are very similar to those found on the Pleistocene Miami Limestone in Florida and highlights the possibility that such crusts are related to regional climate conditions and may therefore enable regional stratigraphic correlation.

Published as: Li., R., Jones, B., 2014. Calcareous crusts on exposed Pleistocene limestones: A case study from Grand Cayman, British West Indies. Sedimentary Geology 299, 88-105.

Chapter 5 — This chapter summarizes the conclusions of the entire thesis.

References

Bar-Matthews, M., Wasserburg, G.J., Chen, J.H., 1993. Diagenesis of fossil coral skeletons: correlation between trace elements, textures, and $^{234}U/^{238}U$. Geochimica et Cosmochimica Acta 57, 257-276.

Bender, M.L., Fairbanks, R.G., Taylor, F.W., Matthews, R.K., Goddard, J.G., Broecker, W.S., 1979. Uranium-series dating of the Pleistocene reef tracts of Barbados, West Indies. Geological Society of America Bulletin 90, 577-594.

Bender, M.L., Taylor, F.T., Matthews, R.K., 1973. Helium-Uranium dating of corals from middle Pleistocene Barbados reef tracts. Quaternary Research 3, 142-146.

Blanchon, P., Eisenhauer, A., 2001. Multi-stage reef development on Barbados during the Last Interglaciation. Quaternary Science Reviews 20, 1093-1112.

Bloom, A.L., Broecker, W.S., Chappell, J.M.A., Matthews, R.K., Mesolella, K.J., 1974. Quaternary sea level fluctuations on a tectonic coast: new $^{230}Th/^{234}U$ dates from the Huon Peninsula, New Guinea. Quaternary Research 4, 185-205.

Braithwaite, C.J.R., Camoin, G.F., 2011. Diagenesis and sea-level change: lessons from Moruroa, French Polynesia. Sedimentology 58: 259-284.

Braithwaite, C.J.R., Montaggioni, L.F., 2009. The Great Barrier Reef: a 700,000 year diagenetic history. Sedimentology 56, 1591-1622.

Broecker, W.S., Thurber, D.L., Goddard, J., KU, T., Matthews, R.K., Mesolella, K.J., 1968. Milankovitch hypothesis supported by precise dating of coral reefs and deep-sea sediments. Science 159, 297-300.

Brunt, M.A., Giglioli, M.E.C., Mather, J.D., Piper, D.J.W., Richards, H.G., 1973. The Pleistocene rocks of the Cayman Islands. Geological Magazine 110, 209-304.

Buchbinder, L.G., Friedman, G.M., 1980. Vadose, phreatic, and marine diagene-

sis of Pleistocene-Holocene carbonates in a borehole: Mediterranean coast of Israel. Journal of Sedimentary Petrology 50, 395-408.

Carew, J.L., Mylroie, J.E., 1995. Depositional model and stratigraphy for the Quaternary Geology of the Bahama Islands. Geological Society of America Special Paper 300, 5-32.

Cerridwen, S.A., 1989. Paleoecology of Pleistocene mollusc from the Ironshore Formation, Grand Cayman, B.W.I.. Unpublished M. Sc. Thesis, University of Alberta, Edmonton, Canada, 217 pp.

Cerridwen, S.A., Jones, B., 1991. Distribution of bivalves and gastropod in the Pleistocene Ironshore Formation, Grand Cayman, British West Indies. Caribbean Journal of Science 27: 97-116.

Chappell, J., 1974. Geology of coral terraces, Huon Peninsula, New Guinea: a study of Quaternary tectonic movements and sea-level changes. Geological Society of America Bulletin 85, 553-570.

Chappell, J., Shackleton, N.J., 1986. Oxygen isotopes and sea level. Nature 324, 137-140.

Chappell, J., Veeh, H.H., 1978. Late Quaternary tectonic movements and sea-level changes at Timor and Atauro Island. Geological Society of America Bulletin 89, 356-368.

Coyne, M.K., 2003. Transgressive-regressive cycles in the Ironshore Formation, Grand Cayman, British West Indies. Unpublished M. Sc. Thesis, University of Alberta, Edmonton, Canada, 98 pp.

Coyne, M.K., Jones, B., Ford, D., 2007. Highstands during Marine Isotope Stage 5: evidence from the Ironshore Formation of Grand Cayman, British West Indies. Quaternary Science Reviews 26, 536-559.

Dodge, R.E., Fairbanks, R.G., Benninger, L.K., Maurrasse, F., 1983. Pleistocene sea levels from raised coral reefs of Haiti. Science 219, 1423-1425.

Emery, K.O., 1981. Low marine terraces of Grand Cayman Island. Estuarine, Coastal and Shelf Science 12, 569-578.

Harrison, R.S., 1977. Caliche profiles: indicator of near surface subaerial diagensis, Barbados, West Indies. Bulletin of Canadian Petroleum Geology 25, 123-173.

Harrison, R.S., Coniglio, M., 1985. Origin of the Pleistocene Key Largo Limestone, Florida Keys. Bulletin of Canadian Petroleum Geology 33, 350-358.

Harrison, R.S., Steinen, R.P., 1978. Subaerial crusts, caliche profiles, and breccia horizons - comparison of some Holocene and Mississippian exposure surfaces, Barbados and Kentucky. Geological Society of America Bulletin 89, 385-396.

Hickey, T.D., Hine, A.C., Shinn, E.A., Kruse, S.E., Poore, R.Z., 2010. Pleistocene carbonate stratigraphy of South Florida: evidence for high-frequency sea-level cyclicity. Journal of Coastal Research 26, 605-614.

Hunter, I.G., 1994. Modern and ancient coral associations of the Cayman Islands. Unpublished Ph.D Thesis, University of Alberta, Edmonton, Canada, 345 pp.

Hunter, I.G., Jones, B., 1996. Coral association of the Pleistocene Ironshore Formation, Grand Cayman. Coral Reefs 15, 249-267.

Imbrie, J., Hays, J.D., Martinson, D.G., McIntyre, A., Mix, A.C., Morley, J.J., Pisias, N.G., Prell, W.L., Shackleton, N.J., 1984. The orbital theory of Pleistocene climate: support from a revised chronology of the marine ^{18}O record. In: Berger, A., Imbrie, J., Hays, J., Kukla, G., Saltzman, B. (Eds.), Milankovitch and Climate, part 1, Dordrecht, pp. 269- 305.

Imbrie, J.D., McIntyre, A., 2006. SPECMAP time scale developed by Imbrie et al., 1984 based on normalized planktonic records (normalized O-18 vs time, specmap.017). doi:10.1594/PANGAEA.441706

James, N.P., 1972. Holocene and Pleistocene calcareous crust (caliche) profiles:

criteria for subaerial exposure. Journal of Sedimentary Petrology 42, 817-836.

Jones, B., 1990. Tunicate spicules and their syntaxial overgrowths: examples from the Pleistocene Ironshore Formation, Grand Cayman, British West Indies. Canadian Journal of Earth Science 27, 525-532.

Jones, B., 1994. Geology of the Cayman Islands. In: Brunt, M.A., Davies, J.E. (Eds.), The Cayman Islands: Natural History and Biogegraphy. Kluwer Academic Publishers, The Netherlands, pp. 13-49.

Jones, B., Hunter, I.G.,1990. Pleistocene paleogeography and sea levels on the Cayman Islands, British West Indies. Coral Reefs 9, 81-91.

Jones, B., Hunter, I.G., Kyser, K., 1994. Revised stratigraphic nomenclature for Tertiary strata of the Cayman Islands, British West Indies. Caribbean Journal of Science 30, 53-68.

Jones, B., Pemberton, S.G., 1988. *Lithophaga* borings and their influence on the diagenesis of corals in the Pleistocene Ironshore Formation of Grand Cayman Island, British West Indies. Palaios 3, 3-21.

Jones, B., Pemberton, S.G., 1989. Sedimentology and ichnology of a Pleistocene unconformity bounded, shallowing upward carbonate sequence: the Ironshore Formation, Salt Creek, Grand Cayman. Palaios 4, 343-355.

Jones, B., Squair, C.A., 1989. Formation of peloids in plant rootlets, Grand Cayman, British West Indies. Journal of Sedimentary Petrology 59, 1002-1007.

Land, C.S., Epstein, S., 1970. Late Pleistocene diagenesis and dolomitization, North Jamaica. Sedimentology 14, 187-200.

Martin, G.D., Wilkinson, B.H., Lohmann, K.C., 1986. The role of skeletal porosity in aragonite neomorphism - *Strombus* and *Montastrea* from the Pleistocene Key Largo Limestone, Florida. Journal of Sedimentary Petrology 56, 194-203.

Martinson, D.G., Pisia, N.G., Hays, J.D., Imbrie, J., Moore, T.C., Shackleton, N.J., 1987. Age dating and the orbital theory of the Ice Ages: Development of

a high-resolution 0 to 300,000 year chronostratigraphy. Quaternary Research 27, 1-29.

Matley, C.A., 1926. The geology of the Cayman Islands (British West Indies), and their relation to the Bartlett Trough. Quarterly Journal of the Geological Society 82, 352-387.

Matthews, R.K., 1967. Diagenetic fabrics in biosparites from the Pleistocene of Barbados, West Indies. Journal of Sedimentary Petrology 37, 1147-1153.

Matthews, R.K., 1973. Relative elevation of Late Pleistocene high sea level stands: Barbados uplift rates and their implications. Quaternary Research 3, 147-153.

McCrea, J.M., 1950. On the isotopic chemistry of carbonates and a paleotemperature scale. The Journal of Chemical Physics 18, 849-857.

McGregor, H.V., Gagan, M.K., 2003. Diagenesis and geochemistry of *Porites* corals from Papua New Guinea: implications for paleoclimate reconstruction. Geochimica et Cosmochimica Acta 67, 2147-2156.

Mesolella, K.J., 1967. Zonation of uplifted Pleistocene coral reefs on Barbados, West Indies. Science 156, 638-640.

Mesolella, K.J., Matthews, R.K., Broecker, W.S., Thurber, D.L., 1969. The astronomical theory of climate change: Barbados data. The Journal of Geology 77, 250-274.

Mitchell, S.F., Pickerill, R.K., Stemann, T.A., 2001. The Port Morant Formation (Upper Pleistocene, Jamaica): high resolution sedimentology and paleoenvironmental analysis of a mixed carbonate clastic lagoonal succession. Sedimentary Geology 144, 291-306.

Multer, H.G., Gischler, E., Lundberg, J., Simmons, K.R., Shinn, E.A., 2002. Key Largo Limestone revisited: Pleistocene shelf-edge facies, Florida Keys, USA. Facies 46, 229-272.

Multer, H.G., Hoffmeister, J.E., 1968. Subaerial laminated crusts of the Florida Keys. Geological Society of America Bulletin 79, 183-192.

Perfit, M.R., Heezen, B.C., 1978. The geology and evolution of the Cayman Trench. Geological Society of America Bulletin 89, 1155-1174.

Perkins, R.D., 1977. Depositional framework of Pleistocene rocks in South Florida. Geological Society of America Memoirs 147, 131-198.

Pirazzoli, P.A., Radtke, U., Hantoro, W.S., Jouannic, C., Hoang, C.T., Causse, C., Borel Best, M., 1991. Quaternary raised coral-reef terraces on Sumba Island, Indonesia. Science 252, 1834-1836.

Pruss, S.B., Clemente, H., 2011. Assessing the role of skeletons in Early Paleozoic carbonate production: insights from Cambro-Ordovician strata, Western Newfoundland. In: Laflamme, M., Schiffbauer, J.D., Dornbos, S.Q. (Eds.), Quantifying the Evolution of Early Life, pp. 161-183.

Rehder, H.A., 1962, The Pleistocene molluscs of Grand Cayman Island, with notes on the geology of the island. Journal of Paleotology 36, 583-585.

Rehman, J., 1992. Diagenetic alteration of *Strombus gigas*, *Siderastrea siderea* and *Montastrea annularis* from the Pleistocene Ironshore Formation of Grand Cayman. Unpublished M. Sc. Thesis, University of Alberta, Edmonton, Canada, 136 pp.

Rehman, J., Jones, B., Hagan, T.H., Coniglio, M., 1994. The Influence of sponge borings on aragonite-to-calcite inversion in Late Pleistocene *Strombus gigas* from Grand Cayman, British West Indies. Journal of Sedimentary Research 64, 174-179.

Rigby, J.K., Roberts, H.H., 1976. Grand Cayman Island: geology, sediments and marine communities, Brigham Young University geology studies volume 4. Brigham Young University, Department of Geology, 122 pp.

Rohling, E.J., Fenton, M., Jorissen, F.J., Bertrand, P., Ganssen, G., Caulet, J.P.,

1998. Magnitudes of sea-level lowstands of the past 500,000 years. Nature 394, 162-165.

Saller, A.H., Moore, C.H., 1991. Geochemistry of meteoric calcite cements in some Pleistocene limestones. Sedimentology 38, 601-621.

Scholle, P.A., Ulmer-Scholle, D.S., 2003. A color guide to the petrography of carbonate rocks: grains, textures, porosity, diagenesis. The American Association of Petroleum Geologists Memoir 77, Tulsa, Oklahoma, 459 pp.

Schroeder, J.H., 1973. Submarine and vadose cements in Pleistocene Bermuda reef rock. Sedimentary Geology 10, 179-204.

Shackleton, N.J., Matthews, R.K., 1977. Oxygen isotope stratigraphy of Late Pleistocene coral terraces in Barbados. Nature 268, 618-620.

Shourie, A., 1993. Depositional architecture of the late Pleistocene Ironshore Formation, Grand Cayman, British West Indies. Unpublished M. Sc Thesis, University of Alberta, Edmonton, Canada, 100 pp.

Siddall, M., Chappell, J., Potter, E.-K., 2007. Eustatic sea level during past interglacials. Developments in Quaternary Science 7, 75-92.

Vacher, H.L., Hearty, P.J., Rowe, M.P., 1995. Stratigraphy of Bermuda: nomenclature, concepts, and status of multiple systems of classification. In: Curran, H.A., White, B. (Eds.), Terrestrial and Shallow Marine Geology of the Bahamas and Bermuda, Geological Society of America Special Paper 300, pp. 271-294.

Vézina, J.L., 1997. Stratigraphy and sedimentology of the Pleistocene Ironshore Formation at Rogers Wreck Point, Grand Cayman: a 400 ka record of sea-level highstands. Unpublished M. Sc. Thesis, University of Alberta, Edmonton, Canada, 131 pp.

Vézina, J.L., Jones, B., Ford, D., 1999. Sea level highstands over the last 500,000 years: evidence from the Ironshore Formation on Grand Cayman, British West

Indies. Journal of Sedimentary Research 69, 317-327.

Vollbrecht, R., Meischner, D., 1996. Diagenesis in coastal carbonates related to Pleistocene sea level, Bermuda platform. Journal of Sedimentary Research 66, 243-258.

Webb, G.E., Nothdurft, L.D., Kamber, B.S., Kloprogge, J.T., Zhao, J.X., 2009. Rare earth element geochemistry of scleractinian coral skeleton during meteoric diagenesis: a sequence through neomorphism of aragonite to calcite. Sedimentology 56, 1433-1463.

Woodroffe, C. D., Stoddart, D. R., Giglioli, M.E.C., 1980. Pleistocene patch reefs and Holocene swamp morphology, Grand Cayman Island, West Indies. Journal of Biogeography 7, 103-113.

Woodroffe, C.D., Stoddart, D.R., Harmon, R.S., Spencer, T., 1983. Coastal morphology and late Quaternary history, Cayman Islands, West Indies. Quaternary Research 19, 64-84.

CHAPTER 2: HETEROGENEOUS DIAGENETIC PATTERNS IN THE PLEISTOCENE IRONSHORE FORMATION OF GRAND CAYMAN, BRITISH WEST INDIES[1]

1. Introduction

Diagenetic studies of Pleistocene limestones have commonly tried to correlate the evolution of their fabrics, mineralogy, and geochemistry to changes in sea level and associated fluctuations in the onshore hydrological zones (e.g., Matthews, 1967, 1968; Schroeder, 1973; Steinen and Matthews, 1973; Allan and Matthews, 1977; Buchbinder and Friedman, 1980; Saller and Moore, 1989; Quinn, 1991; Vollbrecht and Meischner, 1996). During a lowstand, previously deposited sediments will experience meteoric diagenesis that will continue until sea-level rises once again and submerges that unit. During the ensuing highstand, new sediments will be deposited on the unconformity that denotes the top of the older unit. Through time, this depositional-exposure cycle can be repeated many times. The diagenetic fabrics that develop in these rock packages will, in theory, reflect (1) the diagenesis that follows each phase of deposition, (2) repeated cycles of diagenetic overprinting of the older units, and (3) multiple cycles of diagenesis. From a global perspective, the critical question is whether or not the diagenetic fabrics in a carbonate succession follow a systematic pattern that can be linked to the transgressive-regressive cycles that governed its formation.

Matthews and Frohlich (1987) applied forward modeling to a static one dimensional model to predict the diagenetic stratigraphy resulting from sea level fluctuations. This model yielded the lithologies expected by the static

1 This chapter was published as: Li, R., Jones, B., 2013. Heterogeneous diagenetic patterns in the Pleistocene Ironshore Formation of Grand Cayman, British West Indies. Sedimentary Geology 294, 251-265.

model, but fluctuations. This model yielded the lithologies expected by the static model, but the relationship of those lithologies to a particular period of subaerial exposure was obscured by the complexity of glacioeustatic sea level changes. Later, Whitaker et al. (1997) used a coupled two dimensional diagenetic model to simulate the diagenetic profile caused by variations in sea level. They generated a stacked sequence of diagenetic zones, which show lateral continuity and distinct trends from the platform interior to margin, but the associations between unconformity surfaces and underlying diagenetic zones were difficult to establish with certainty. Braithwaite and Montaggioni (2009) and Braithwaite and Camoin (2011) examined this question by analyzing cores through Pleistocene limestones from the Great Barrier Reef and Moruroa (French Polynesia) in the western Pacific Ocean. As with the modeling studies, they had difficulty relating the diagenetic history to the multiple episodes of diagenesis that had acted on the succession.

The Pleistocene Ironshore Formation on Grand Cayman, formed of six unconformity-bounded depositional units (A to F), provides an excellent opportunity to examine the diagenetic response to sea level change because the internal stratigraphy is well established (Jones et al., 1994; Vézina, 1997; Vézina et al., 1999; Coyne, 2003; Coyne et al., 2007) and the constituent limestones have been modified by many different diagenetic processes (Jones and Pemberton, 1988; Jones and Squair, 1989; Rehman, 1992; Rehman et al., 1994). Using samples collected from this formation, this study examines the stratigraphic and geographic variations in the mineralogy, fabrics, and stable isotope geochemistry, and compares the diagenetic evolution of the corals with their associated matrices. By integrating all these data, this study ascertains if (1) the corals and their coeval matrices underwent the same diagenetic changes, (2) the diagenetic patterns in the Ironshore Formation are stratigraphically systematic, and (3) if the different styles

of diagenesis can be related to specific Pleistocene lowstands.

2. Geological Setting

Grand Cayman (Fig. 2-1A) is relatively flat with most of the island being less than 6 m above sea level (Jones et al., 1997, their figure 8-2). The Pleistocene limestones that unconformably overlie the Tertiary Bluff Group (Fig. 2-1B) were originally assigned to the Ironshore Formation by Matley (1926). Although found mostly on the central and western parts of the island, large stretches of the formation are covered by mangrove swamps. On the eastern part of island, the formation is largely restricted to small embayments (Jones et al., 1994). A maximum thickness of 19 m is known from a well drilled in the Rogers Wreck Point area (Fig. 2-2) (Vézina, 1997; Vézina et al., 1999).

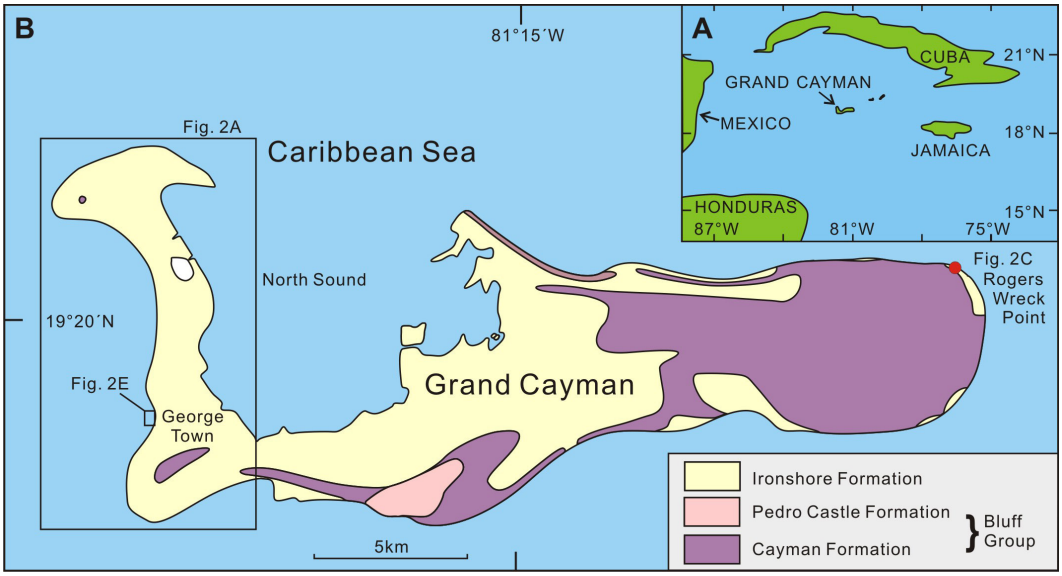

Fig. 2-1. (A) Location of Grand Cayman. (B) Geological map of Grand Cayman (modified from Jones, 1994) showing locations of western onshore (WA), offshore George Town (GT) and Rogers Wreck Point (RWP).

Division of the formation into Units A to F (Fig. 2-3A) is based on lithology, biota, unconformities, and U/Th radiometric ages (Vézina, 1997; Vézina et al., 1999; Coyne, 2003; Coyne et al., 2007). Relative to sea level today,

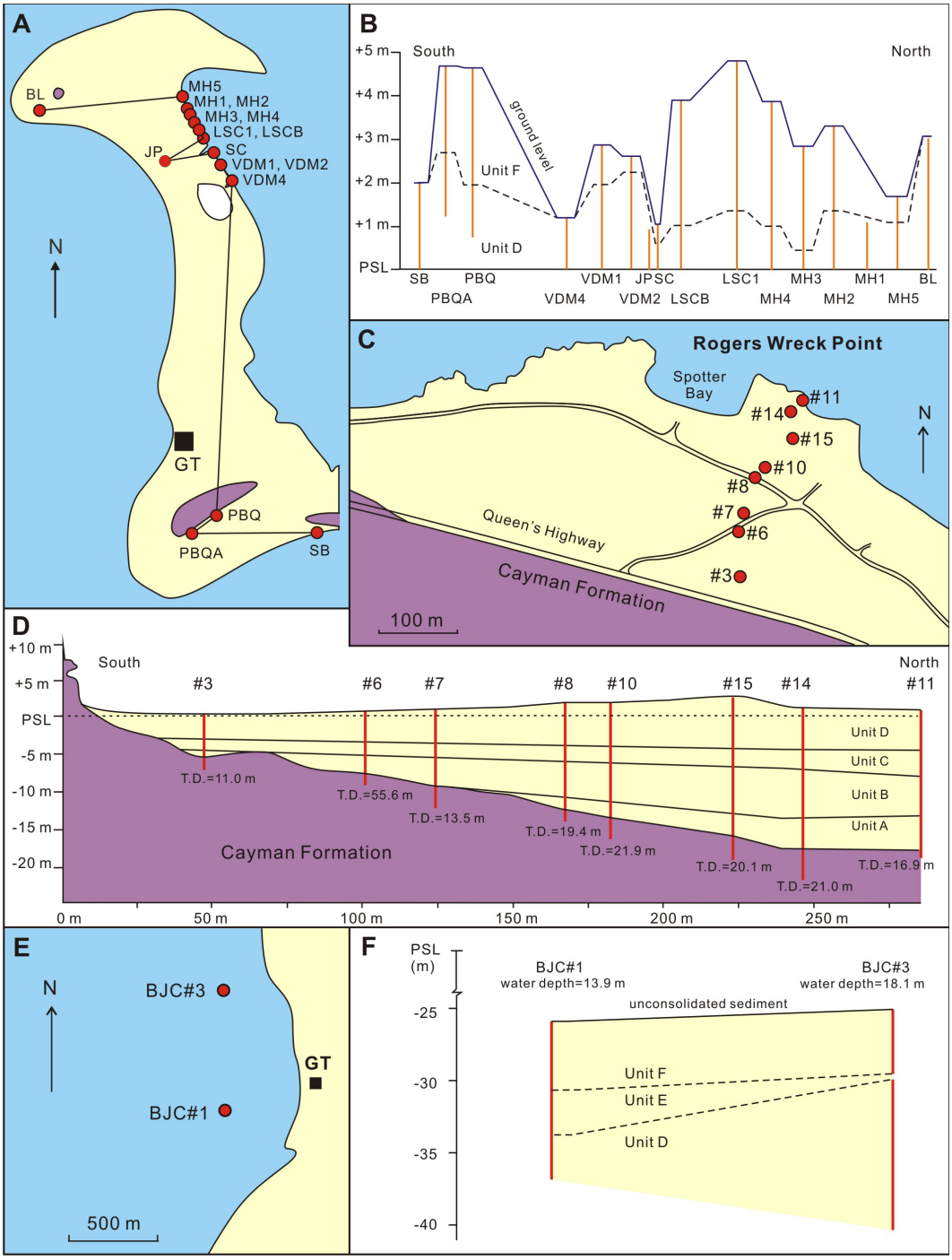

Fig. 2-2. (A) Location of outcrops and quarries where the Ironshore Formation was sampled. (B) Correlation of units D and F on western part of Grand Cayman (modified from Coyne et al., 2007). (C) Location of sampled cores in Rogers Wreck Point area (modified from Vézina, 1997; Vézina et al., 1999). (D) Correlation of units A, B, C, and D in the Ironshore Formation in the eight studied cores from Rogers Wreck Point area (modified from

Vézina, 1997). (E) Location of cores through Ironshore Formation offshore Vézina, 1997). (E) Location of cores through Ironshore Formation offshore from George Town (GT) (modified from Coyne, 2003; Coyne et al., 2007). (F) Correlation of units D, E, and F between BJC#1 and BJC#3 from offshore George Town (modified from Coyne, 2003).

sea levels at the times of deposition of those units were: Unit A, –9.0 to –5.5 m; Unit B, –3.0 to +0.5 m; Unit C, –2.5 to +1.0 m; Unit D, +2.5 to +6.0 m, Unit E, +2.0 to +5.0 m; and Unit F, +3.0 to +5.0 m (Vézina, 1997; Vézina et al., 1999; Coyne, 2003; Coyne et al., 2007). Units A, B, C, D, E, and F correlate with Marine Isotope Stages (MIS) 11, 9, 7, 5e, 5c, and 5a, respectively (Fig. 2-3B; Vézina, 1997; Vézina et al., 1999; Coyne, 2003; Coyne et al., 2007).

A

Age (ka)	Unit	Lithology	Biota	Sea level elevation (m)
84	F	Cross-bedded ooid grainstones; coral floatstone; *Halimeda* floatstone	Head corals, branching corals, *Halimeda*	+3.0 to +5.0
104	E	Coral floatstones	Head corals	+2.0 to +5.0
131	D	Grainstones	Head corals, branching corals	+2.5 to +6.0
229	C	Rudstones, packstones, grainstones,bafflestone	Head corals, branching corals	-2.5 to +1.0
346	B	Packstones, grainstones, minor wackstones	Head corals, branching corals	-3.0 to +0.5
>400	A	Grainstones	Head corals, branching corals	-9.0 to -5.5

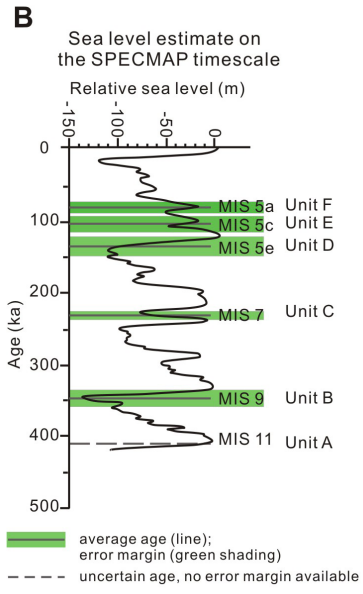

Fig. 2-3. (A) Internal stratigraphy of Ironshore Formation. Ages and sea-levels (relative to modern sea level) from Vézina et al. (1999) and Coyne et al. (2007). (B) Positions of units A to F in Ironshore Formation relative to sea level curve of Siddall et al. (2007).

3. Material and Methods

The samples used in this study came from (1) Rogers Wreck Point (RWP),

(2) offshore George Town (GT), and (3) the western onshore area (WA) (Fig. 2-2). The samples from RWP came from cores from eight wells (RWP#3, #6, #7, #8, #10, #11, #14, #15; Fig. 2-2C, 2-2D). The GT samples came from two cores (BJC#1, BJC#3; Fig. 2-2E, 2-2F), whereas the WA samples came from scattered outcrops and quarries (BL, JP, MH1, MH2, MH3, MH4, MH5, LSC1, LSCB, PBQA, PBQ, SB, SC, VDM1, VDM2, VDM4; Fig. 2-2A, 2-2B). Collectively, these samples provide coverage of units A to F.

The samples from RWP and GT are formed of corals held in wacke/pack/grainstone to floatstone matrices. Samples from the WA localities are typically formed of corals that are held in friable ooid grainstones formed of aragonitic ooids that are variably lithified by calcite cement. In this study, the corals and the matrices were analyzed separately so that the two could be compared. For the ooid grainstones, the ooids and calcite cement were also analyzed separately.

The proportion of each type of skeletal grain in the matrices was determined by point counting of 50 thin sections (200 points per section) using the method outlined by Pruss and Clemente (2011). Identifications of the skeletal grains were verified by comparison with images in Scholle and Ulmer-Scholle (2003). Visual charts for estimating abundances of constituents in the thin section (Scholle and Ulmer-Scholle, 2003, their figure on page xii) were used to assess the proportion of skeletal grains, micrite matrix, and cements found between the corals.

The mineralogies of 183 coral, 161 matrix, and 19 ooid grainstone samples were determined by X-ray diffraction (XRD) analysis. The powdered samples (each weighing ~1 g) were analyzed on a Rigaku Ultima IV Powder XRD system that was run at 38 kV and 38 mA using an Ultima IV X-ray generator with a Co tube. All scans were run from 5° to 90° 2θ at a speed of 2°θ/min. The aragonite and calcite weight percentages were calculated from the intensities of the d_{110}, d_{021},

and d_{104} peaks using an aragonite-calcite calibration curve that had been derived from the analyses of artificial samples with known calcite:aragonite ratios. The values obtained using this method are accurate at ±2 wt.%.

The diagenetic features of the limestones were determined from 117 thin sections that had each been impregnated with blue epoxy. Minor amounts of dolomite were detected in some samples by XRD analyses. The distribution of dolomite was determined by examining small (~1 cm^3) fractured rock samples on a JEOL 6301 Field Emission Scanning Electron Microscope (SEM). The samples were mounted on SEM stubs using conductive glue and then sputter coated with gold before being examined using an accelerating voltage of 5 kV. The composition of the dolomite crystals was confirmed by using the energy dispersive X-ray (EDX) analyzer that is attached to the SEM (operated at an accelerating voltage of 20 kV).

Oxygen and carbon isotope ratios were determined for 95 corals and 44 matrix samples that contained >85% aragonite or >85% calcite, and 16 bulk ooid grainstone samples with calcite wt.% between 15% and 85%, as determined by XRD analyses and confirmed by thin section analyses. Individual aragonitic ooids from 6 ooid grainstone samples were manually picked under binocular microscope and run for stable isotope compositions. Powder samples were dissolved in H_3PO_4 at 25°C in a constant temperature water bath for 60 minutes following the protocol outlined by McCrea (1950). The evolved gases were analyzed on a Finnigan MAT 251 mass spectrometer. The isotope values are calibrated relative to the Vienna Peedee Belemnite using the NBS 19 ($\delta^{18}O$ = –2.20‰, $\delta^{13}C$ = +1.95‰) and NBS 18 ($\delta^{18}O$ = –23.00‰, $\delta^{13}C$ = –5.00‰) standards. The accuracy is better than 0.2‰ for $\delta^{13}C$, and better than 0.6‰ for $\delta^{18}O$.

4. Results

4.1. Corals

The dominant corals found in the RWP and GT areas are *Montastrea annularis* and *Acropora palmata* (Li and Jones, 2013). At the WA localities, *M. annularis*, *Porites* thickets, and other head corals dominate (Hunter and Jones, 1996; Coyne et al., 2007). The aragonitic coral skeletons have been calcified to varying degrees, but no systematic variations in calcitization or diagenetic diversity of *M. annularis* and *A. palmata* were found from Units A to F (Li and Jones, 2013). The geographic variations in the degree of skeletal calcification between *M. annularis* and *A. palmata* from RWP and GT are related to the intrinsic coral skeleton structures and extrinsic diagenetic environments (Li and Jones, 2013).

Li and Jones (2013) focused solely on the *M. annularis* and *A. palmata* whereas the data for corals used in this study came from all of the corals (Fig. 2-4).

4.2. Matrix compositions

4.2.1. Rogers Wreck Point

The groundmasses in these limestones are composed of skeletal pack/grain/floatstones with subordinate wackestones that are formed of micrite, allochem grains, and cements. From units A to D, the matrices are formed, on average, of 30%, 40%, 60%, and 50% micrite, 55%, 50%, 33%, and 40% skeletal grains, and 15%, 10%, 7%, and 10% cements, respectively (Fig. 2-4D). The increase in micrite from units A to C is matched by a decrease in the cements and skeletal grains (Fig. 2-4D). The skeletal grains were derived largely from benthic foraminifera (41.5%), red algae (30%), Halimeda (13.4%), and mollusc (8.8%)

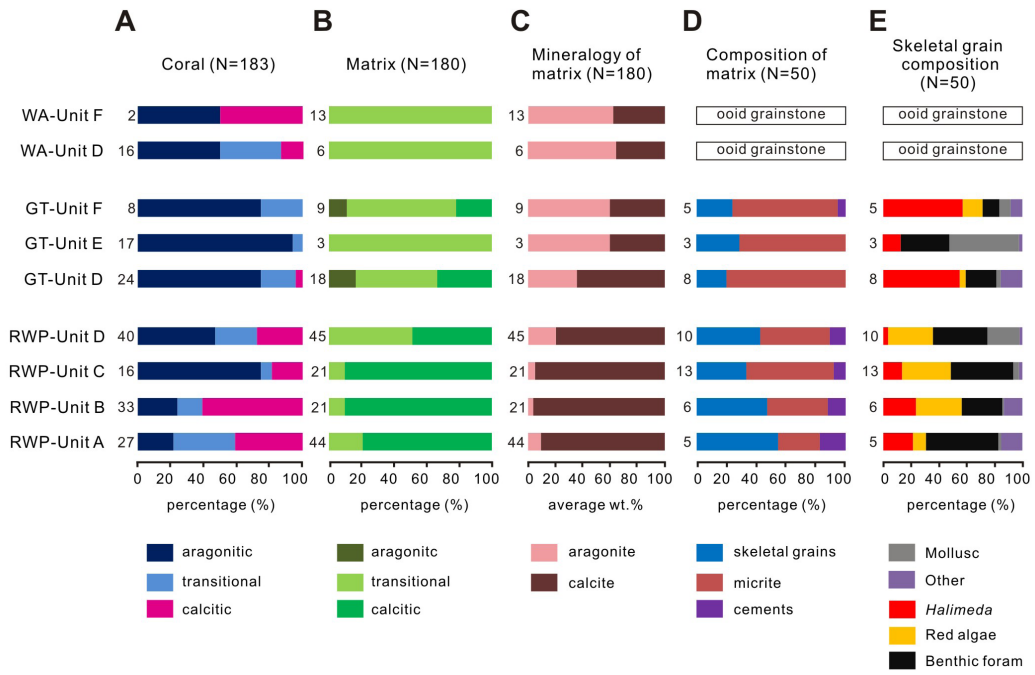

Fig. 2-4. Summary statistics for mineralogy of coral, mineralogy and composition of matrices from the Ironshore Formation, Grand Cayman. N represents total sample size. (A) Percentages of aragonitic, transitional, and calcitic corals from WA, GT, and RWP. Numbers derived by XRD analyses. (B) Percentages of aragonitic, transitional, and calcitic matrices from WA, GT, and RWP, derived by XRD analyses. (C) Average wt.% calcite and aragonite of matrices from WA, GT, and RWP. Numbers derived by XRD analyses. (D) Proportions of skeletal grains, micrites, and cements in matrices from GT and RWP. Numbers derived from point counting with 200 points per thin section. (E) Estimated composition of matrices from GT and RWP. Numbers derived from thin section analyses.

grains along with fewer from worm tubes, and echinoids (Table 2-1, Fig. 2-4E). Encrusting foraminifera and red algae are associated with many of the coral grains. Mollusc fragments are present in Units C and D.

4.2.2. Offshore George Town

In these samples, the matrices range from skeletal wacke/pack/grainstone to Halimeda floatstone. From units D to F, the amounts of micrite are 80%, 60%, and 70%, whereas the amounts of skeletal grains are 20%, 40%, and 25%,

Table 2-1. Composition of constituent grains in Pleistocene Ironshore Formation from Rogers Wreck Point and offshore George Town area. Statistics based on point-counting (200 points) of thin sections.

Unit	Rogers Wreck Point				Offshore George Town		
	A	B	C	D	D	E	F
Composition	Average (%)	Average (%)	Average (%)	Average (%)	Average (%)	Average (%)	Average (%)
Peloid/Ooid	0	6.6	0	0	0	0	0
Halimeda	21.2	23.4	13.1	3.7	54.8	13.0	56.7
Red algae	9.5	32.8	35.2	32.0	4.3	0	14.9
Benthic foraminifera	51.9	28.9	45.1	39.0	22.4	35.0	11.8
Mollusc	2.4	0.5	3.8	23.2	2.7	50.0	8.0
Worm tubes	0	0.4	0.7	0.3	8.1	0	0
Echinoid	0.2	0	0.5	0.4	2.7	2.0	5.8
Unidentified	14.8	7.4	1.6	1.4	5.0	0	2.8

respectively (Fig. 2-4D). The is no more than 5% cement in any of the samples. The percentage of micrite is generally higher than that in the matrices from RWP (Fig. 2-4D). In units D and F, the skeletal grains are dominated by Halimeda (up to 55% of skeletal grains) along with fewer benthic foraminifera, red algae and mollusc (Fig. 2-4E). In Unit E, however, skeletal grains are derived largely from mollusc (50%) and foraminifera (35%) grains, with fewer Halimeda (13%) and echinoids (Table 2-1, Fig. 2-4E). Large worm tubes are found in Unit D (37.0 mbsl, BJC#1).

4.2.3. Western onshore area

The Ironshore Formation (mostly units D and F) exposed on the western part of the island is formed mainly of oolitic limestones (Brunt et al., 1973; Woodroffe et al., 1980; Jones and Goodbody, 1984; Jones and Pemberton, 1989; Jones and Hunter, 1990; Shourie, 1993; Hunter and Jones, 1996; Coyne, 2003;

Coyne et al., 2007). Corals, bivalve, and conch shells are common in unit D at many of these localities (Coyne, 2003; Coyne et al., 2007).

4.3. Mineralogy

XRD analyses show that the corals and their associated matrices are formed of various mixtures of aragonite and/or calcite. For the purpose of this study, aragonitic refers to samples formed of >85% aragonite, calcitic refers to samples formed of >85% calcite, and transitional refers to samples that have between 15 and 85% aragonite.

4.3.1. Corals

In the RWP area, the percentage of calcitic corals in units A, B, C, and D is 40%, 60%, 20%, and 30%, respectively. In the GT samples, only 5% of the corals from Unit D are calcitic, and all corals from units E and F are aragonitic (Fig. 2-4A). About 10% of the corals from Unit D found in the WA localities are calcitic (Fig. 2-4A). These comparisons clearly show that the corals from RWP area are more calcitic than those from GT and WA. The calcitic corals are randomly distributed in each unit with no clear relationship to the unconformities found at the top of each unit (Fig. 2-5). In Unit C in RWP#11, for example, almost all of the corals are aragonitic, whereas corals from Unit B in RWP#14 are almost all calcitic (Fig. 2-5A, 2-5B).

4.3.2. Matrices

For each unit in the Ironshore Formation, the amount of calcite in the matrices can be expressed as (1) the percentage of samples that are calcitic (Fig. 2-4B), or (2) the average weight % calcite based on all the samples analyzed from a particular unit (Fig. 2-4C).

In the RWP area, (1) the percentage of calcitic samples in units A to C is

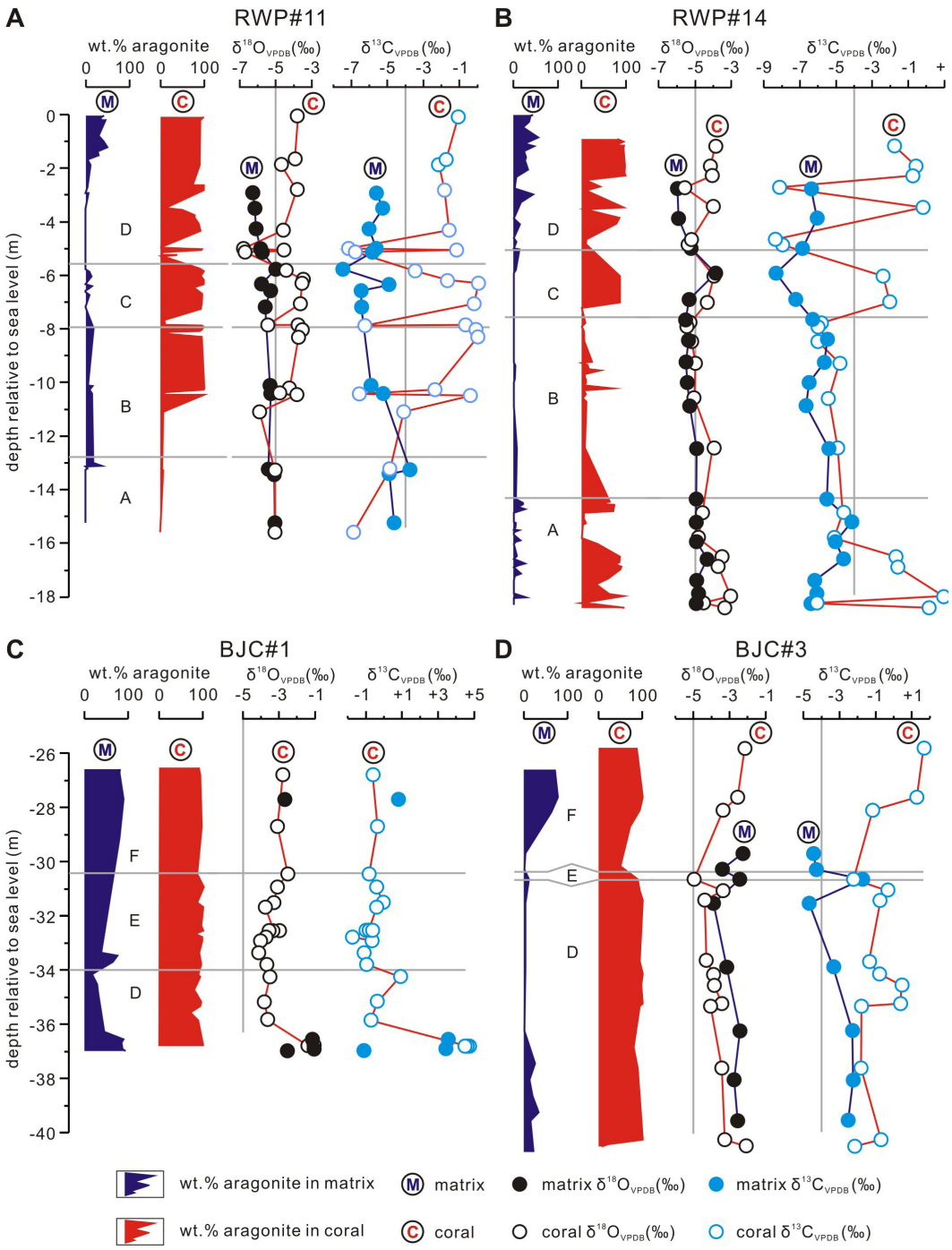

Fig. 2-5. Down-hole variation of weight percent (wt.%) aragonite, δ18O, and δ13C of corals and coeval matrices in cores from wells (A) RWP#11, (B) RWP#14, (C) BJC#1, and (D) BJC#3.

higher than that in Unit D, (2) none of the analyzed matrix samples are aragonitic (Fig. 2-4B), and (3) the average wt.% calcite in units A to C (91-97%) is higher

than that in Unit D (81%) (Fig. 2-4C). In Unit A from core RWP#14 (15.4 to 17.9 mbsl), the limestone matrices contain up to 12% dolomite.

In the GT area, the matrices are less calcitic than those from RWP. In Units D to F from GT, calcitic matrices form less than 35% of the samples, whereas 50% to 90% of the matrices in the limestones from Units A to D at RWP are calcitic (Fig. 2-4B). Furthermore, the average wt.% calcite of matrices from Units D to F in GT is 20-50% lower than that from Units A to D in RWP (Fig. 2-4C). In the GT cores, the average wt.% calcite of matrices in units E and F (40%) is 25% lower than that in Unit D (65%). Some of the limestones in Units D and F from core BJC#3 contain up to 3% dolomite.

There are no consistent relationships between the mineralogy of matrices and the unconformities (Fig. 2-5). In the RWP area, the matrices in units A to C are all calcitic (Fig. 2-5A, 2-5B), whereas the matrices in unit D change from calcitic in the lower part to mixed aragonite-calcite towards the top of the unit (Fig. 2-5A, 2-5B). In Unit D in the GT area, however, the opposite is true (Fig. 2-5C, 2-5D).

4.3.3. Ooid grainstone

The oolitic grainstones consist of aragonitic ooids cemented by calcite. The wt.% calcite in these grainstones ranges from 25% to 60% with an average of about 40% (Fig. 2-4C).

4.4. Diagenetic features

In the RWP area, unconformities at the tops of units A, B, C, and D are highlighted by terra rossa and/or calcrete crusts (Vézina, 1997). In WA and GT, unconformities at the tops of units D, E, and F are characterized by a hard calcrete crust and/or an erosional surface with high relief (Coyne, 2003; Coyne et al., 2007). Diagenetic features evident in the corals and the allochems found in

the matrices include bioerosion, dissolution and neomorphism, cementation, and internal sediments.

4.4.1. Bioerosion

Many skeletal grains have been extensively bored with sponge borings being common in the corals and shell fragments (Fig. 2-6A, 2-6B). Bivalve borings are common in M. annularis and many of the encrusting red algae were intensely bored by worms (Fig. 2-6C). Microbial microborings, ~1 μm in diameter, are common. Most of the borings are partially or fully filled by sediments (Fig. 2-6A-C). Micrite envelopes, up to 200 μm thick, are developed around many grains.

4.4.2. Dissolution and neomorphism

Many of the foraminifera, ooids, Halimeda plates, and mollusc shells (Fig. 2-6D) have been completely dissolved. Some of the resultant vugs are coated with a thin crust of microcrystalline calcite (Fig. 2-6E).

Aragonitic biofragments, including those from mollusc shells (Fig. 2-6F), Halimeda, corals, and worms have been variably altered to calcite. Some of the red algae grains have been partially recrystallized to blocky low-Mg calcite.

4.4.3. Cementation

Acicular aragonite cement, found in many of the corals, developed largely as epitaxial overgrowths on the aragonite crystals that form the coral skeletons (Fig. 2-7A). The distribution of this cement is highly irregular in individual coral heads and from coral head to coral head.

High-magnesium calcite (HMC) cement, found mostly in the GT samples, is present as isopachous fibrous (Fig. 2-7B) or prismatic calcite (Fig. 2-7C) crystals, 50-100 μm long, coating skeletal grains, or lining chamber walls.

Low-magnesium calcite (LMC) cements are found as blocky, equant

calcite crystals, 30 μm to 3 mm long, that coat grains (Fig. 2-7D), fill intergranular (Fig. 2-7C, 2-7E) and intragranular pore spaces (Fig. 2-6F) and fill cavities.

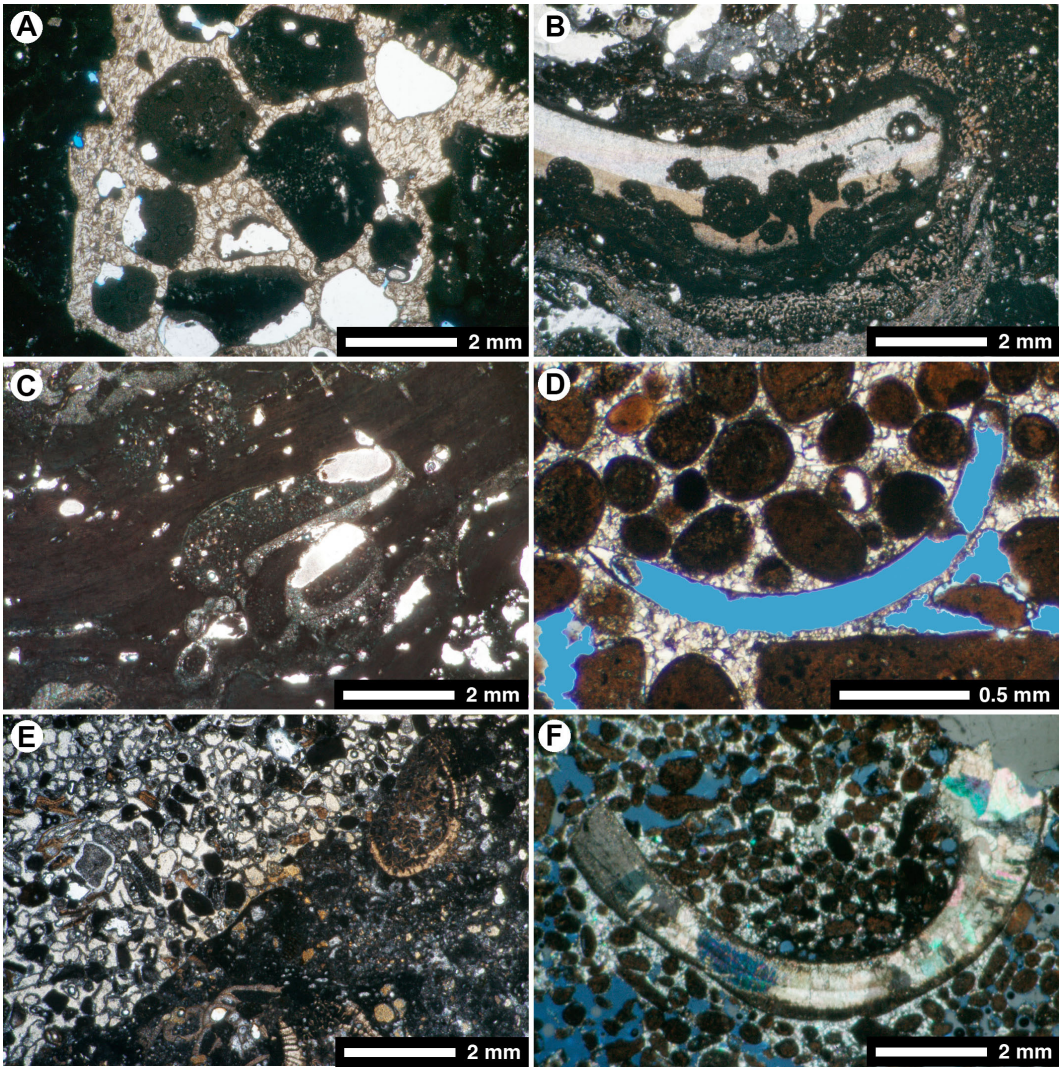

Fig. 2-6. Thin section microphotographs showing bioerosion, dissolution and neomorphism in Ironshore Formation. A to E are taken under plane polarized light, F is taken under cross polarized light. (A) Sponge boring in coral head partially to completely filled with micrite. BJC#1, Unit D, 37.1 mbsl. (B) Boring in mollusc shell completely filled with micrite. RWP#6, Unit D, 0.9 m. (C) Geopetal fabrics in borings in red algae. RWP#11, Unit C, 6.9 m. (D) Moldic porosity after mollusc shell. MH4, Unit F, 1.2 masl. (E) Poorly cemented grainstone overlying a hardground developed on a packstone. RWP#10, Unit A, 13.3 m. (F) Neomorphosed mollusc shell. MH4, Unit F, 1.2 masl.

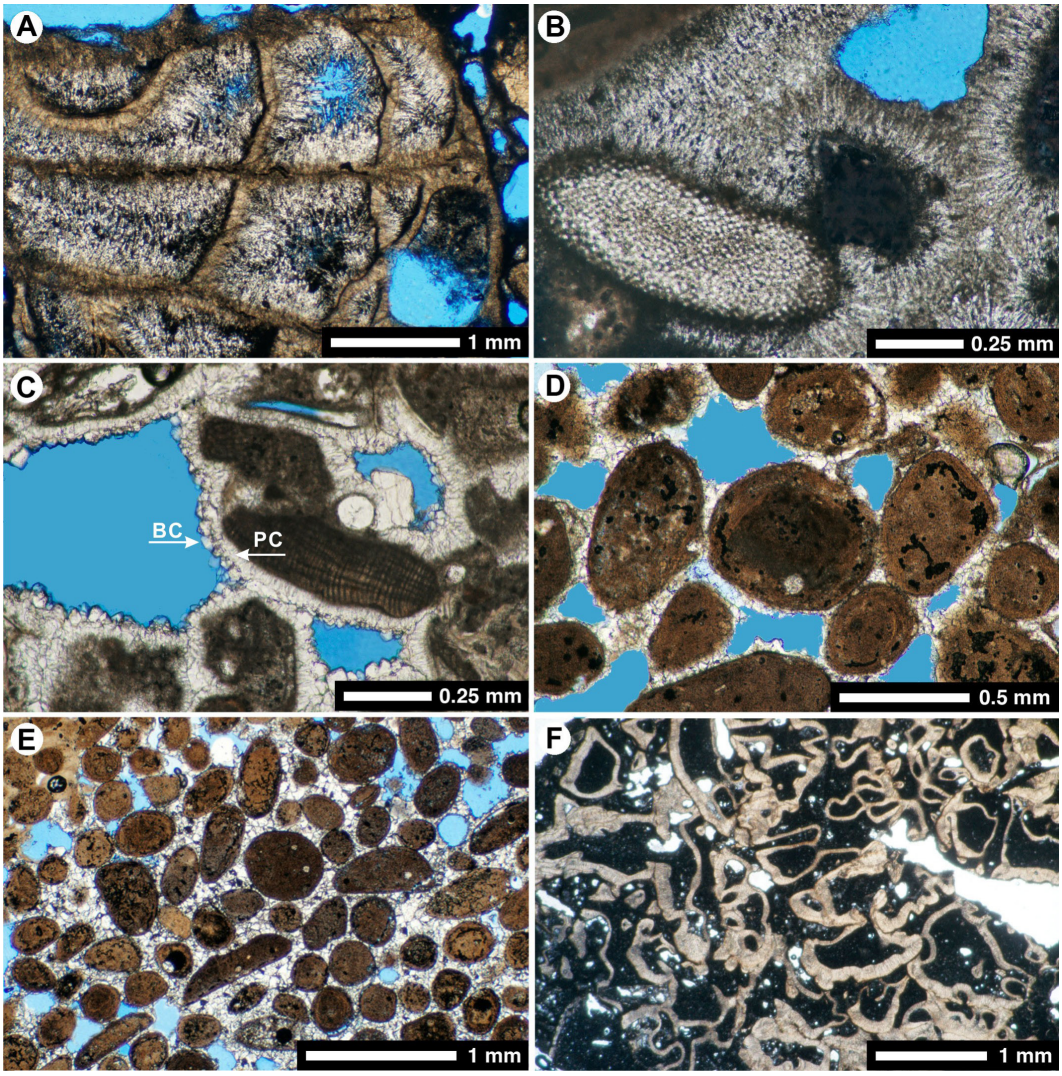

Fig. 2-7. Thin section microphotographs showing cementation and internal sediments in limestones from Ironshore Formation. All images with plane polarized light; blue = porosity. (A) Acicular aragonite cements in coral skeletal voids. BJC#3, Unit F, 26.5 mbsl. (B) Fibrous calcite cements around allochem grains. BJC#3, Unit F, 28.8 mbsl. (C) Two generations of cements, prismatic calcite (PC) and blocky calcite (BC). RWP#11, Unit A, 13.0 m. (D) Meniscus calcite cements in ooid/peloid grainstone. LSC1, Unit F, 1.4 masl. (E) Evenly distributed blocky calcite cements and remnants of meniscus calcite cements. MH2, Unit F, 1.8 masl. (F) Internal sediments in chambers of Carpenteria. RWP#7, Unit C, 6.4 m.

4.4.4. Internal sediments

Internal sediments formed largely of micrite are common in all types of

cavities (Fig. 2-6C, 2-7F). Some of the internal sediment contains tunicates, spores, and peloids.

4.4.5. Dolomitization

Dolomite crystals, ~1 μm long, present in some samples from well RWP#14, occur as individual rhombs associated with blocky calcite, or in thin layers that coat the allochems.

4.5. Distribution of diagenetic features

4.5.1. Corals

There are no systematic stratigraphic trends in the diagenetic fabrics found in the corals from units A to F. Calcification ranges from 0 to 100%. Borings, common in all the head corals, have been partly to totally filled with internal sediments (Fig. 2-6A) with geopetal fabrics being evident in some. Framework voids in the corals are variously lined with isopachous calcite cements (Fig. 2-8A), blocky calcite cements (Fig. 2-8B), and filled with mud/wacke/grainstones (Fig. 2-8A). Acicular aragonite cements are common in unit F from GT (Fig. 2-7A).

4.5.2. Matrices

In the RWP area, diagenetic features evident in the matrices of the limestones from units A to D generally includes various combinations of (1) borings in molluscan (Fig. 2-6B) and red algae biofragments (Fig. 2-6C), (2) sediment filling of borings with geopetal fabrics being common (Fig. 2-6C), (3) filling of skeletal body chambers with internal sediments (Fig. 2-6F), (4) lining of skeletal body chambers with isopachous calcite cement (Fig. 2-8C), (5) micrite envelopes, (6) partial to complete dissolution and neomorphism of Halimeda plate, foraminifera (Fig. 2-8D), mollusk (Fig. 2-6D, 2-6F), and worm tubes.

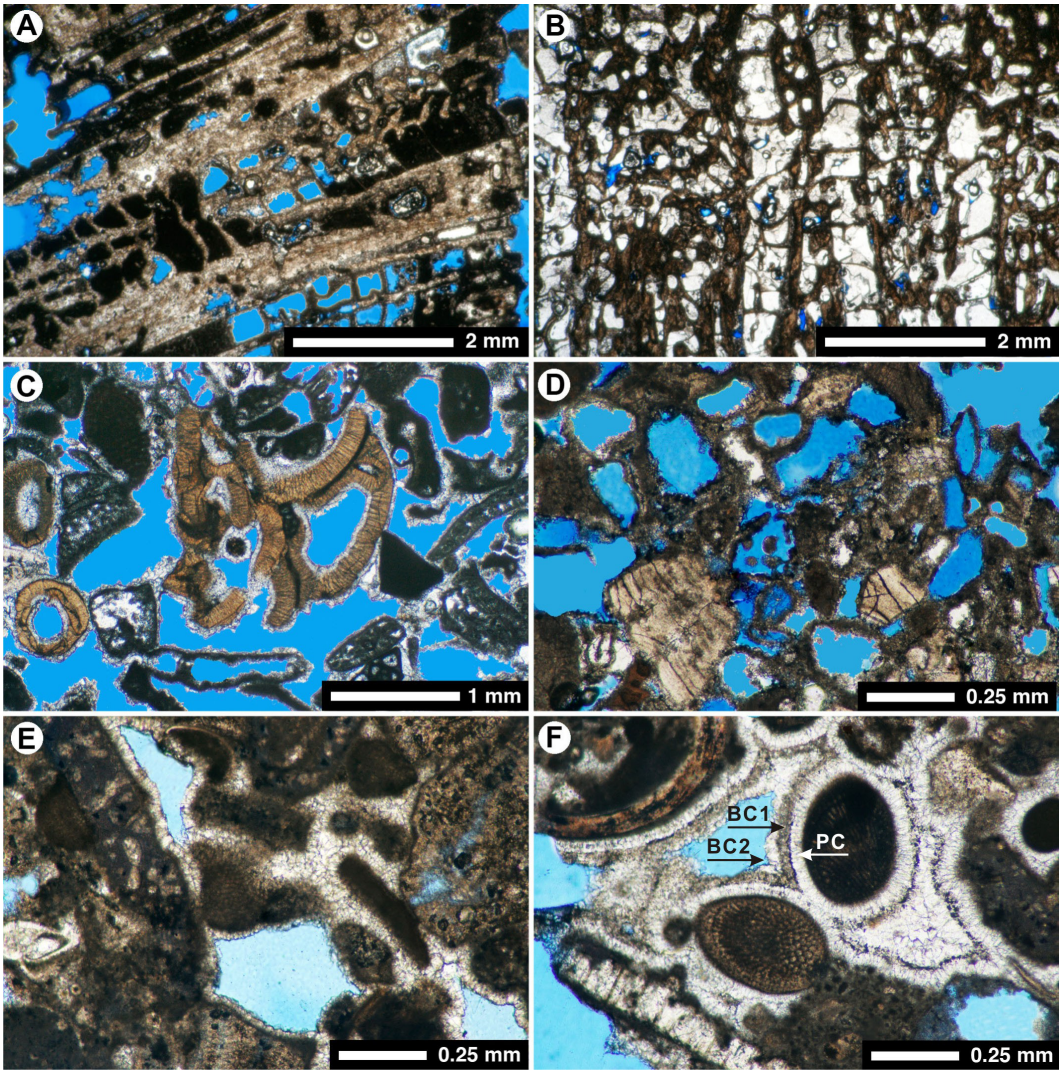

Fig. 2-8. Thin section microphotographs showing diagenetic fabrics in Ironshore Formation. All images with plane polarized light; blue = porosity. (A) Neomorphosed coral skeleton with internal sediments and/or calcite cements in skeletal voids. RWP#11, Unit A, 15.6 m. (B) Blocky calcite cements in coral skeletal voids. RWP#11, Unit B, 11.1 m. (C) Porous grainstone with thin layer of isopachous calcite cements lining inside and outside of allochem grains. RWP#11, Unit A, 13.4 m. (D) Moldic porosity. RWP#11, Unit C, 7.1 m. (E) Prismatic calcite cements around allochems. BJC#1, Unit D, 34.9 mbsl. (F) Prismatic calcite cements (PC) and two generations of blocky calcite cements (BC1, BC2). BJC#3, Unit F, 28.4 mbsl.

Other diagenetic features restricted to specific samples from this area include (1) two generations of cement around the grains in Unit A (Fig. 2-7C) and (2) a

hardground in Unit A (RWP#10, 13.3 mbsl) that is highlighted by grain truncation in the underlying packstone (Fig. 2-6E).

Diagenetic fabrics in the GT samples include (1) selective dissolution of Halimeda grains in units D to F, (2) fibrous HMC cements in worm chambers from Unit D in BJC#1, (3) isopachous calcite cements in Unit D (Fig. 2-8E), and (4) isopachous and blocky calcite (Fig. 2-8F) cements in Unit F.

Diagenetic fabrics in the ooid grainstones from Units D to F in the WA area include (1) meniscus calcite cement (Fig. 2-7D), (2) blocky intergranular calcite cements (Fig. 2-7E), (3) dissolution of some ooids (SC, LSC), (4) non-fabric selective vugs that are filled by large blocky calcite crystals that are up to 3 mm long, and (5) some partly recrystallized biofragments (Fig. 2-6F).

4.6. Porosity and Permeability

Six core pieces (each 6 cm diameter and 6.5 to 14.5 cm long) from units D to F in BJC#1 and BJC#3 yielded tested porosities of 18 to 40% (average = 28%), and tested permeabilities of 187 to 5510 mD (average 1574 mD) (Table 2-2). These cores are representative of the matrices found in units D, E, and F.

4.7. Stable isotope

4.7.1. Corals

In the RWP area, the average $\delta^{18}O_{VDPB}$ values of the aragonitic corals from Units A to C range from –3.88‰ to –3.41‰, whereas the $\delta^{13}C$ values range from –1.47‰ to –0.55‰ (Table 2-3). Corals from Unit D in the WA and RWP areas have similar $\delta^{18}O_{VDPB}$ values of –4.1‰, and their $\delta^{13}C$ values are within the range of those from Units A to C (Table 2-3). Corals from Unit D in the GT area have more positive $\delta^{18}O$ and $\delta^{13}C$ values than those from the RWP area (Table 2-3). In the GT area, corals from Unit E yielded slightly more negative $\delta^{18}O$ and $\delta^{13}C$

values than those from Unit D, whereas corals from Unit F yielded more positive $\delta^{18}O$ and $\delta^{13}C$ values than those from Unit E (Table 2-3). Samples from Unit F in the WA area have the most positive average $\delta^{18}O$ and $\delta^{13}C$ values (Table 2-3). In general, the aragonitic corals from each area have consistent average $\delta^{18}O$ values, from –4.15‰ to –2.57‰, whereas the $\delta^{13}C$ values range from –1.47‰ to +3.22‰.

The $\delta^{18}O$ values of calcitic corals from the RWP and WA areas, ranging from –5.96‰ to –4.82‰, are more negative than the $\delta^{18}O$ values (–4.15‰ to –2.57‰) of the aragonitic corals (Table 2-3). In Unit D from GT, however, the average $\delta^{18}O$ value of the calcitic corals is –2.11‰, which is 2‰ more positive than all the other calcitic corals (Table 2-3).

Table 2-2. Porosity and permeability of matrices in Pleistocene Ironshore Formation from offshore George Town area (modified from Coyne, 2003).

Core	Depth (mbsl)	Unit	Cylindrical plugs		Composition	Permeability (mD)			Porosity (%)
			Diameter (cm)	Length (cm)		K_{max}	K_{90}	K_{vert}	
BJC#1	26.8	F	6.0	6.8	Matrix with coral grains	5510	5200	2440	29.8
BJC#1	31.6	E	6.0	6.5	Matrix	2060	2440	1060	36.2
BJC#1	36.6	D	6.0	10.0	Matrix with coral grains	542	248	34.2	24.7
BJC#3	26.5	F	6.0	14.5	Matrix	254	211	25.6	19.1
BJC#3	27.9	F	6.0	10.0	Matrix with coral grains	187	69.3	182	18.1
BJC#3	38.9	D	6.0	6.8	Matrix	895	844	462	40.0

The $\delta^{13}C$ and $\delta^{18}O$ of the corals generally have a positive correlation (Fig. 2-5). In the profiles analyzed, however, there were no systematic trends in the

stable isotope values that could be related to any of the unconformities.

Table 2-3. Stable oxygen and carbon isotope composition of corals from Ironshore Formation, Grand Cayman. Total sample number is 95. N = number of samples. WA = Western onshore area; GT = offshore George Town; RWP = Rogers Wreck Point.

Unit	Coral (aragonite)					Coral (calcite)				
	N	$\delta^{18}O_{VPDB}$ mean (‰)	$\delta^{18}O_{VPDB}$ 1σ	$\delta^{13}C_{VPDB}$ mean (‰)	$\delta^{13}C_{VPDB}$ 1σ	N	$\delta^{18}O_{VPDB}$ mean (‰)	$\delta^{18}O_{VPDB}$ 1σ	$\delta^{13}C_{VPDB}$ mean (‰)	$\delta^{13}C_{VPDB}$ 1σ
F (WA)	1	-2.57	NA	3.22	NA	1	-5.96	NA	0..36	NA
F (GT)	5	-2.79	0.5	0.16	1.2	0				
E (GT)	13	-3.46	0.4	-0.76	0.4	0				
E (WA)	0					0				
D (WA)	7	-4.11	0.3	-0.81	0.7	3	-5.72	0.3	-1.17	1.3
D (GT)	18	-3.08	1.3	0.78	2.6	3	-2.11	0.02	-2.21	0.08
D (RWP)	10	-4.15	0.3	-1.28	0.6	5	-5.95	0.7	-7.67	0.7
C (RWP)	7	-3.88	0.4	-1.47	1.3	1	-5.37	NA	-6.21	NA
B (RWP)	4	-3.83	0.3	-0.7	1.1	8	-5.09	0.5	-5.45	0.8
A (RWP)	4	-3.41	0.3	-0.55	1.3	5	-4.82	0.2	-5.51	0.9

4.7.2. Matrices

The calcitic matrices in Units A to C in Rogers Weck Point area have $\delta^{18}O$ values between –5.34‰ and –4.94‰ with an average of about –5‰ (Table 2-4). The corresponding average $\delta^{13}C$ values, which range from –6.80‰ to –5.12‰, become more negative from Units A to C (Table 2-4). The matrices in unit D are ~1‰ more negative than the $\delta^{18}O$ values in Units A to C, whereas the $\delta^{13}C$ values are within the same range as for Units A to C (Table 2-4).

In the GT samples, the average $\delta^{18}O$ values for the calcitic matrices in Units D and F are –2.90‰ and –2.85‰, whereas the average $\delta^{13}C$ values are –2.81‰ and –4.37‰, respectively (Table 2-4). Compared to the $\delta^{18}O$ and $\delta^{13}C$ values from the RWP area, the values derived from the GT samples are about 2‰ more positive. For the GT samples, the calcitic matrices have more negative $\delta^{13}C$ values than the aragonitic matrices (Table 2-4).

Table 2-4. Stable oxygen and carbon isotope composition of matrices from Ironshore Formation, Grand Cayman. Total sample number is 44. N = number of samples. WA = Western onshore area; GT = offshore George Town; RWP = Rogers Wreck Point.

Unit	matrix (aragonite)					matrix (calcite)				
	N	$\delta^{18}O_{VPDB}$ mean (‰)	$\delta^{18}O_{VPDB}$ 1σ	$\delta^{13}C_{VPDB}$ mean (‰)	$\delta^{13}C_{VPDB}$ 1σ	N	$\delta^{18}O_{VPDB}$ mean (‰)	$\delta^{18}O_{VPDB}$ 1σ	$\delta^{13}C_{VPDB}$ mean (‰)	$\delta^{13}C_{VPDB}$ 1σ
F (WA)	0					0				
F (GT)	1	-2.69	NA	0.80	NA	2	-2.85	0.8	-4.37	0.1
E (GT)	0					0				
D (WA)	0					0				
D (GT)	3	-1.58	0.8	1.96	2.7	6	-2.90	0.6	-2.81	1.1
D (RWP)	0					8	-5.91	0.3	-5.95	0.5
C (RWP)	0					6	-5.15	0.7	-6.80	1.2
B (RWP)	0					8	-5.34	0.2	-5.90	0.5
A (RWP)	0					10	-4.94	0.3	-5.12	0.9

The $\delta^{13}C$ and $\delta^{18}O$ are generally positively correlated (Fig. 2-5). In general, there is no evidence of systematic changes that can be linked to the unconformities that occur at the top of each unit. Nevertheless, the calcitic

matrices of Unit C from RWP#11 (at 5.8 mbsl) and RWP#14 (at 5.9 mbsl), which are close to the unconformity at the top of Unit C, yielded $\delta^{18}O$ values that are shifted towards less negative values, and the $\delta^{13}C$ values shifted towards more negative values relative to the $\delta^{13}C$ and $\delta^{18}O$ values of the calcitic matrices from units A to C (Fig. 2-5A, 2-5B).

4.7.3. Ooid grainstones

Bulk samples of the ooid grainstones in units D and F yielded $\delta^{18}O$ values between –3.91‰ and –2.22‰, and $\delta^{13}C$ values between +0.29‰ and +3.49‰. In contrast, the $\delta^{18}O$ and $\delta^{13}C$ of the ooids (separated from matrix) range from –1.66‰ to +0.48‰, and from +3.20‰ to +4.18‰, respectively.

5. Interpretation

5.1. Original matrix mineralogy

Given that diagenetic changes have taken place, the original amounts of calcite and aragonite in the matrices of the limestones can only be estimated by considering (1) the proportions of the micrite, allochems, and cement (Fig. 2-4D), and (2) the proportions of biofragments (Fig. 2-4E) in terms of their original mineralogy.

Samples from GT have the highest amount of micrite, whereas samples from WA have the lowest. Samples from RWP are intermediate between these two extremes. The amount of calcite cement increases as the amount of micrite decreases (Fig. 2-4D). The allochems and micrite form >95% of the matrices in the GT samples and 80-90% of the matrices in the RWP samples. The calcite cements are not included in the calculation of the original amount of calcite and aragonite in matrices.

In the RWP and GT areas, Halimeda, benthic foraminifera, red algae,

and mollusc collectively form at least 80% of the skeletal grains (Table 2-1, Fig. 2-4E). Halimeda and mollusc (Strombus gigas) contributed aragonite to the sediment whereas red algae and the dominant foraminifera (Homotrema, Carpenteria) contributed HMC to the sediment (cf., Blackmon and Todd, 1959; Gross, 1961). This means that the biofragments were formed predominantly of aragonite and HMC with little LMC. Most of the micrite in the matrices was probably derived from (1) the breakdown of skeletal grains, and/or (2) direct chemical precipitation from the seawater. Given that abiotic sediments precipitated during the Pleistocene were mainly aragonite (Sandberg, 1983), it seems reasonable to suggest that most of the micrite in the matrices of the limestones in the Ironshore Formation were also formed largely of aragonite.

Based on all the data obtained, the estimated amounts of aragonite in the original matrices from units A to D in RWP are 50%, 60%, 70%, and 65%, respectively, whereas the amount of aragonite in the original matrices from units D to F in GT is about 90%. The ooids from the ooid grainstones in the WA samples, are formed entirely of aragonite.

5.2. Post-diagenesis mineralogy

In the RWP and GT areas, the corals are generally less calcitic than the surrounding matrix (Fig. 2-4A, 2-4B). The same is true in the Barbados Pleistocene coral-cap where the mineralogical stabilization of the matrices is more advanced than that of the corals (Matthews, 1968). This can probably be attributed to the presence of (1) HMC biofragments that are the first to stabilize during incongruent dissolution (Gavish and Friedman, 1969), and (2) aragonitic mud that may have stabilized before the aragonitic grains (Matthews, 1968; Brand, 1989). In the Ironshore Formation, the amount of HMC allochems in the original matrices of the limestones is greater in the RWP samples than the GT

samples (Fig. 2-4D, 2-4E). Thus, the matrices in the RWP area are more stable than those from the GT area (Fig. 2-4B). The distribution of calcitic matrix and calcitic coral samples is irregular with no clearly defined association with any of the unconformities that cap each unit.

In the RWP area, the degree of mineralogic stabilization in the matrices does not systematically increase from Units D to A. In the RWP area, the calculated percentages of aragonite that have been diagenetically altered to calcite, which are 40%, 55%, 65%, and 45% in units A to D (Fig. 2-9) respectively, shows that the amount of transformed aragonite is not stratigraphically controlled. In the GT area, the mineralogy of the matrices in Unit D are more stable than the matrices in Units E and F (Fig. 2-4B, 2-4C).

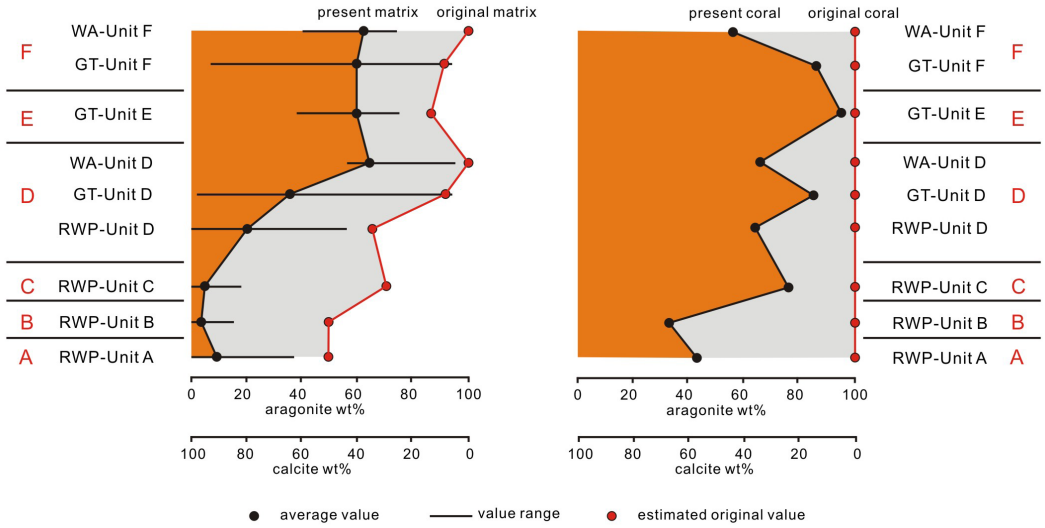

Fig. 2-9. Weight percent aragonite in present day limestones compared to original sediments (estimated) for (A) matrices and (B) corals from units A to F of Ironshore Formation, Grand Cayman. Total number for analyzed matrices is 180, and for analyzed corals is 183. Total number of estimated matrices is 50. The original mineralogy of scleractinian coral is 100% aragonite.

The corals from the RWP area are generally more calcified than those from the GT area (Fig. 2-4A). A similar geographic difference in the degree of calcitization is evident in Pleistocene corals collected ~16 km apart on Barbados

(Matthews, 1968). Those differences were attributed to differences in the rainfall and evaporation rates of the two areas with the high calcification levels in the central west coast area being linked to the high rainfall and low evaporation of that area (Matthews, 1968). The situation on Grand Cayman, however, is different because the highest mineral stability, in the RWP area, is today the area with the lowest rainfall and highest evaporation rates (Ng et al., 1992). Such linkages must be treated with caution because there is no guarantee that the patterns of rainfall and evaporation evident on these islands today were the same as those that were operative at the time when diagenesis took place.

Mineralogic stabilization is a dissolution-reprecipitation process (Land, 1967; Matthews, 1968; James, 1974) with the rate of calcitization being a function of variables such as climate, diagenetic environments, original mineralogy, and skeletal structures. Given the different elevations of RWP (top of unit D is ~1 m above sea level) and GT (top of unit D is ~34 m below sea level) (Li and Jones, 2013), the geographic differences in the mineralogical stabilization rates evident in the Ironshore Formation may reflect (1) differences in the periods of time that the sequences spent in the freshwater phreatic zone (cf., Steinen and Matthews, 1973; Budd, 1988), and/or (2) the different amounts of meteoric waters that flushed through the vadose zone (e.g., Harris and Matthews, 1968; Holail, 1999). Thus, for both the corals and the matrices, the more stable mineralogy found in the RWP succession as compared to that in GT succession suggests that (1) the Ironshore Formation at RWP spent more time in the freshwater phreatic environment, or (2) the larger volume of meteoric water that flowed through the Ironshore Formation at RWP in vadose environment.

5.3. Diagenetic fabrics

Diagenetic fabrics found in Units A to F include evidence of alteration

that took place in the marine zone, the freshwater phreatic zone, and the subaerial vadose zone. Marine diagenetic fabrics include (1) bioerosion of the corals and biofragments that probably started while the animals were alive (Acker and Risk, 1985) and continued after their death (Schroeder, 1986), (2) micrite envelopes, (3) internal sediments, and (4) isopachous fibrous HMC (Fig. 2-7B), acicular aragonite (Fig. 2-7A), and isopachous prismatic calcite cements (Fig. 2-8E) that are similar to those reported from many recent reefs (e.g., James and Ginsburg, 1979; Aissaoui et al., 1986; Braithwaite and Montaggioni, 2009; Braithwaite and Camoin, 2011; Perrin, 2011; Sayani et al., 2011).

Freshwater phreatic diagenetic fabrics includes (1) blocky calcite cements precipitated evenly or randomly around the allochems (e.g., Halley and Harris, 1979; Budd, 1988) (Fig. 2-7C, 2-7E), and (2) extensive leaching of grains with resultant pores lined by isopachous blocky calcite cements (cf., Buchbinder and Friedman, 1980) (Fig. 2-6E).

Vadose diagenetic fabrics include (1) meniscus calcite cements (cf., Schroeder, 1973) (Fig. 2-7D), and (2) blocky calcite cements filling primary or secondary voids (Pingitore, 1976; Buchbinder and Friedman, 1980) (Figs. 2-6F, 2-8B).

Marine diagenetic fabrics are evident throughout the Ironshore Formation with the greatest diversity being in Unit F in the GT area. Nevertheless, vadose fabrics are the most common diagenetic features in the formation. Phreatic diagenetic fabrics are largely restricted to Unit A in the RWP area and units D and F in the GT and WA areas. Evidence of multiphase vadose diagenetic fabrics such as multiple generations of calcite cements, however, is rare. In the ooid grainstones from the WA area, vadose cements and phreatic cements are present (Fig. 2-7E), which may imply proximity to a paleo-water table.

The origin of the dolomite in Unit A of RWP#14 is open to debate, largely

because the small crystal size precludes detailed geochemical analyses of the dolomite.

5.4. Stable isotopes

The $\delta^{18}O - \delta^{13}C$ values for the matrices (Fig. 2-10A) and the corals and ooids (Fig. 2-10B), which follow similar trend lines, can be divided into Groups I, II, and III. The aragonitic samples (Group I) occupy the upper-middle part of the trend, whereas the calcitic samples (Groups II and III) cluster along the lower part of the trend (Fig. 2-10). The calcitic samples are divided into Groups II that includes samples from GT and WA, and Group III, which includes all the samples

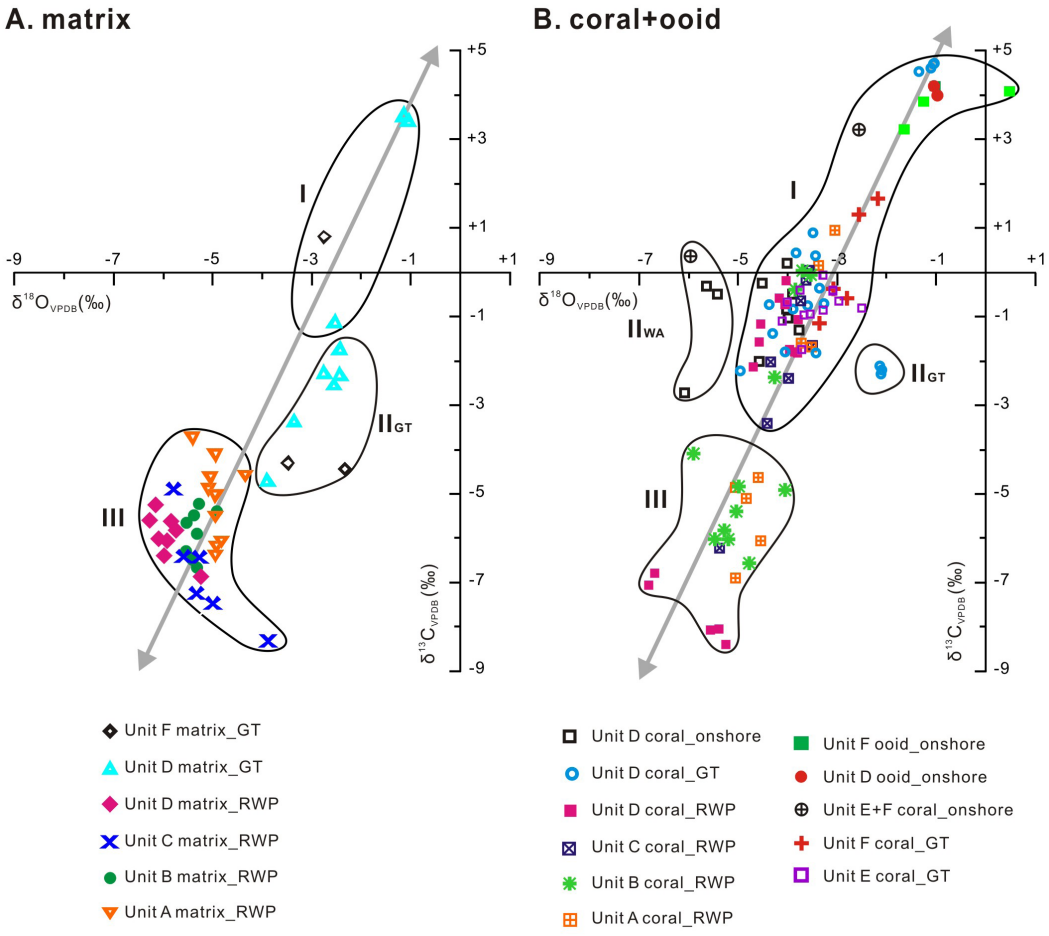

Fig. 2-10. Cross plots of δ13C versus δ18O for the (A) matrices, and (B) corals and ooids from Ironshore Formation, with interpreted stable isotopic groups.

from RWP. From an interpretive perspective, the most important aspects of the stable isotope data are as follows.

- Group I is indicative of the marine environment. The aragonitic ooids plot in the field close to that occupied by modern peloids and ooids (data from Gischler et al., 2009) and the expected values for Pleistocene aragonite (data from Chafetz and Rush, 1994). This indicates that the present isotopic compositions may have been in equilibrium with the marine water in which they formed. The deviation in the $\delta^{18}O$ values for some of the ooids (–1.3 to –1.7‰), however, suggests that some may have been influenced by meteoric diagenesis. If the measured $\delta^{18}O$ value of the aragonitic ooids (average is –0.92‰) is used to calculate ambient water temperature using the equation of Grossman and Ku (1986) with present-day seawater values of $\delta^{18}O$ (SMOW), then:

  $$T\ (°C) = 20.6 - 4.34 * (\delta^{18}O_{aragonite} - \delta^{18}O_{water})$$

  This indicates that the ambient seawater temperature was ~25°C at the time of ooid formation.

- The $\delta^{18}O$ (–4.96‰ to –2.16‰) and $\delta^{13}C$ (–3.43‰ to +3.22‰) values (Fig. 2-10B) of the aragonitic corals are similar to those from modern corals in the Caribbean Sea (Fairbanks and Matthews, 1978; Fairbanks and Dodge, 1979; Swart et al., 1996; Leder et al., 1996; Smith, 2006; Gischler et al., 2009). This implies that meteoric processes have had little impact on the aragonitic corals. Isotopic variations between the aragonitic corals are probably due to taxonomic differences in the "vital effect" and isotopic variations within individual skeletons may reflect changes in environment factors (e.g., temperature) as the corals grew (Weber and Woodhead, 1970). The extremely positive $\delta^{13}C$ values (+4.52‰ to +4.73‰) in some corals are attributed to precipitation of aragonite cements in the skeletal

voids of the corals (Li and Jones, 2013).

- The isotopic values of the aragonitic matrices ($\delta^{18}O$ = –3.2 to +2.3‰, $\delta^{13}C$ = –1.6 to +5.3‰) plot in the field of modern skeletal sediments from the Belize-Yucatan platform, the Belize barrier reef, and the Maldives (data from Gischler et al., 2009). Such values also indicate minimal meteoric diagenetic alteration.
- The aragonitic ooids found in WA samples are commonly cemented by calcite (Fig. 2-7D, 7E). Based on the stable isotope composition of 13 ooid grainstone samples, the relationship between $\delta^{18}O$ of ooid grainstones and the aragonite content can be expressed by:

  $$\delta^{18}O_{VPDB}\ (‰) = [0.04 * \text{aragonite weight } (\%)] - 5.38$$

  From this equation, the intercept on the y-axis at –5.38‰ is an estimate for a sample that is formed entirely of calcite.
- Most samples in Group III have $\delta^{13}C$ values that are less than –4‰ and indicate subaerial vadose diagenesis. These values are similar to those derived from Pleistocene limestones on Barbados (Allan and Matthews, 1977). The average $\delta^{18}O$ values for the calcitic matrix and calcitic coral are –5.32‰ and –5.26‰ respectively, which is essentially the same as that estimated for the meteoric calcite (–5.38‰) in ooid grainstones.
- Group II contains two subgroups, II_{GT} and II_{WA}, which have different $\delta^{18}O$ values (Fig. 2-10). The average $\delta^{18}O$ value in II_{WA} is about –6‰, whereas the average $\delta^{18}O$ value in II_{GT} is about –2‰. The more positive $\delta^{18}O$ values in II_{GT} suggest precipitation of calcite from pore fluids enriched in ^{18}O due to evaporation at or near the surface.
- Group II, like Group III, is formed entirely of calcitic samples. Unlike Group III, the samples in Group II have more positive $\delta^{13}C$ values (Fig. 2-10), suggesting that factors other than the change in mineralogy

were responsible. Probably, the calcitization in Group II occurred in a freshwater phreatic zone. First, the $\delta^{13}C$ trend of calcitic matrix in GT resembles that indicated by Allan and Matthews (1977), characterizing the vadose/phreatic transition to phreatic zone. The $\delta^{13}C$ shifted towards more negative values ($\delta^{13}C$ = –4.7‰) at 31.7 mbsl; then increases with depth from 31.7 mbsl towards 36.5 mbsl; thereafter, $\delta^{13}C$ values remain constant (Fig. 2-5D). In addition, phreatic calcite cements (Fig. 2-7E) are found in samples from the WA localities.

From the above interpretations, it can be argued that units D to F in GT and WA localities underwent marine and freshwater phreatic diagenesis, whereas units A to D in the RWP area underwent marine and subaerial vadose diagenesis.

6. Discussion

The stable isotope trend lines for the matrices and the corals and ooids have similar slopes (Fig. 2-10) that reflect a common diagenetic pathway between the marine (Group I) and meteoric diagenetic (Groups II and III) environments. Among the aragonitic samples in Group I, the ooids have the most positive $\delta^{18}O$ and $\delta^{13}C$ values whereas the corals yielded the most negative values (Fig. 2-10B). The isotope values of the matrices in this group plot between the corals and the ooids (Fig. 2-10A). The contrast between the ooids, corals, and matrices is probably related to differences in biogenic isotope fractionation (i.e., "vital effect") effects. The ooids seem to have formed in isotopic equilibrium with Pleistocene seawater, whereas the isotopes from the corals reflect a "vital effect" that was more pronounced than those associated with the mollusc, red algae, foraminifera, and Halimeda from which most grains in the matrices were derived. This interpretation is consistent with the data presented by Gischler et al. (2009), who showed that corals have more negative isotopic compositions than

echinoderms, Halimeda, molluscs, red algae, and foraminifera.

The aragonitic corals in the Ironshore Formation are characterized by larger variations in the $\delta^{18}O$ and $\delta^{13}C$ values than their associated aragonitic matrices (Fig. 2-10). Land (1989) also noted a similar contrast in Holocene shallow marine carbonate sediments from the Caribbean Sea and the Pacific Ocean. Gischler et al. (2009) suggested that the lower variance in the matrices reflected the mixing of different grains with different isotope values.

Contrary to the aragonitic samples in Group I, the calcitic matrices in Group III have more negative $\delta^{18}O$ values than the calcitic corals. This probably indicates that the matrices were more susceptible to meteoric diagenesis than the corals. Although the diagenetic alteration of individual allochems have been studied (Crickmay, 1945; Emery et al., 1954; Friedman, 1964), the changes that take place when they are found together in a matrix is poorly documented. Irrespective of this issue, the original composition of the matrix is important because the HMC will be transformed to LMC before the aragonite (Gavish and Friedman, 1969). The subsequent changes, however, are not constant throughout the Ironshore Formation. In units A to D of the RWP area, the matrices have been largely changed to calcite, whereas most of the corals are still aragonitic (Fig. 2-5A, 2-5B). Analysis of the matrices shows that the matrices, although originally formed of 50-70% aragonite, have been changed largely to calcite (Fig. 2-9). In contrast, the matrices and corals in units E and F in the GT area are largely aragonitic with little evidence of calcitization (Fig. 2-5C, 2-5D).

Similar contrasts between the stabilization rates of corals and matrices has been documented from the Pleistocene limestones of Barbados by Matthews (1968). He argued that the aragonite to calcite transformation in freshwater depends on the dissolution of aragonite, calcite nucleation, calcite precipitation, and the amount and percolation rate of water through the rocks. Matthews (1968)

assumed that aragonite dissolution was fast and argued that the contrasts between the matrices and the corals were due to "rate step" differences. For the corals, the rate step was deemed to be the nucleation of calcite, whereas the availability and movement of water were considered the rate steps for the growth of calcite in the matrices (Matthews, 1968).

In the Pennsylvanian Boggy Formation in Oklahoma, Brand (1989) found that the matrices (originally aragonite lime-mud) were more altered than the coeval fossils (mainly molluscs). He argued that grain size and/or surface area may have controlled the different degrees of alteration. Walter and Morse (1984) argued that the dissolution rate of aragonite is controlled by grain size, grain microstructure (crystal size and arrangement), and the saturation state of the diagenetic fluids. If the diagenetic fluid is saturated with respect to $CaCO_3$, the dissolution process is surface reaction-controlled (Constantz, 1986) with the dissolution rate being proportional to the surface area (approximately equal to the reciprocal of the grain radius), and the grain surface roughness factors (Walter and Morse, 1984). The matrices of the limestones in the Ironshore Formation originally included aragonite muds, Halimeda plates, and mollusc fragments (<2 cm), all of which were smaller than the coral skeletal grains that are typically >4 cm long. In addition, the surface roughness factor of Halimeda is ~2.5 times higher than that for coral (Walter and Morse, 1984). Hence, aragonite in the matrices dissolved faster than that in corals. If the diagenetic fluids are undersaturated with respect to $CaCO_3$, the dissolution process is diffusion-controlled and the surface area of the grains will not influence the diagenetic rate (Constantz, 1986). Under this scenario, dissolution will be focused on the grain exteriors (Constantz, 1986) because the grain interiors are isolated from chemical exchange with the fluids (Walter and Morse, 1984).

The porosity and permeability of the limestones are crucial because they

ultimately control the amount of water held in the rock and the rate at which it passes through the limestone. According to Constantz (1986), Acropora palmata, Montastrea annularis, and Porites porites, which are most common corals in the Ironshore Formation, have average porosities of 48, 69, and 71% and permeabilities of 450 mD, 120 mD, and 870 mD, respectively. By comparison, the porosities of the matrices in units D, E, and F range from 18 to 40% (average 28%) with K_{max} values of 187 to 5510 mD (average 1574 mD), respectively. The values from the matrices in the cores must be regarded as minimum values because diagenetic changes have, with time, reduced their porosities and permeabilities. Comparisons of these data show that the corals, irrespective of taxa, have higher porosities but generally lower permeabilities than the matrices. Such data indicate that water will flow more freely through the matrices than the corals.

During the aragonite-to-calcite transformation, the volume of water that flushes through the rocks is critically important because it will, in part, control the rate of diagenesis. This is fundamentally related to the climatic conditions that existed during each of the lowstand periods. During the Pleistocene, the climate in the Caribbean area during lowstands periods was generally more arid than during highstands (Bonatti and Gartner, 1973). Hughes et al. (2007) and Osipova et al. (2013), however, demonstrated that the MIS 6 (after Unit C) and MIS5d (after Unit D) stages were characterized by wet climates with high annual precipitation. Estimated exposure times following deposition of units C and D were 65 ka and 8 ka, respectively (Li and Jones, 2013). Critically, the unconformities at the tops of Unit C and Unit D represent the periods of exposure that led to the development of the two lowest diagenetic packages in the Ironshore Formation. In the lowest package, formed of Units A to C, the mineralogy and stable isotope compositions are relative consistent, the matrices

are largely calcitic, and the average $\delta^{18}O$ value is about –5‰. Important features in this package include (1) an increase in the degree of diagenetic alteration of the matrices from units A to C (Fig. 2-9), and (2) abnormally negative $\delta^{13}C$ values that came from samples just below the unconformity at the top of unit C.

Unit D, is characterized by variable composition, mineralogy and stable isotope signatures among RWP, WA, and GT, but the amount of transformed aragonite is relatively consistent (Fig. 2-9). The uppermost package, composed of units E and F, mostly consist of aragonite and show the lowest level of diagenetic alteration (Fig. 2-9).

The petrographic and geochemical signatures of units A to F in the Pleistocene Ironshore Formation on Grand Cayman show clear evidence of diagenesis that took place in the marine, vadose, and freshwater phreatic zones. Thus, it might be expected that individual limestone samples from the older units should be characterized by paragenetic sequences that reflect multiple cycles of diagenesis. The expectation, however, is not true here. Similarly, stable isotopic signature trends, that have been used elsewhere for locating ancient exposure surfaces (cf., Allan and Matthews, 1982, their figure 11A) are not apparent in the Ironshore Formation. Thus, it has proven impossible to link specific diagenetic features to the unconformities that define the upper boundary of each depositional unit. Similar problems have also been documented for the Pleistocene carbonate successions found on mid-oceanic atolls (e.g., Quinn, 1991; Braithwaite and Camoin, 2011), uplifted coral-reef terraces (e.g., Matthews and Frohlich, 1987), and along continental coasts (e.g., Braithwaite and Montaggioni, 2009). From these examples and Grand Cayman, it is apparent that the correlation between diagenetic profiles and specific unconformities is difficult to ascertain for the following reasons.

- The accurate timing and the amplitude of the sea level lowstand after each

cycle of sediment deposition are, in general, poorly constrained. Most studies focused on the timing and height of sea level during interglacial periods and various sea level curves are estimated (Siddall et al., 2007).

- The diagenetic features in a particular unit may not record every cycles of sea level change. In the case of the Ironshore Formation, for example, there are six unconformities that each reflect a period of subaerial exposure. There is, however, scant evidence of multigenerational cements in the limestones of this formation. This is also true for the cement sequences found in Pleistocene carbonate successions on Moruroa (Braithwaite and Camoin, 2011) and the Great Barrier Reef (Braithwaite and Montaggioni, 2009).
- It is generally impossible to determine precise ages for the diagenetic events found throughout the succession.

7. Conclusions

Detailed assessment of the diagenetic signatures found in units A to F in the Pleistocene Ironshore Formation on Grand Cayman has produced the following important conclusions.

- The corals and matrices underwent similar diagenetic processes and display similar diagenetic features.
- In general, the corals underwent less diagenetic alteration than their surrounding matrices. This can probably be attributed to the higher permeabilities in the matrices that allowed greater volumes of water to flow through them.
- From a depositional perspective, the Ironshore Formation is divided into six units (A to F). From a diagenetic perspective, however, the succession can be divided into three packages that are formed of Units A to C, Unit D,

and Units E and F.

- Maximum diagenesis took place during the lowstands that followed the deposition of units C and D. These two periods of maximum diagenesis can be attributed to lowstand conditions that existed for long periods of time during which the climate was wet with high annual rainfalls.
- Although the Ironshore Formation developed through repeated lowstand-highstand cycles, the diagenetic fabrics found in individual limestone samples do not reflect all of those cycles. Indeed, it is generally impossible to link specific diagenetic features evident in the Ironshore Formation with the unconformities that denote specific lowstands.

The Ironshore Formation on Grand Cayman, like Pleistocene carbonate successions on other islands, records complex diagenetic features that formed in response to the Pleistocene sea level change history. The heterogeneous diagenetic patterns evident in the Ironshore Foramtion reflect the complex interplay between many different intrinsic and extrinsic factors.

References

Acker, K.L., Risk, M.J., 1985. Substrate destruction and sediment production by the boring sponge Cliona caribbaea on Grand Cayman Island. Journal of Sedimentary Petrology 55, 705-711.

Aissaoui, D.M., Buigues, D., Purser, B.H., 1986. Model of reef diagenesis: Mururoa Atoll, French Polynesia. In: Schroeder, J.H., Purser, B.H. (Eds.), Reef Diagenesis. Springer Verlag, Berlin, pp. 27-52.

Allan, J.R., Matthews, R.K., 1977. Carbon and oxygen isotopes as diagenetic and stratigraphic tools: surface and subsurface data, Barbados, West Indies. Geology 5, 16-20.

Allan, J.R., Matthews, R.K., 1982. Isotope signatures associated with early meteoric diagenesis. Sedimentology 29, 797-817.

Blackmon, P.D., Todd, R., 1959. Mineralogy of some foraminifera as related to their classification and ecology. Journal of Paleontology 33, 1-15.

Bonatti, E., Gartner, S., 1973. Caribbean climate during Pleistocene Ice Ages. Nature 244, 563-565.

Braithwaite, C.J.R., Camoin, G.F., 2011. Diagenesis and sea-level change: lessons from Moruroa, French Polynesia. Sedimentology 58, 259-284.

Braithwaite, C.J.R., Montaggioni, L.F., 2009. The Great Barrier Reef: a 700,000 year diagenetic history. Sedimentology 56, 1591-1622.

Brand, U., 1989. Aragonite-calcite transformation based on Pennsylvanian molluscs. Geological Society of America Bulletin 101, 377-390.

Brunt, M.A., Giglioli, M.E.C., Mather, J.D., Piper, D.J.W., Richards, H.G., 1973. The Pleistocene rocks of the Cayman Islands. Geological Magazine 110, 209-304.

Buchbinder, L.G., Friedman, G.M., 1980. Vadose, phreatic, and marine diagenesis of Pleistocene-Holocene carbonates in a borehole: Mediterranean coast of

Israel. Journal of Sedimentary Petrology 50, 395-408.

Budd, D.A., 1988. Petrographic products of freshwater diagenesis in Holocene ooid sands, Schooner Cays, Bahamas. Carbonates and Evaporites 3, 143-163.

Chafetz, H.S., Rush, P.F., 1994. Diagenetically altered sabkha-type Pleistocene dolomite from the Arabian Gulf. Sedimentology 41, 409-421.

Constantz, B.R., 1986. The primary surface area of corals and variations in their susceptibility to diagenesis. In: Schroeder, J.H., Purser, B.H. (Eds.), Reef Diagenesis. Springer Verlag, Berlin, pp. 53-76.

Coyne, M.K., 2003. Transgressive-regressive cycles in the Ironshore Formation, Grand Cayman, British West Indies. Unpublished M. Sc. Thesis, University of Alberta, Edmonton, Canada, 98 pp.

Coyne, M.K., Jones, B., Ford, D., 2007. Highstands during Marine Isotope Stage 5: evidence from the Ironshore Formation of Grand Cayman, British West Indies. Quaternary Science Reviews 26, 536-559.

Crickmay, G.W., 1945. Petrography of limestones. In: Ladd, H.S., Hoffmeister, J.E. (Eds.), Geology of Lau, Fiji. Bernice P. Bishop Museum, pp. 211-250.

Emery, K.O., Tracey, J.I., Jr., Ladd, H.S., 1954. Geology of Bikini and Nearby Atolls. Geological Survey Professional Paper 260-A, 1-265.

Fairbanks, R.G., Dodge, R.E., 1979. Annual periodicity of the $^{18}O/^{16}O$ and $^{13}C/^{12}C$ ratios in the coral Montastrea annularis. Geochimica et Cosmochimica Acta 43, 1009-1020.

Fairbanks, R.G., Matthews, R.K., 1978. Marine oxygen isotope record in Pleistocene coral, Barbados, West Indies. Quaternary Research 10, 181-196.

Friedman, G.M., 1964. Early diagenesis and lithification in carbonate sediments. Journal of Sedimentary Petrology 34, 777-813.

Gavish, E., Friedman, G.M., 1969. Progressive diagenesis in Quaternary to Late Tertiary carbonate sediments: sequence and time scale. Journal of Sedimenta-

ry Petrology 39, 980-1006.

Gischler, E., Swart, P.K., Lomando, A.J., 2009. Stable isotopes of carbon and oxygen in modern sediments of carbonate platforms, barrier reefs, atolls and ramps: patterns and implications. In: Swart, P.K., Eberli, G.P., McKenzie, J.A. (Eds.), Perspectives in Carbonate Geology: A Tribute to the Career of Robert Nathan Ginsburg. International Association of Sedimentologists Special Publication, pp. 61-74.

Gross, M.G., 1961. Carbonate sedimentation and diagenesis of Pleistocene limestones in the Bermuda Islands. Unpublished Ph. D. Thesis, California Institute of Technology, Pasadena, USA, 242 pp.

Grossman, E.L., Ku, T.L., 1986. Oxygen and carbon isotope fractionation in biogenic aragonite: temperature effects. Chemical Geology 59, 59-74.

Halley, R.B., Harris, P.M., 1979. Fresh-water cementation of a 1,000-year-old oolite. Journal of Sedimentary Petrology 49, 969-988.

Harris, W.H., Matthews, R.K., 1968. Subaerial diagenesis of carbonate sediments: efficiency of the solution-reprecipitation process. Science 160, 77-79.

Holail, H., 1999. The isotopic composition and diagenetic history of Pleistocene carbonates, North Qatar. Carbonates and Evaporites 14, 41-55.

Hughes, P.D., Woodward, J.C., Gibbard, P.L., 2007. Middle Pleistocene cold stage climates in the Mediterranean: new evidence from the glacial record. Earth and Planetary Science Letters 253, 50-56.

Hunter, I.G., Jones, B., 1996. Coral associations of the Pleistocene Ironshore Formation, Grand Cayman. Coral Reefs 15, 249-267.

James, N.P., 1974. Diagenesis of scleractinian corals in the subaerial vadose environment. Journal of Paleontology 48, 785-799.

James, N.P., Ginsburg, R.N., 1979. The seaward margin of Belize barrier and atoll reefs. International Association of Sedimentologists Special Publication 3,

Blackwell Scientific Publications, Oxford, London, Edinburgh, Melbourne, 191 pp.

Jones, B., 1994. Geology of the Cayman Islands. In: Brunt, M.A., Davies, J.E. (Eds.), The Cayman Islands: Natural History and Biogeography. Kluwer Academic Publishers, The Netherlands, pp. 13-49.

Jones, B., Goodbody, Q.H., 1984. Biological factors in the formation of quiet water ooids. Bulletin of Canadian Petroleum Geology 32, 190-200.

Jones, B., Hunter, I.G., 1990. Pleistocene paleogeography and sea levels on the Cayman Islands, British West Indies. Coral Reefs 9, 81-91.

Jones, B., Pemberton, S.G., 1988. Lithophaga borings and their influence on the diagenesis of corals in the Pleistocene Ironshore Formation of Grand Cayman Island, British West Indies. Palaios 3, 3-21.

Jones, B., Pemberton, S.G., 1989. Sedimentology and ichnology of a Pleistocene unconformity-bounded, shallowing-upward carbonate sequence: the Ironshore Formation, Salt Creek, Grand Cayman. Palaios 4, 343-355.

Jones, B., Squair, C.A., 1989. Formation of peloids in plant rootlets, Grand Cayman, British West Indies. Journal of Sedimentary Petrology 59, 1002-1007.

Jones, B., Hunter, I.G., Kyser, K., 1994. Revised stratigraphic nomenclature for Tertiary strata of the Cayman Islands, British West Indies. Caribbean Journal of Science 30, 53-68.

Jones, B., Ng, K.C., Hunter, I.G., 1997. Geology and hydrogeology of the Cayman Islands. In: Vacher, H.L., Quinn, T. (Eds.), Geology and Hydrogeology of Carbonate Islands. Elsevier, pp. 299-325.

Land, L.S., 1967. Diagenesis of skeletal carbonates. Journal of Sedimentary Petrology 37, 914-930.

Land, L.S., 1989. The carbon and oxygen isotope chemistry of surficial Holocene shallow marine carbonate sediment and Quaternary limestone and dolomite.

In: Fritz, P., Fontes, J.C. (Eds.), Handbook of Environmental Isotope GeoIn: Fritz, P., Fontes, J.C. (Eds.), Handbook of Environmental Isotope Geochemistry. Elsevier, pp. 191-217.

Leder, J.J., Swart, P.K., Szmant, A.M., Dodge, R.E., 1996. The origin of variations in the isotopic record of scleractinian corals: I. Oxygen. Geochimica et Cosmochimica Acta 60, 2857-2870.

Li, R., Jones, B., 2013. Temporal and spatial variations in the diagenetic fabrics and stable isotopes of Pleistocene corals from the Ironshore Formation of Grand Cayman, British West Indies. Sedimentary Geology 286-287, 58-72.

McCrea, J.M., 1950. On the isotopic chemistry of carbonates and a paleotemperature scale. The Journal of Chemical Physics 18, 849-857.

Matley, C.A., 1926. The geology of the Cayman Islands (British West Indies), and their relation to the Bartlette Trough. Quarterly Journal of the Geological Society 82, 352-387.

Matthews, R.K., 1967. Diagenetic fabrics in biosparites from the Pleistocene of Barbados, West Indies. Journal of Sedimentary Petrology 37, 1147-1153.

Matthews, R.K., 1968. Carbonate diagenesis: equilibration of sedimentary mineralogy to the subaerial environment; coral cap of Barbados, West Indies. Journal of Sedimentary Petrology 38, 1110-1119.

Matthews, R.K., Frohlich, C., 1987. Forward modeling of bank-margin carbonate diagenesis. Geology 15, 673-676.

Ng, K.C., Jones, B., Beswick, R., 1992. Hydrogeology of Grand Cayman, British West Indies: a karstic dolostone aquifer. Journal of Hydrology 134, 273-295.

Osipova, E., Danukalova, G., Marković, S., 2013. Malacological characteristics of the Middle to Upper Pleistocene transitional interval (MIS 7-5) observed in the Batajnica locality (Serbia). Quaternary International 292, 86-100.

Perrin, C., 2011. Diagenesis. In: Hopley, D. (Ed.), Enclyclopedia of Modern Coral

Reefs: Structure, Form and Process. Springer, pp. 309-321.

Pingitore, N.E., 1976. Vadose and phreatic diagenesis: processes, products and their recognition in corals. Journal of Sedimentary Petrology 46, 985-1006.

Pruss, S.B., Clemente, H., 2011. Assessing the role of skeletons in Early Paleozoic carbonate production: insights from Cambro-Ordovician strata, Western Newfoundland. In: Laflamme, M., Schiffbauer, J.D., Dornbos, S.Q. (Eds.), Quantifying the Evolution of Early Life, pp. 161-183.

Quinn, T.M., 1991. Meteoric diagenesis of Plio-Pleistocene limestones at Enewetak Atoll. Journal of Sedimentary Petrology 61, 681-703.

Rehman, J., 1992. Diagenetic alteration of Strombus gigas, Siderastrea siderea, and Montastrea annularis from the Pleistocene Ironshore Formation of Grand Cayman. Unpublished M. Sc. Thesis, University of Alberta, Edmonton, Canada, 136 pp.

Rehman, J., Jones, B., Hagan, T.H., Coniglio, M., 1994. The influence of sponge borings on aragonite-to-calcite inversion in Late Pleistocene Strombus gigas from Grand Cayman, British West Indies. Journal of Sedimentary Research 64, 174-179.

Saller, A.H., Moore, C.H., 1989. Meteoric diagenesis, marine diagenesis, and microporosity in Pleistocene and Oligocene limestones, Enewetak Atoll, Marshall Islands. Sedimentary Geology 63, 253-272.

Sandberg, P.A., 1983. An oscillating trend in Phanerozoic non-skeletal carbonate mineralogy. Nature 305, 19-22.

Sayani, H.R., Cobb, K.M., Cohen, A.L., Elliott, W.C., Nurhati, I.S., Dunbar, R.B., Rose, K.A., Zaunbrecher, L.K., 2011. Effects of diagenesis on paleoclimate reconstructions from modern and young fossil corals. Geochimica et Cosmochimica Acta 75, 6361-6373.

Scholle, P.A., Ulmer-Scholle, D.S., 2003. A color guide to the petrography of car-

bonate rocks: grains, textures, porosity, diagenesis. The American Association of Petroleum Geologists Memoir 77, Tulsa, Oklahoma, 459 pp.

Schroeder, J.H., 1973. Submarine and vadose cements in Pleistocene Bermuda reef rock. Sedimentary Geology 10, 179-204

Schroeder, J.H., 1986. Diagenetic diversity in Paleocene coral knobs from the Bir Abu El-Husein area, S Egypt. In: Schroeder, J.H., Purser, B.H. (Eds.), Reef Diagenesis. Springer Verlag, Berlin, pp. 132-158.

Shourie, A., 1993. Depositional architecture of the Late Pleistocene Ironshore Formation, Grand Cayman, British West Indies. Unpublished M. Sc. Thesis, University of Alberta, Edmonton, Canada, 100 pp.

Siddall, M., Chappell, J., Potter, E.-K., 2007. Eustatic sea level during past interglacials. Developments in Quaternary Science 7, 75-92.

Smith, J.M., 2006. Geochemical signatures in the coral Montastraea: modern and mid-Holocene perspectives. Unpublished Ph. D. Thesis, University of South Florida, Tampa, USA, 125 pp.

Steinen, R.P., Matthews, R.K., 1973. Phreatic vs. vadose diagenesis: stratigraphy and mineralogy of a cored borehole on Barbados, W. I. Journal of Sedimentary Petrology 43, 1012-1020.

Swart, P.K., Leder, J.J., Szmant, A.M., Dodge, R.E., 1996. The origin of variations in the isotopic record of scleractinian corals: II. Carbon. Geochimica et Cosmochimica Acta 60, 2871-2885.

Vézina, J.L., 1997. Stratigraphy and sedimentology of the Pleistocene Ironshore Formation at Rogers Wreck Point, Grand Cayman: a 400 ka record of sea-level highstands. Unpublished M. Sc. Thesis, University of Alberta, Edmonton, Canada, 131 pp.

Vézina, J.L., Jones, B., Ford, D., 1999. Sea level highstands over the last 500,000 years: evidence from the Ironshore Formation on Grand Cayman, British West

Indies. Journal of Sedimentary Research 69, 317-327.

Vollbrecht, R., Meischner, D., 1996. Diagenesis in coastal carbonates related to Pleistocene sea level, Bermuda platform. Journal of Sedimentary Research 66, 243-258.

Walter, L.M., Morse, J.W., 1984. Reactive surface area of skeletal carbonates during dissolution: effect of grain size. Journal of Sedimentary Petrology 54, 1081-1090.

Weber, J.N., Woodhead, P.M.J., 1970. Carbon and oxygen isotope fractionation in the skeletal carbonate of reef-building corals. Chemical Geology 6, 93-117.

Whitaker, F., Smart, P., Hague, Y., Waltham, D., Bosence, D., 1997. Coupled two-dimensional diagenetic and sedimentological modeling of carbonate platform evolution. Geology 25, 175-178.

Woodroffe, C.D., Stoddart, D.R., Giglioli, M.E.C., 1980. Pleistocene patch reefs and Holocene swamp morphology, Grand Cayman Island, West Indies. Journal of Biogeography 7, 103-113.

CHAPTER 3: TEMPORAL AND SPATIAL VARIATIONS IN THE DIAGENETIC FABRICS AND STABLE ISOTOPES OF PLEISTOCENE CORALS FROM THE IRONSHORE FORMATION OF GRAND CAYMAN, BRITISH WEST INDIES[1]

1. Introduction

Corals found in Pleistocene to Holocene successions have been used to (1) decipher original depositional environments (e.g., Lighty et al., 1982), (2) extrapolate past sea levels by combining the elevation of in situ specimens with ages determined by radiogenic isotopes (e.g., Bard et al., 1996; Anderson et al., 2010), and (3) delineate changes in ocean conditions by interpreting various geochemical proxies obtained from their skeletons (e.g., Fallon et al., 2003; McGregor and Gagan, 2003). Freshwater diagenesis can, however, lead to calcitization of their skeletons and radically alter the geochemical proxies (e.g., Dullo, 1986; Bar-Matthews et al., 1993; Lazar et al., 2004; Rabier et al., 2008). Attempts to unravel the diagenetic processes that have affected these corals have commonly been based on the physical changes to their aragonitic skeletons (Pingitore, 1970, 1976; Spiro, 1971; James, 1974; Gvirtzman and Friedman, 1977; Buchbinder, 1977; Schroeder, 1984; Aissaoui and Purser, 1985; Constantz, 1986; Dullo, 1987; Ribaud-Laurenti et al., 2001; Perrin, 2003; Nothdurft, 2007; McGregor and Abram, 2008; Rabier et al., 2008; Nothdurft and Webb, 2009) and/or geochemical proxies derived from the skeletal aragonite and the calcite that has replaced it (Pingitore, 1976; Scherer and Seitz, 1980; Cross and Cross, 1983;

1 This chapter was published as: Li, R., Jones, B., 2013. Temporal and spatial variations in the diagenetic fabrics and stable isotopes of Pleistocene corals from the Ironshore Formation of Grand Cayman, British West Indies. Sedimentary Geology 286-287, 58-72.

Pingitore and Eastman, 1985; Pingitore et al., 1989; Bar-Matthews et al., 1993; McGregor and Gagan, 2003; Webb et al., 2009). Explaining these diagenetic signals, however, is difficult because they reflect the interplay between many signals, however, is difficult because they reflect the interplay between many different intrinsic (e.g., skeletal architecture of the corals, primary porosity of coral) and extrinsic (e.g., climate, sea level, depositional facies) factors (James, 1974; Buchbinder, 1977; Schroeder, 1984; Dullo, 1986, 1987; Constantz, 1986).

On Grand Cayman, the Ironshore Formation (Middle to Late Pleistocene) is divided into units A to F (Vézina, 1997; Vézina et al., 1999; Coyne, 2003; Coyne et al., 2007). This succession is ideal for the study of coral diagenesis because (1) it contains numerous corals, (2) the corals in the different units display different degrees of diagenetic alteration, (3) the ages of units A to F are known, and (4) the Ironshore Formation has not been dolomitized. For this study, attention was focused mainly on *Montastrea annularis* and *Acropora palmata* because they are the most common corals found in the cores obtained from wells drilled in the Rogers Wreck Point area and offshore George Town (Fig. 3-1). This study examines the temporal and spatial variance in the diagenesis of these corals by documenting the stratigraphic and geographic variance in coral diagenesis evident from the diagenetic fabrics in the corals and their stable oxygen and carbon signatures. These results are used to assess the roles that the intrinsic factors, extrinsic factors, and sea-level oscillations played in the diagenetic evolution of the corals.

2. Geological setting

Grand Cayman, located south of Cuba and northwest of Jamaica, is about 35 km long and 6-14 km wide with most of the island being less than 3 m above sea level (Fig. 3-1A). There, Pleistocene limestones belonging to the Ironshore

Formation unconformably overlie the Tertiary limestones and dolostones of the Bluff Group (Matley, 1926; Jones, 1994) (Fig. 3-1B).

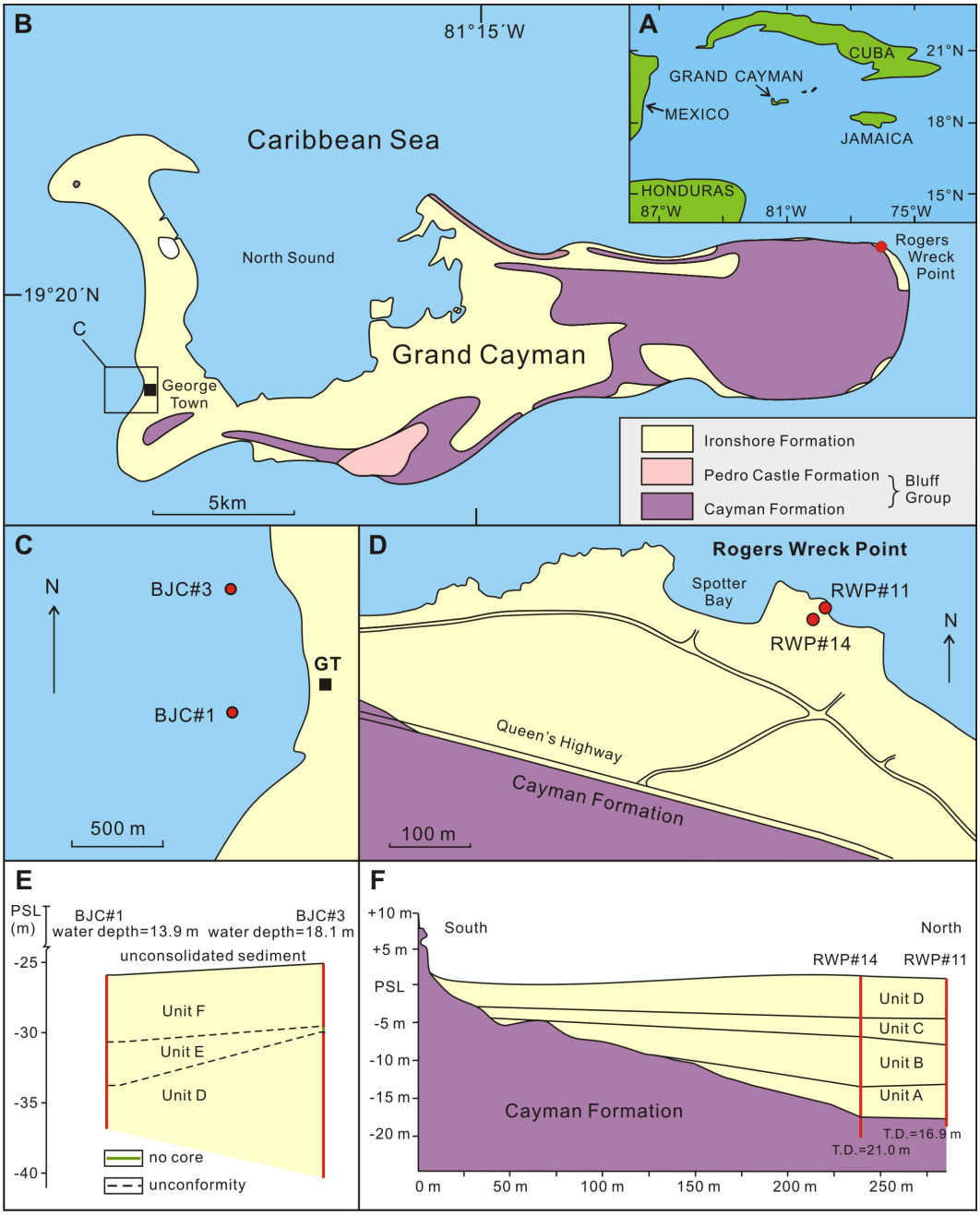

Fig. 3-1. (A) Location of Grand Cayman. (B) Geological map of Grand Cayman (modified from Jones, 1994) showing locations of George Town and Rogers Wreck Point. (C) Location of cores through Ironshore Formation offshore from George Town (GT) (modified from Coyne, 2003; Coyne et al., 2007). (D) Location of cores RWP#11 and RWP#14 in Rogers Wreck Point area (modified from Vézina, 1997; Vézina et al., 1999). (E) Correlation of

units D, E, and F between BJC#1 and BJC#3 from offshore George Town (modified from Coyne, 2003). (F) Correlation of units A, B, C, and D in the Ironshore Formation in cores RWP#11 and RWP#14 (modified from Vézina, 1997).

The Ironshore Formation in the Rogers Wreck Point area and offshore from George Town is up to 19 m thick (Fig. 3-1C-F). Units A to F are delineated by their lithologies, biota, and the unconformities that are commonly highlighted by calcrete crusts (Fig. 3-2A). U/Th radiometric dating of each unit allows

A

Age (ka)	Unit	Lithology	Biota	Sea level elevation (m)
84	F	Cross-bedded ooid grainstones; coral floatstone; *Halimeda* floatstone	Head corals, branching corals, *Halimeda*	+3.0 to +5.0
104	E	Coral floatstones	Head corals	+2.0 to +5.0
131	D	Grainstones	Head corals, branching corals	+2.5 to +6.0
229	C	Rudstones, packstones, grainstones,bafflestone	Head corals, branching corals	-2.5 to +1.0
346	B	Packstones, grainstones, minor wackstones	Head corals, branching corals	-3.0 to +0.5
>400	A	Grainstones	Head corals, branching corals	-9.0 to -5.5

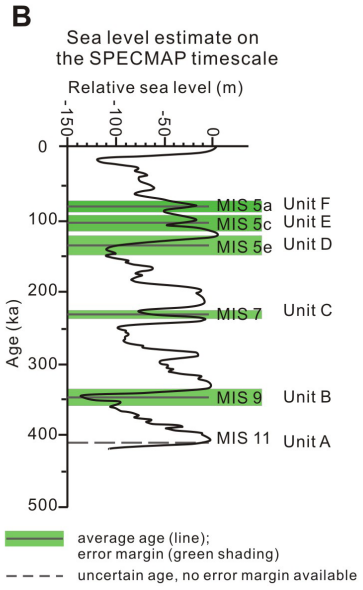

Fig. 3-2. (A) Internal stratigraphy of Ironshore Formation. Ages and sea-levels (relative to modern sea level) from Vézina et al. (1999) and Coyne et al. (2007). (B) Positions of units A to F in Ironshore Formation relative to sea level curve of Siddall et al (2007).

correlation with the highstands that led to their development (Vézina et al., 1999; Coyne et al., 2007). Units A (>400 ka), B (~ 346 ka), C (226-232 ka), D (121-147 ka), E (95-110 ka), and F (74-87 ka) correlate with Marine Isotope Stages (MIS) 11, 9, 7, 5e, 5c, and 5a, respectively (Vézina, 1997; Vézina et al., 1999; Coyne, 2003; Coyne et al., 2007) (Fig. 3-2B). Facies in the Ironshore Formation represent many different shallow-water depositional settings (Brunt et al., 1973;

Rigby and Roberts, 1976; Woodroffe et al., 1980; Jones and Pemberton, 1989; Jones and Hunter, 1990; Vézina, 1997; Vézina et al., 1999; Coyne, 2003; Coyne et al., 2007). Corals are common with *Montastrea annularis*, *M. cavernosa*, *Acropora palmata*, *A. cervicornis*, and *Porites porites* being the most numerous (Hunter, 1994; Hunter and Jones, 1996). Although most corals are still formed of aragonite, many have been replaced, to varying degrees, by calcite (Rehman, 1992).

3. Methods

Cores BJC#1 and BJC#3 (6 cm diameter) from offshore George Town (Fig. 3-1C) and cores RWP#11 and RWP#14 (3.5 cm diameter) from the Rogers Wreck Point area (Fig. 3-1D) were used in this study because core recovery was good and they collectively include Units A to F (Vézina, 1997; Vézina et al., 1999; Coyne, 2003; Coyne et al., 2007). The tops of cores BJC#1 (10.8 m long) and BJC#3 (15.2 m long) are 26.6 m and 25.8 m below present sea level (bsl), respectively, whereas the tops of cores RWP#11 (16.9 m long) and RWP#14 (21.0 m long) are 0.5 m and 1 m above present sea level (asl), respectively (Fig. 3-1E, 3-1F). By using all of the corals found in these cores, this study is based on 99 samples of *Montastrea* (94 of *M. annularis*, 5 of *M. cavernosa*) and 44 of *Acropora* (41 of *A. palmata*, 3 of *A. cervicornis*).

The percentage of calcite in each coral sample was determined by X-ray diffraction (XRD) analysis. Each powder sample, weighing ~1 g, obtained from each coral using a Dremel drill, was analyzed on a Rigaku Ultima IV Powder XRD system that was run at 38 kV and 38 mA using an Ultima IV X-ray generator with a Co tube. All scans were run from 5° to 90° 2θ at a speed of 2°θ/min. The aragonite and calcite weight percentages were calculated from the intensities of the d_{110}, d_{021}, and d_{104} peaks using an aragonite-calcite calibration

curve that had been derived from the analyses of artificial samples with known calcite:aragonite ratios. The values obtained using this method are accurate at ±2 wt%.

The presence of aragonite cement, secondary calcite (cement and inverted aragonite), and dissolution of the coral samples were established from thin sections that were made from the coral as close as possible to where the XRD sample had been obtained. All samples were impregnated with blue epoxy in order to highlight the porosity. Images of thin sections were captured using a Polaroid DMC digital camera mounted on a Leica petrographic microscope.

The skeletal microarchitecture and diagenetic fabrics of the corals were determined by examination on a JEOL 6301FE scanning electron microscope (SEM). For this purpose, small fractured samples of the aragonitic (aragonite wt% >85%) and calcitic (calcite wt% >85%) corals were obtained from the same corals that had been used for XRD and thin section analyses. These samples were mounted on SEM stubs using double sided tape and conductive glue and sputter coated with gold before being examined on the SEM using an accelerating voltage of 5 kV.

Oxygen and carbon isotope ratios were determined for 45 samples that contained >85% aragonite and 19 samples that contained >85% calcite. For these analyses, 10-18 mg of powder samples were dissolved in H_3PO_4 at 25°C in a constant temperature water bath for 60 minutes following the protocol outlined by McCrea (1950). The evolved gases were analyzed on a Finnigan MAT 251 mass spectrometer. The isotope values are calibrated relative to the Vienna Peedee Belemnite using the NBS 19 ($\delta^{18}O$ = -2.20‰, $\delta^{13}C$ = +1.95‰) and NBS 18 ($\delta^{18}O$ = -23.00‰, $\delta^{13}C$ = -5.00‰) standards. The accuracy is better than 0.2‰ for $\delta^{13}C$, and better than 0.6‰ for $\delta^{18}O$.

4. Results

4.1. Mineralogy

M. annularis and *A. palmata*, which came from all units in the Ironshore Formation, have been calcified to different degrees. Based on the samples used in this study, 38.3% of all the *M. annularis* and 65.9% of all the *A. palmata* retained their aragonite skeletons. Although there are distinct stratigraphic trends in the degree of calcification of the corals, those trends are not consistent from genus to genus. The percentage of aragonitic *M. annularis* varies from 11-16% in Units A and B, to 50-70% in Units C and D, to 100% in Units E and F (Table 3-1). For *A. palmata* from Units A to F, the percentages with aragonitic skeletons are 43%, 100%, 92%, 70%, 67%, and 67%, respectively. *M. annularis* from Units A to C have been extensively calcified whereas those from Units E and F are still formed of aragonite. For *A. palmata*, however, there is no obvious correlation between the degree of calcification and stratigraphic position (Table 3-1).

Table 3-1. Average percentage of aragonitic (aragonite wt% >85%) Montastrea annularis and Acropora palmata in each unit of the Ironshore Formation. Unit ages are based on U-Th dating, from Vézina (1997) and Coyne (2003). n = total sample size.

Unit	Age (ka)	*Montastrea annularis*		*Acropora palmata*	
		offshore	RWP	offshore	RWP
F	80-73	100% (n=2)	-	66.7% (n=6)	-
E	109-103	100% (n=8)	-	66.7% (n=3)	-
D	133-120	87.5% (n=8)	39.3% (n=28)	66.7% (n=8)	50.0% (n=2)
C	232-226	-	50.0% (n=2)	-	91.7% (n=12)
B	346	-	11.1% (n=27)	-	100% (n=3)
A	>400	-	15.8% (n=19)	-	42.9% (n=7)

The degree of coral calcification varies from location to location. In Unit D, for example, 39.3% of *M. annularis* from Rogers Wreck Point are aragonitic,

whereas 87.5% remain aragonitic in the offshore George Town cores (Table 3-1). The geographic variation in the calcification of *M. annularis* in Unit D is larger than the stratigraphic variation found between units A to D in the Rogers Wreck Point area. In the cores from offshore George Town, *A. palmata* is more calcified than the *M. annularis,* whereas the opposite is true in the Rogers Wreck Point area (Table 3-1).

The degree of calcification can vary in a single coral head. In core BJC#1, the aragonite content of four samples from a single *M. annularis* head (about 1 m high) in Unit E varied from 91 to 100%. In contrast, the aragonite content of five samples from a single head of *M. cavernosa* from Unit D (BJC#1) varied from 72 to 96%. Critically, the variation in this single *M. cavernosa* is (1) slightly higher than the variation in calcification for all *M. annularis* sampled from Unit D (20% in BJC#3), and (2) is larger than the stratigraphic variation in the degree of calcification for *M. annularis* from the offshore George Town cores.

4.2. Diagenesis

The progressive changes in diagenetic textures are correlated with the degree of calcification of the coral skeleton. This assessment, however, must be treated with caution because thin section analyses show that some *Montastrea* formed of 100% aragonite as determined by XRD, contains secondary aragonite, internal sediments, evidence of dissolution, and some calcite cement. The discrepancies between the XRD and thin section analyses can be attributed to (1) the two samples, although close together, cannot be from precisely the same spot in the coral skeleton, (2) the difference in sizes of the XRD samples (~1 g) and the thin section (3 x 2 cm), (3) dissolution (e.g., loss of skeleton) that cannot be shown by XRD analysis, and/or (4) detection limits associated with the XRD whereby <1 wt% calcite cannot be detected. Thus, assessment of the diagenetic

fabrics of coral skeletons, as noted by McGregor and Abram (2008), must be based on a combination of XRD, thin section, and SEM analyses.

4.2.1. Montastrea

Modern *Montastrea* are characterized by pristine aragonitic skeletons that do not contain internal sediments, aragonite cement, or calcite cement (cf., Gischler and Storz, 2009). Well-preserved *Montastrea* from the Ironshore Formation have aragonitic skeletons with well-preserved synapticula, dissepiments, trabeculae and porous centers of calcification but no evidence of calcification, borings, or internal sediments (Fig. 3-3A-C). Nevertheless, minor amounts of aragonite cement are present in some of the primary pores and/or coating the septa.

With less than 10% calcite, evidence of diagenesis includes acicular aragonite cement (Fig. 3-3D), an aragonite skeleton partly replaced by calcite (Fig. 3-3E), calcite cement lining some skeletal voids (Fig. 3-3E), internal sediments, and borings that can be filled with micrite (Fig. 3-3F).

With 50 to 70% calcite, the general skeletal morphology is still evident even though it has been largely calcified (Fig. 3-3G, 3-3H). In some corals, there is evidence of microbial infestations with many filaments being calcified and partially encased by later calcite cements (Fig. 3-3I).

With 90 to 100% calcite, the aragonite skeletons have been almost completely transformed to calcite (Fig. 3-3J). Framework voids are partly or entirely filled by calcite cements (Fig. 3-3J, 3-3K) and/or micrite and geopetal fabrics are evident in some cavities (Fig. 3-3L).

4.2.2. Acropora

Acropora with 100% aragonite are characterized by well-preserved porous coenosteum (Fig. 3-4A) even though the internal structures of the radial

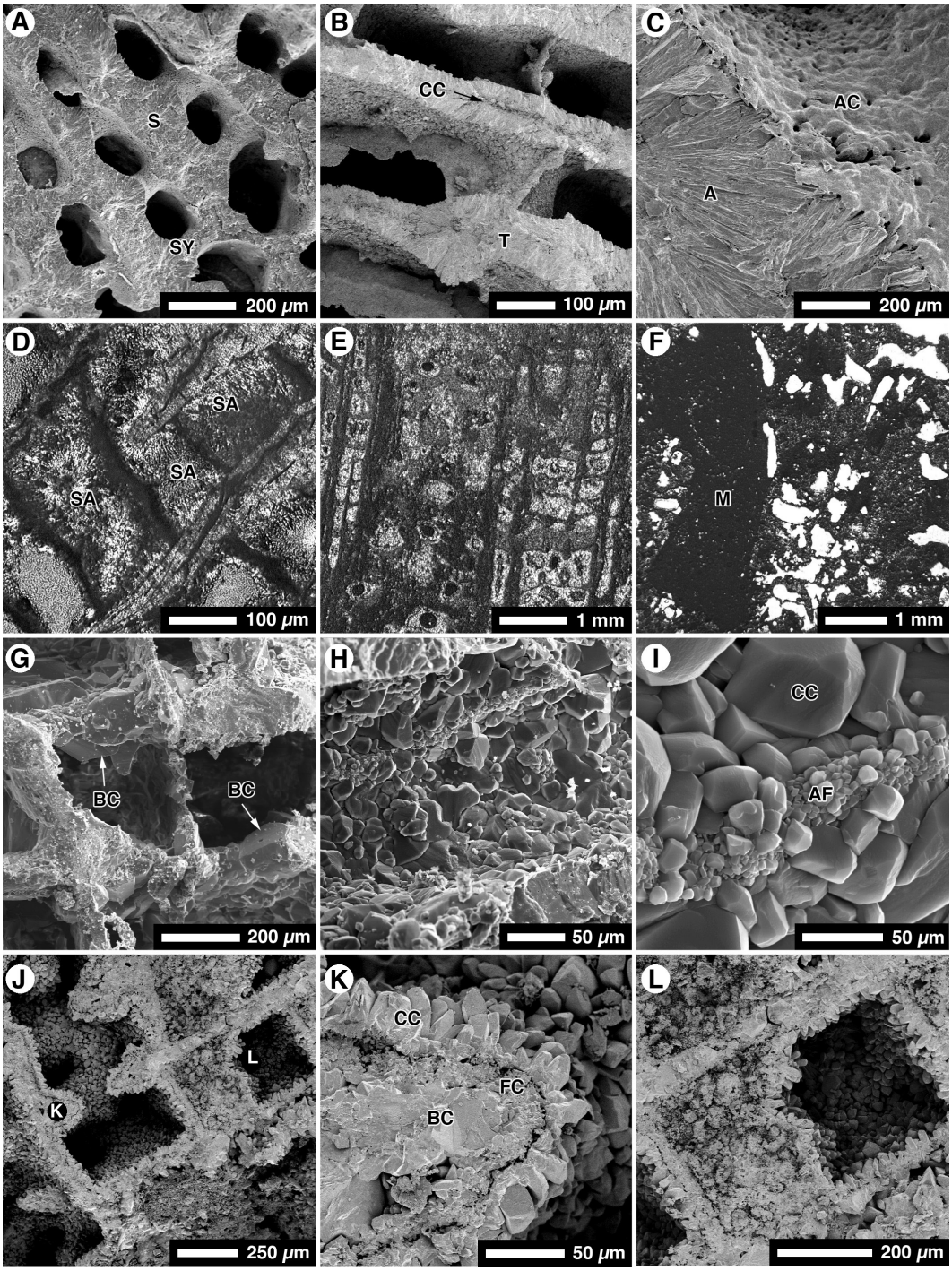

Fig. 3-3. SEM (A-C, G-L) and thin section (D-F) photomicrographs of Montastrea with 100% aragonite (A-C), 63% calcite (G-I), and 90-100% calcite from Ironshore Formation. (A) Montastrea with well preserved septa (S) and synapticula (SY). BJC#1, Unit F, 14.4 m. (B) Trabecula (T) showing center of calcification (CC). BJC#1, Unit F, 14.4 m. (C) Aragonite cement (AC) coating surface of aragonitic septa (A). BJC#1, Unit F, 14.4 m. (D)

Montastrea, 94% aragonite, with skeletal voids partly filled by acicular secondary aragonite (SA). BJC#3, Unit F, 10.2 m. (E) Montastrea, 94% aragonite, with skeletal voids rimmed and/or filled by blocky calcite cement. RWP#14, Unit A, 18.0 m. (F) Montastrea, 93% aragonite, with boring filled by micritic sediments (M). RWP#11, Unit D, 1.9 m. (G) Skeleton with blocky calcite (BC). RWP#11, Unit D, 5.2 m. (H) Skeletal voids with calcite cements. RWP#11, Unit D, 5.2 m. (I) Algae filament (AF) encased by calcite cements (CC). RWP#11, Unit D, 5.2 m. (J) Skeletal voids lined with calcite cement (CC). White K and L indicate positions of panels K and L, respectively. RWP#11, Unit A, 15.6 m. (K) Skeleton with coarser blocky calcite (BC) in the center and finer calcite (FC) in the rim overlain by calcite cement (CC). RWP#11, Unit A, 15.6 m. (L) Geopetal fabric and calcite cement in skeletal void. RWP#11, Unit A, 15.6 m.

corallites are generally destroyed and surfaces of the corallite tubes are typically coated with aragonite cements (Fig. 3-4B, 3-4C). Scleroderimites (Fig. 3-4D)

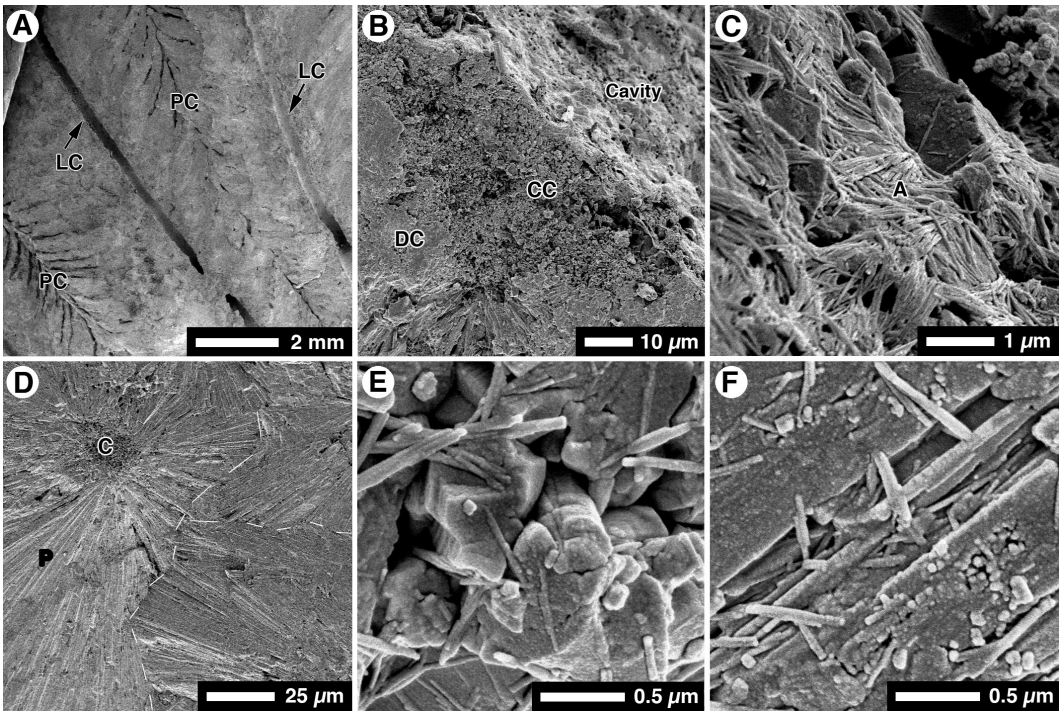

Fig. 3-4. SEM photomicrographs showing well preserved Acropora from the Ironshore Formation. BJC#1,Unit D, 22.6 m. (A) Longitudinal section of Acropora with porous coenosteum (PC) and leached corallite (LC). (B) Leached corallite, chalky coenosteum (CC), and dense coenosteum (DC). (C) Leached corallite tube with surface coated by acicular aragonite (A). (D)

Sclerodermite with porous center (C) and dense peripheral area (P) formed of aragonite fibers. (E) Porous center of sclerodermite showing amalgamation of very fine acicular aragonite into larger aragonite crystal. (F) Peripheral aragonite bundles of sclerodermite showing amalgamation of very fine acicular aragonite into dense aragonite skeleton.

located around the corallite tubes are commonly chalkified (cf., James, 1974) and transformed into loosely packed aragonite crystals (Fig. 3-4B). In tightly packed sclerodermites away from the chalkified area, fine acicular aragonite crystals, ~1 μm long, are commonly amalgamated into the aragonite fibers of sclerodermites (Fig. 3-4E, 3-4F). Organic materials partly coat the aragonite skeletons (Fig. 3-5A) and many of the primary framework pores (Fig. 3-5B) are lined with columnar aragonite (Fig. 3-5C) and euhedral calcite (Fig. 3-5D, 3-5E) cements. Microbial borings are locally common in the coenosteum (Fig. 3-5F).

In *Acropora* with 1% calcite, most of the coenosteum trabeculae have been transformed to chalky aragonite (Fig. 3-5G), dense arrays of aragonite needles rim the pore walls (Fig. 3-5H, 3-5I) and cavities are completely or partly filled with internal sediments (Fig. 3-5J) and aragonite cements.

In *Acropora* with 10-20% calcite, the centers of the coenosteums have undergone extensive dissolution (Figs. 3-5K, 3-5L, 3-6A). Many cavities are filled with various types of sediments that commonly include scalloped grains (Fig. 3-6A,3-6B), ~50 μm long, that were produced by boring sponges. The grains are cemented by calcite and acicular aragonite. Other cavity walls are rimmed with dense arrays of aragonite needles that commonly developed as syntaxial overgrowth on the skeletal aragonite crystals (Fig. 3-6C).

Acropora with 50% calcite are characterized by severely dissolved coenosteums (Fig. 3-6D) and partly filled skeletal voids. The coenosteum centers are formed of chalky aragonite and walls are rimmed by larger aragonite crystals (Fig. 3-6E, 3-6F). Aragonite cements are well developed in some primary skeletal

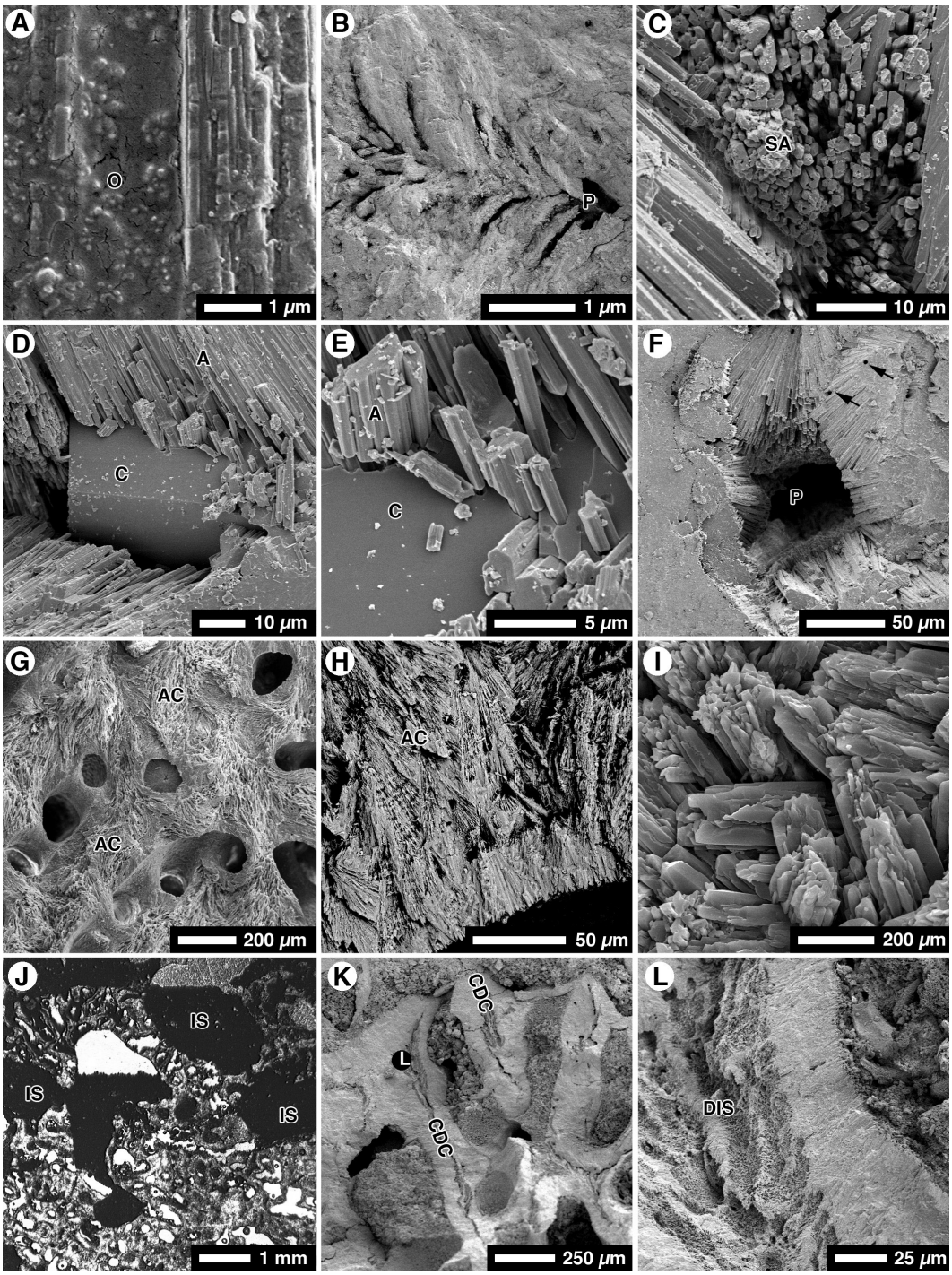

Fig. 3-5. SEM photomicrographs showing well preserved Acropora with 100% aragonite (A-F: all from BJC#1, Unit D, 22.6 m) and 1-20% calcite (G-L) from Ironshore Formation. (A) Skeleton coated by organic material (O). (B) Longitudinal section of Acropora showing framework pores (P) in coenosteum. (C) Framework pores partly filled with columnar secondary aragonite (SA). (D) Euhedral calcite (C) crystals forming cement in

framework pore between aragonite (A). (E) Calcite (C) crystal with relics of aragonite (A) crystals. (F) Framework pore (P) and coenosteum with microbial borings (arrows). (G) Acropora, 1% calcite, showing coenosteum with chalky porous aragonite center (AC). RWP#11, Unit C, 6.3 m. (H) Porous aragonite center (AC) and dense arrays of aragonite needles lining pore walls. RWP#11, Unit C, 6.3 m. (I) Dense skeleton rim with aragonite fiber bundles. RWP#11, Unit C, 6.3 m. (J) Acropora, 1% calcite, with cavities fully or partly filled by internal sediments (IS). BJC#3, Unit F, 9.7 m. (K) Acropora, 14% calcite, showing extensive dissolution of center of calcification (COC). White L indicates position of panel L. (L) Coenosteum with dissolution (DIS). BJC#1, Unit E, 17.2 m.

voids (Fig. 3-6G, 3-6H). Blocky calcite cement commonly overlies the aragonite crystals (Fig. 3-6I).

In *Acropora* with more than 90% calcite, the original coenosteum centers have been completely dissolved (Fig. 3-6J), the primary aragonite in the coenosteum walls is almost completely transformed to calcite (Fig. 3-6K) and cavities are pervasively coated by acicular aragonite cements and organic materials (Fig. 3-6K). Calcified algal filaments are common in many of the pores (Fig. 3-6L).

4.3. Geochemistry

Twenty-two samples of *A. palmata* and 42 samples of *M. annularis* formed of >85 wt% aragonite or calcite were analyzed for $\delta^{18}O$ (Table 3-2) and $\delta^{13}C$ (Table 3-3). Both *Montastrea* and *Acropora* show progressively more positive $\delta^{18}O_{VPDB}$ values from Unit C to Unit F, and average $\delta^{18}O_{VPDB}$ values in Units A and B that are more positive than those from Unit C (Table 3-2).

The calcified skeletons of *Montastrea* have more negative $\delta^{18}O_{VPDB}$ and $\delta^{13}C_{VPDB}$ values than the aragonitic skeletons (Table 3-4, Fig. 3-7A, 3-7B). For calcitic *Montastrea*, the $\delta^{18}O_{VPDB}$ ranges from -6.80‰ to -4.05‰, and the $\delta^{13}C_{VPDB}$

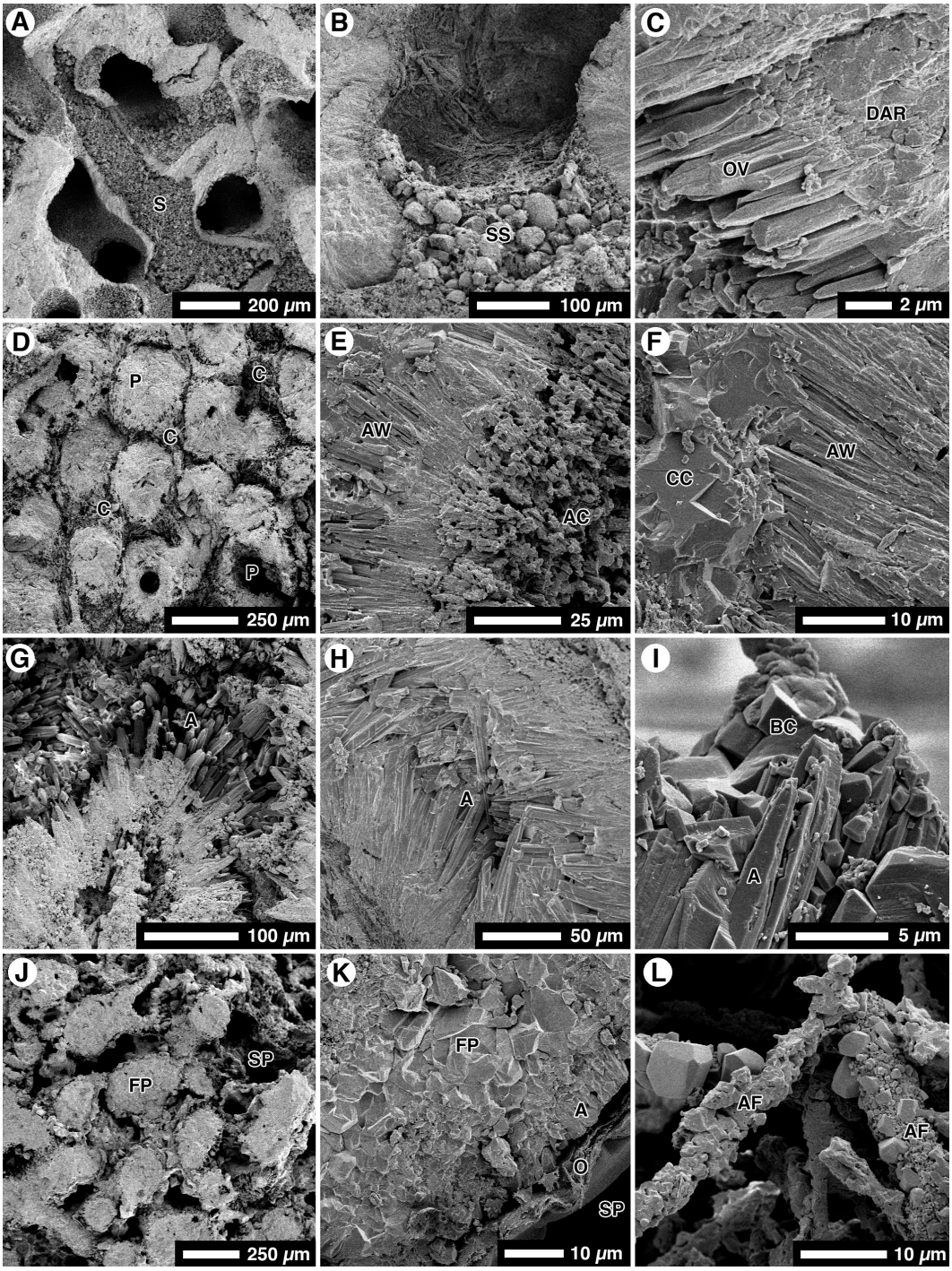

Fig. 3-6. SEM photomicrographs showing well preserved Acropora with 1-20% calcite (A-C), and 50-100% calcite (D-L) from Ironshore Formation. (A) Leached coenosteum filled with sediments (S). BJC#1, Unit E, 17.2 m. (B) Skeletal voids filled with scalloped sponge (SS) grains. BJC#1, Unit E, 17.2 m. (C) Syntaxial overgrowth (OV) of skeletal aragonite needles (DAR). BJC#1, Unit E, 17.2 m. (D) Acropora, 50% aragonite, with coenosteum (C)

severely dissolved and framework pores (P) fully or partly filled. BJC#3, Unit F, 12.1 m. (E) Coenosteum with chalky porous aragonite center (AC) and dense aragonite wall (AW). BJC#3, Unit F, 12.1 m. (F) Dense aragonite wall (AW) of coenosteum coated by calcite cement (CC). BJC#3, Unit F, 12.1 m. (G) Skeletal voids filled with aragonite (A) crystals. BJC#3, Unit F, 12.1 m. (H) Skeletal pores filled with columnar aragonite (A) cements. BJC#3, Unit F, 12.1 m. (I) Aragonite (A) fibers partly transformed to blocky calcite (BC). BJC#3, Unit F, 12.1 m. (J) Acropora, 93% calcite, with framework pores (FP) filled with calcite and secondary pores (SP) formed by dissolution of coenosteum. BJC#3, Unit D, 22.6 m. (K) Coenosteum with walls transformed to calcite, framework pores (FP) filled with calcite crystals, and secondary pore (SP) coated by very fine aragonite (A) crystals and organic (O) matter. BJC#3, Unit D, 22.6 m. (L) Calcified algae filaments (AF) in skeletal pores. BJC#3, Unit D, 22.6 m.

varies from -8.39‰ to -4.10‰, respectively. In comparison, the aragonitic *Montastrea* yielded $\delta^{18}O_{VPDB}$ values of 4.96‰ to -2.97‰, and $\delta^{13}C_{VPDB}$ values of -2.37‰ to +0.94‰. With 100%, 99%, 85-99%, and <15% aragonite, the average

Table 3-2. Average oxygen isotope composition of *Acropora palmata* and *Montastrea annularis* from Pleistocene Ironshore Formation.

Unit	*Montastrea* Aragonite $\delta^{18}O_{VPDB}$ (‰)			*Acropora* Aragonite $\delta^{18}O_{VPDB}$ (‰)			*Montastrea* Calcite $\delta^{18}O_{VPDB}$ (‰)			*Acropora* Calcite $\delta^{18}O_{VPDB}$ (‰)		
	n	mean	1σ	*n*	mean	1σ	*n*	mean	1σ	*n*	mean	1σ
F	2	-3.22	0.19	3	-2.50	0.32	-	-	-	-	-	-
E	4	-3.37	0.40	2	-2.89	0.55	-	-	-	-	-	-
D	12	-4.20	0.46	7	-3.23	1.00	5	-6.21	0.74	1	-5.44	NA
C	1	-4.34	NA	6	-3.80	0.35	1	-5.37	NA	-	-	-
B	2	-4.05	0.29	2	-3.61	0.12	7	-5.03	0.56	-	-	-
A	3	-3.31	0.24	1	-3.72	NA	5	-4.82	0.24	-	-	-

$\delta^{18}O_{VPDB}$ values of *Montastrea* are -3.69‰, -4.06‰, -3.96‰, and -5.32‰, the average $\delta^{13}C_{VPDB}$ values are -0.93‰, -0.71‰, -1.19‰, and -6.04‰, respectively (Table 3-4). The $\delta^{18}O_{VPDB}$ and $\delta^{13}C_{VPDB}$ are positively correlated (Fig. 3-7C) and

the $\delta^{18}O_{VPDB}$ values decrease as the aragonite content decreases (Fig. 3-7D).

Table 3-3. Average carbon isotope composition of *Acropora palmata* and *Montastrea annularis* from Pleistocene Ironshore Formation.

Unit	*Montastrea* Aragonite $\delta^{13}C_{VPDB}$ (‰)			*Acropora* Aragonite $\delta^{13}C_{VPDB}$ (‰)			*Montastrea* Calcite $\delta^{13}C_{VPDB}$ (‰)			*Acropora* Calcite $\delta^{13}C_{VPDB}$ (‰)		
	n	mean	1σ	*n*	mean	1σ	*n*	mean	1σ	*n*	mean	1σ
F	2	-0.76	0.56	3	0.78	1.21	-	-	-	-	-	-
E	4	-0.61	0.26	2	-0.44	0.54	-	-	-	-	-	-
D	12	-1.41	0.57	7	0.58	2.01	5	-7.48	0.70	1	-8.04	NA
C	1	-2.02	NA	6	-1.38	1.36	1	-6.21	NA	-	-	-
B	2	-1.39	1.38	2	-0.01	0.05	7	-5.37	0.83	-	-	-
A	3	-0.02	1.34	1	-1.61	NA	5	-5.51	0.94	-	-	-

Table 3-4. Average oxygen and carbon isotope compositions for *Acropora palmata* and *Montastrea annularis* (range in brackets) with different aragonite contents.

Aragonite content	*Montastrea annularis*		*Acropora palmata*	
	Mean $\delta^{18}O$ (‰ PDB)	Mean $\delta^{13}C$ (‰ PDB)	Mean $\delta^{18}O$ (‰ PDB)	Mean $\delta^{13}C$ (‰ PDB)
100%	-3.69 (-4.37 to -2.97)	-0.93 (-2.37 to -0.40)	-2.97 (-4.42 to -1.05)	+0.55 (-3.43 to +4.70)
99%	-4.06 -	-0.71 -	-3.20 (-3.55 to -2.55)	-0.11 (-1.65 to +1.29)
85%-99%	-3.96 (-4.96 to -3.05)	-1.19 (-2.23 to +0.94)	-3.41 (-4.04 to -2.16)	-0.38 (-2.39 to +1.65)
0-15%	-5.32 (-6.80 to -4.05)	-6.04 (-8.39 to -4.10)	-5.44 -	-8.04 -

One *Acropora* from Unit D, formed of 100% aragonite, however, has the maximum $\delta^{18}O_{VPDB}$ and $\delta^{13}C_{VPDB}$ values of -1.05‰ and +4.70‰, respectively, whereas one completely calcified specimen yielded a $\delta^{18}O_{VPDB}$ value of -5.44‰ and a $\delta^{13}C_{VPDB}$ value of -8.04‰ (Tables 3-2, 3-3; Fig. 3-8A, 3-8B). The

average values of $\delta^{18}O_{VPDB}$ and $\delta^{13}C_{VPDB}$ become more negative as the degree of calcification increases in *Acropora*, and there is generally a positive correlation between the $\delta^{18}O_{VPDB}$ and $\delta^{13}C_{VPDB}$ values (Table 3-4, Fig. 3-8C). For aragonitic *Acropora*, the $\delta^{18}O_{VPDB}$ values from Unit E and Unit F are generally more positive than those specimens from the underlying units (Fig. 3-8D).

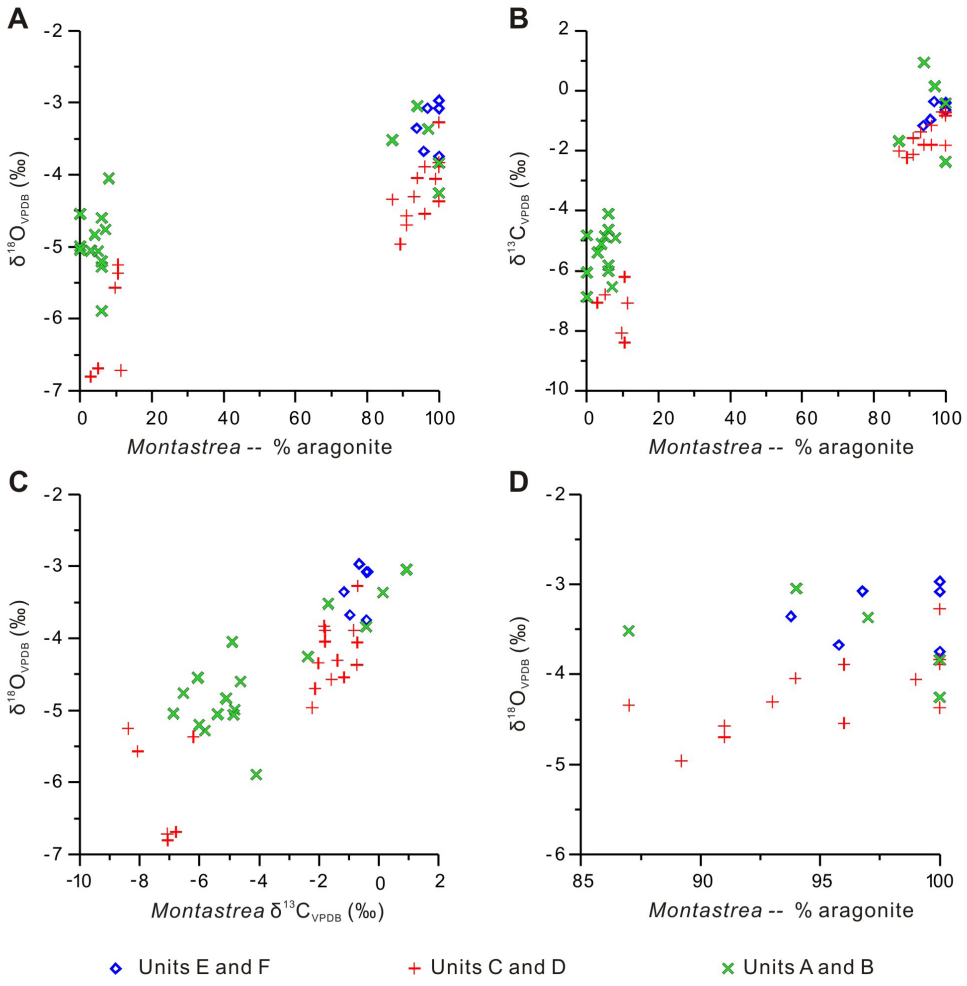

Fig. 3-7. Cross plots showing relationships between mineralogy and stable isotope values in *Montastrea annularis* from Ironshore Formation. (A) $\delta^{18}O$ versus aragonite content. (B) $\delta^{13}C$ versus aragonite content. (C) $\delta^{18}O$ versus $\delta^{13}C$. (D) $\delta^{18}O$ versus aragonite content.

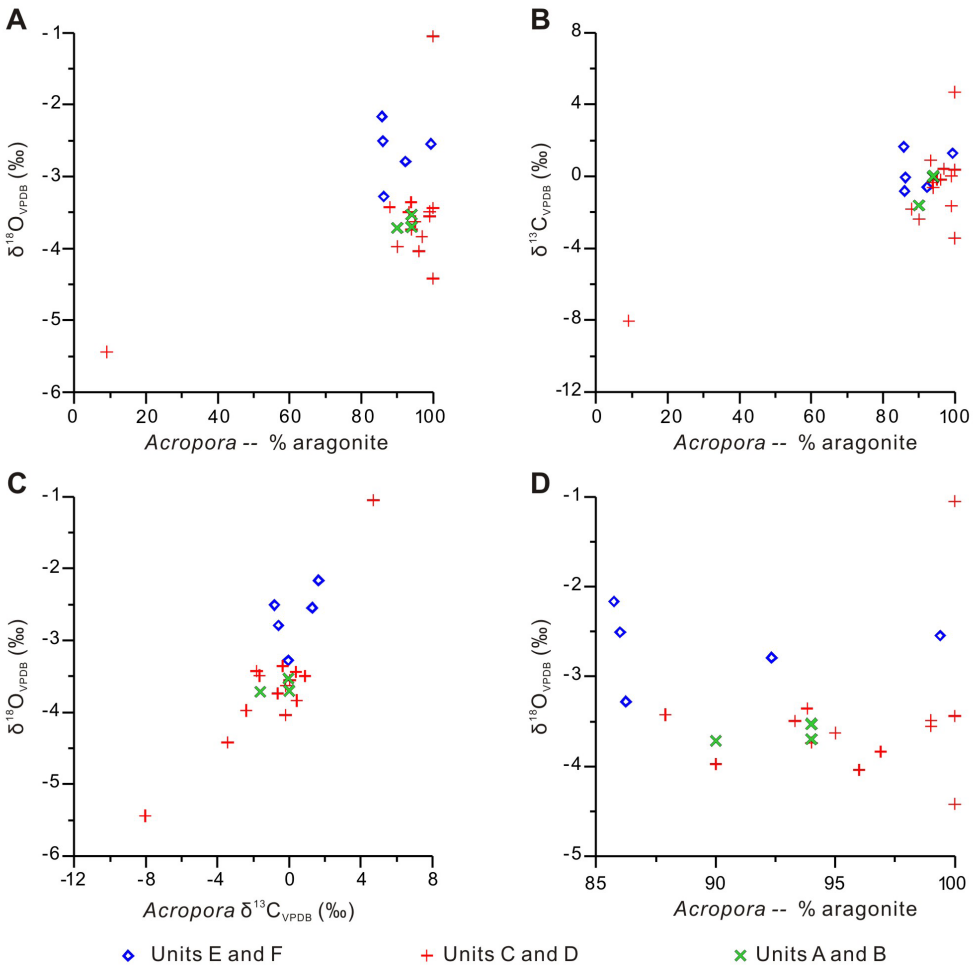

Fig. 3-8. Cross plots showing relationships between mineralogy and stable isotope values in *Acropora palmata* from Ironshore Formation. (A) $\delta^{18}O$ versus aragonite content. (B) $\delta^{13}C$ versus aragonite content. (C) $\delta^{18}O$ versus $\delta^{13}C$. (D) $\delta^{18}O$ versus aragonite content.

5. Interpretations

5.1. Elevations of Units A to F

At Rogers Wreck Point, the Ironshore Formation unconformably overlies an erosional bench that was cut into the dolostones of the Cayman Formation (Fig. 3-1F). Available evidence indicates that the positions of the depositional units have not been displaced since their original formation. A wave-cut notch, evident 6 m above present day sea level (mid-point) in the cliff face exposed

along the south side of the area, is associated with deposition of Unit D (Jones and Hunter, 1990; Vézina et al., 1999). With the base of Unit D being no more than 5 m below present day sea level, this means that the maximum water depth for sediment deposition in Unit D was 11 m. The facies and corals in this unit are consistent with this shallow water interpretation.

In the two cores from off-shore George Town, the top of Unit D lies at depths between 34 m and 41 m. Coupled with the 6 m highstand position for this unit, this implies that the water was 40 to 47 m deep at the time of deposition. The presence of *A. palmata* in these cores, however, is inconsistent with these depths because this taxon is typically associated with water that is < 5 m deep (e.g., Goreau, 1959; Geister, 1977; Adey and Burke, 1977; Lighty et al., 1982; Blanchon et al., 2002). Potentially, this can be attributed to (1) tectonic movement of the island with the western part of the island now being lower than at the time of coral growth, (2) transportation of *A. palmata* from their original shallow water growth zone into deeper water, or (3) a temporary standstill in sea level as it rose to the + 6 m highstand. Option 1 is discounted because unit D elsewhere on the western part of Grand Cayman is at the same position as unit D in the Rogers Wreck Point area. In this case, option 3 is deemed viable because the corals appear to be in or close to growth position and there is no evidence to indicate that they underwent any significant transportation from their place of growth (option 2).

5.2. Alteration of skeleton structure

The rate of diagenetic alteration of scleractinian corals is controlled by their skeletal architecture (Constanz, 1986; Dullo, 1986) and the external diagenetic environment (Schroeder, 1984; Constantz, 1986). The reaction surface area of *Acropora* is higher than that of *Montastrea* because skeletal

aragonite fibers in *Acropora* are smaller than those in *Montastrea*. This factor, however, is offset by the higher primary porosity of *Montastrea* skeletons (Constantz, 1986). Under vadose environments, the diagenetic reaction rate is controlled by the diffusion rate and the surface area of coral will not substantially influence the reaction rates (Constantz, 1986). Under phreatic conditions, however, the dissolution rate is controlled largely by the surface area of the skeleton (Constantz, 1986), and higher alteration rates of *Acropora* relative to *Montastrea* are expected. In the Ironshore Formation, however, the results conflict because *Montastrea* from Rogers Wreck Point have undergone more alteration than *Acropora*, whereas in the cores from offshore George Town, the *Acropora* skeletons are more altered than those of *Montastrea* (Table 3-1). These differences suggest that the two localities experienced different diagenetic histories.

Montastrea and *Acropora* from the Ironshore Formation on Grand Cayman were prone to the following sequence of diagenetic changes (Fig. 3-9). It is important to note, however, that not all diagenetic phases are evident in all corals.

- Syndepositional precipitation of acicular aragonite cements on internal skeletal surfaces (Figs. 3-3A, 3-3C, 3-4C) that is indicative of early marine cementation (cf., Perrin, 2011; Sayani et al., 2011).
- Bioerosion by fungi, bacteria, and algae followed by filament calcification (Figs. 3-3I, 3-6L).
- Deposition of marine aragonitic and calcitic sediments in skeletal voids that included scalloped sponge grains, diatoms, coccoliths, and other biofragments.
- Precipitation of columnar aragonite (Figs. 3-5C, 3-6H) and/or blocky calcite cements (Fig. 3-3J, 3-3K) in skeletal voids.

• Calcification of aragonitic coral skeletons through meteoric alteration involved dissolution of the skeletal aragonite (Figs. 3-3K, 3-6D) and precipitation of blocky calcite cements in the skeletal voids and secondary pores. In *Montastrea* and *Acropora*, leaching that started in the trabecular centers produced chalky trabecular centers rimmed by dense layers of aragonite needles (Fig. 3-5G, 3-5L). In *Montastrea*, the secondary pores are commonly filled with blocky calcite cements

• Indiscriminate dissolution of coral skeletons produced cavities that cross-cut

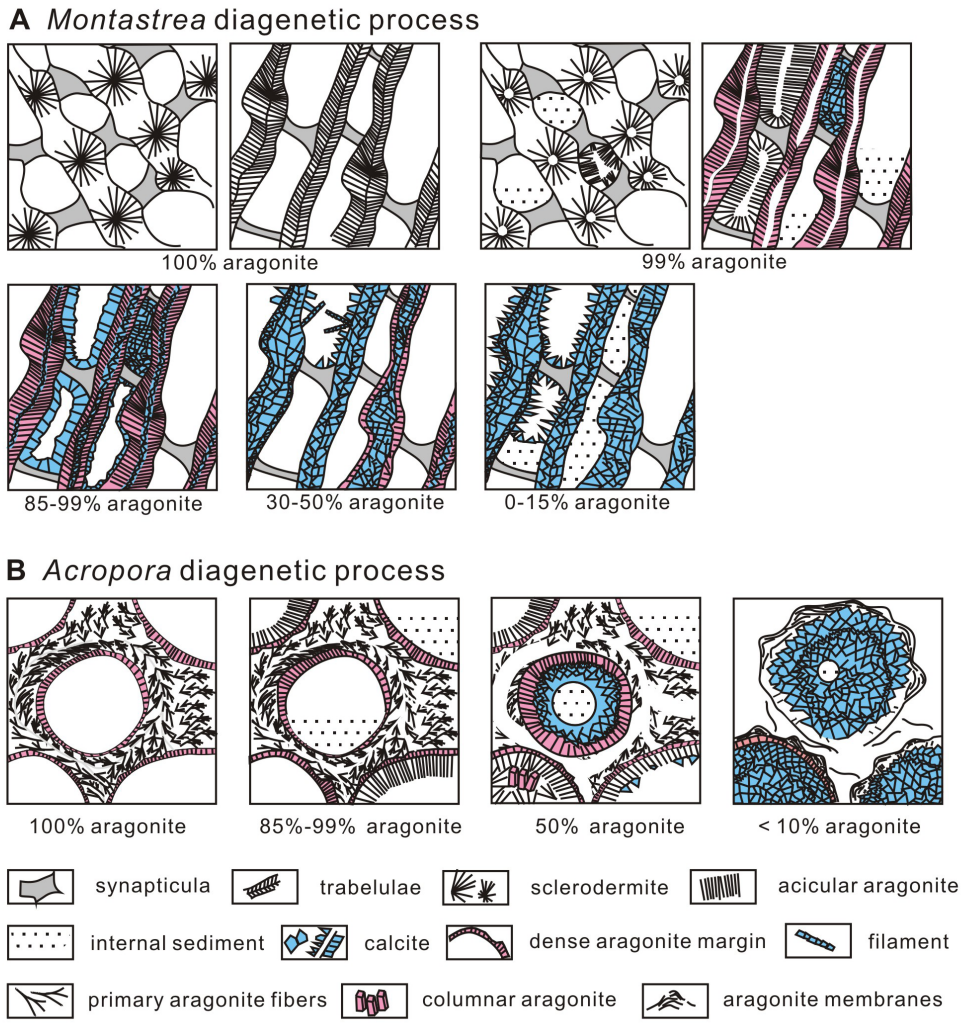

Fig. 3-9. Sketch summarizing diagenetic processes that have modified the skeletons of *Montastrea* (A) and *Acropora* (B) from the Ironshore Formation on Grand Cayman.

the primary microstructures. Many of these cavities are partly filled with micrite (Fig. 3-5J).

5.3. Alteration of skeletal $\delta^{18}O$ and $\delta^{13}C$

A cross plot of $\delta^{18}O$ against $\delta^{13}C$ shows a linear trend and three groups that correspond to Units E and F, Unit D, and Units A to C (Fig. 3-10C). Although the three groups plot along the same trend line, their positions on that trend are different. Corals from Units E and F have a narrow range of $\delta^{18}O$ (-4‰ to -2‰) and $\delta^{13}C$ (-2‰ to +2‰) values (Fig. 3-10B) with the oxygen isotope values being similar to those reported by Fairbanks and Matthews (1978) for Pleistocene *A. palmata* from Barbados. Compared with the isotope compositions of modern corals (Fairbanks and Matthews, 1978; Fairbanks and Dodge, 1979; Swart et al., 1996; Leder et al., 1996; Smith, 2006), the $\delta^{18}O$ and $\delta^{13}C$ of the corals from Units E and F are heavier, implying that meteoric processes have not significantly influenced the corals.

From Units A to C, the progressive increase in skeletal calcification (Table 3-1) is matched by a decrease in $\delta^{18}O$ values from -5‰ to -3‰ to -6‰ to -4‰, and in $\delta^{13}C$ from values from -4‰ to +1‰ to -7‰ to -4‰ (Fig. 3-10A). The highly negative $\delta^{13}C$ values (<-4‰) in the calcitic corals, which is consistent with whole-rock inter-coral matrix from the Pleistocene *A. palmata* facies of Barbados, as reported by Allan and Matthews (1977), indicate that the corals were exposed to subaerial vadose environment. Although the stable isotope values for the calcitic corals relative to the aragonitic corals from Unit D follow the same trend as for the corals from Units A to C, the calcitic corals from Unit D have more negative $\delta^{18}O$ (-7‰ to -5‰) and $\delta^{13}C$ (-9‰ to -7‰) values (Fig. 3-10A, 3-10C). This indicates that the corals from Unit D underwent more extensive meteoric diagenesis than those in Units A to C.

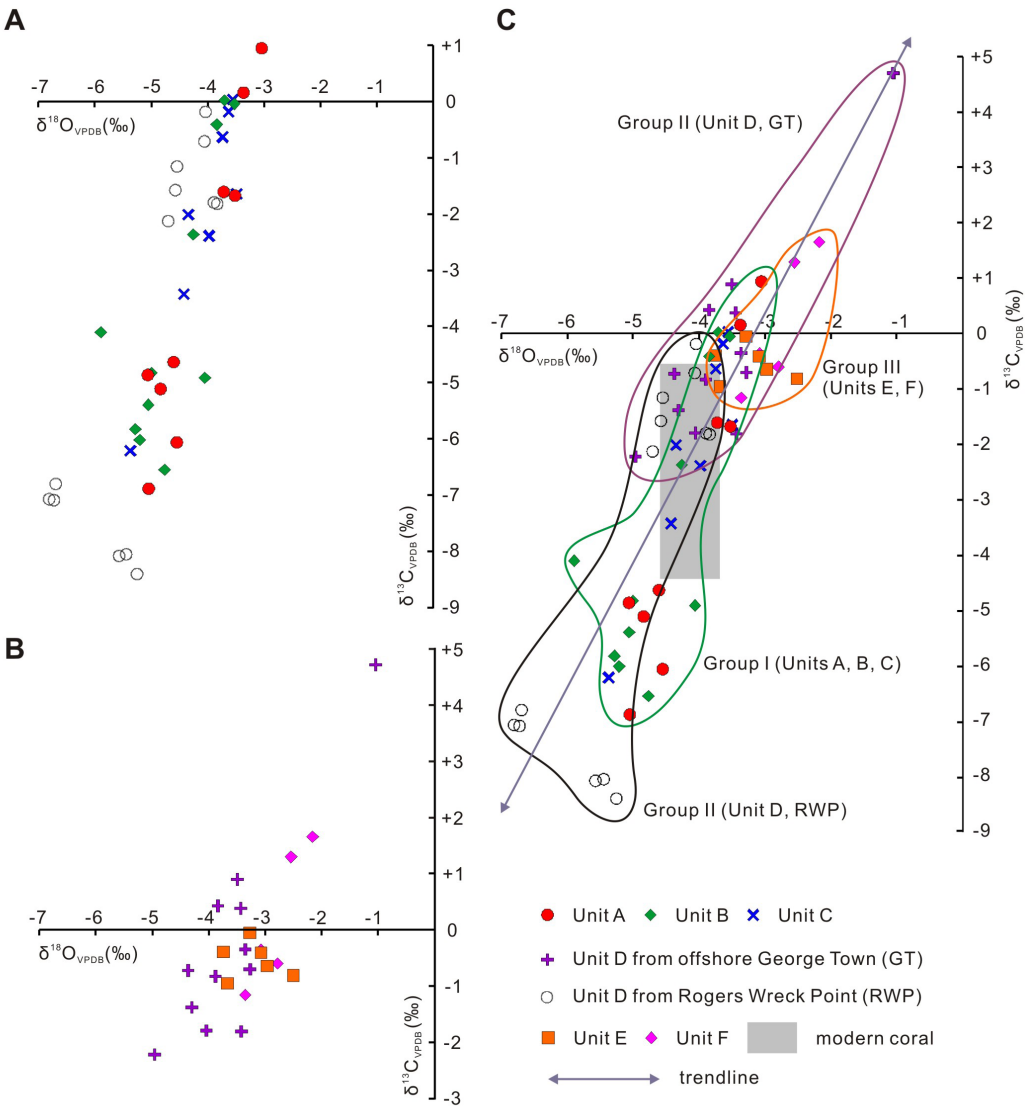

Fig. 3-10. Cross plots of $\delta^{13}C$ versus $\delta^{18}O$ for the corals from Ironshore Formation, Grand Cayman. (A) $\delta^{13}C$ versus $\delta^{18}O$ for corals from Rogers Wreck Point area. (B) $\delta^{13}C$ versus $\delta^{18}O$ for corals from offshore George Town area. (C) $\delta^{13}C$ versus $\delta^{18}O$ for corals from Pleistocene Ironshore Formation relative to modern *Montastrea* and *Acropora* (Fairbanks and Matthews, 1978; Fairbanks and Dodge, 1979; Swart et al., 1996; Leder et al., 1996;

For *Montastrea* from the Ironshore Formation, the relationship between the aragonite content and oxygen isotope composition can be expressed by:

$$\delta^{18}O_{VPDB}\ (‰) = (0.016 \times \text{aragonite weight } (\%)) - 5.41 \quad (1)$$

The $\delta^{18}O$ values of *Montastrea* formed of 100% aragonite (-4.37‰ to

-2.97‰, this study) are within the range of modern *Montastrea* (-4.49‰ to -3.74‰, Fairbanks and Dodge, 1979 and Leder et al., 1996, respectively) and that estimated for pristine *Montastrea* (-3.8‰) from equation (1). The precipitation of calcite cement in the coral skeletons leads to a decrease in the overall $\delta^{18}O$ values because the calcite cement is depleted in ^{18}O relative to the primary aragonite of the coral (cf., McGregor and Gagan, 2003). In the Ironshore Formation, 100% calcitic *Montastrea* from Units A and B have relative constant $\delta^{18}O_{VPDB}$ (-5.04‰ to -4.55‰, average -4.86‰) with the minimum value being the least affected by marine carbonate. If that $\delta^{18}O$ value (-5.04‰) is used in the paleotemperature equation of Epstein et al. (1953) with an average water temperature of 27°C (Ng et al., 1992; Rehman et al., 1994), then the water from which the calcite was precipitated was approximately -2.5‰$_{SMOW}$. This value is close to the highest $\delta^{18}O$ values of -2.0‰$_{SMOW}$ for modern meteoric precipitation on Grand Cayman (Jones et al., 1997).

The highly variable relationship between carbon and oxygen isotopes of scleractinian corals (Weber and Woodhead, 1970; Goreau, 1977; Emiliani et al., 1978; Swart, 1983; McConnaughey, 1989; Smith, 2006) reflects the ratio between the photosynthesis and respiration rates of the corals (Swart, 1983; McConnaughey, 1989; McConnaughey et al., 1997). A positive correlation, like that between $\delta^{18}O$ and $\delta^{13}C$ for aragonitic *Acropora* and *Montastrea* from the Ironshore Formation (Fig. 3-7C, 3-8C), typically develops when respiration is several times faster than photosynthesis (Swart, 1983; Davies, 1980).

6. Discussion

Units A to F in the Ironshore Formation on Grand Cayman are the physical record of deposition associated with six different highstands (Fig. 3-2). Given that (1) a lowstand followed each phase of deposition, and (2) the older units have

probably spent more cumulative time in the vadose zone, it might be expected that the corals from each unit would be distinct in terms of their diagenetic alteration. This, however, is not the case because the corals belong to three diagenetic groups: Group I with corals from Units A to C, Group II with corals from Unit D, and Group III with corals from Units E and F. Although the stable isotope compositions of these groups plot along the same trendline, their occupancy on different parts of that trendline reflects the different degrees of meteoric diagenesis that they underwent.

The extent of vadose diagenesis is controlled by many factors including the time that the corals and their host rocks spent in the vadose zone. Units A, B, C, D, E, and F in the Ironshore Formation on Grand Cayman have been correlated with Marine Isotope Stages (MIS) 11, 9, 7, 5e, 5c, and 5a, respectively (Vézina, 1997; Vézina et al., 1999; Coyne, 2003; Coyne et al., 2007). Based on the timing of the sea-level highstands during these stages for Grand Cayman (Vézina, 1997; Coyne, 2003), Moruroa (Braithwaite and Camoin, 2011), the Bahama Islands (Robinson et al., 2002; Mylroie, 2008), Henderson Island (Anderson et al., 2010), and Barbados (Schellmann et al., 2004), the maximum durations of exposure after deposition of Units A, B, C, D, E, and F are estimated at 52,000, 67,000, 65,000, 8,000, 8,000, and 66,000 years, respectively. These estimates must, however, be treated with caution because of the uncertainties associated with the precise ages of some of the highstands (e.g., Siddall et al., 2007, their Table 7.1). Nevertheless, if the degree of diagenesis was related solely to time, then the maximum diagenesis might be expected in Units A, B, C, and F. The fact that this is not the case indicates that other factor(s) must have influenced diagenesis.

The “exposure window”, where vadose diagenesis takes place, is dictated by the elevation of the lowstand relative to the elevation of the land surface and the lower boundary of the stratigraphic unit. Although the highstand positions

associated with each depositional unit in the Ironshore Formation are known with some certainty (Jones and Hunter, 1990; Vézina et al., 1999; Coyne et al., 2007), little is known about the positions of the lowstands that followed each depositional phase. In the Rogers Wreck Point area, the maximum known thickness of the Ironshore Formation is 18.6 m (well RWP#14). Thus, if each lowstand throughout the Middle to Late Pleistocene was >18.6 m below present sea level (bsl), then each unit (A-D) would have been repeatedly exposed to

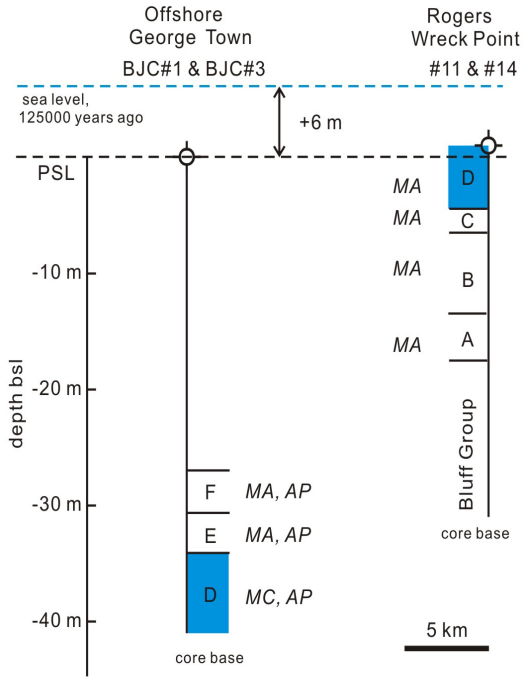

Fig. 3-11. Positions of Units A to F in Ironshore Formation in cores from Rogers Wreck Point and offshore George Town area relative to sea level about 125,000 years ago. MA = *Montastrea annularis*, MC = *Montastrea cavernosa*, AP = *Acropora palmata*.

vadose diagenetic cycles and the maximum exposure times would apply. If, however, any of the lowstands were <18.6 m bsl, then the older units would have remained below sea level. In the offshore George Town area, Units D, E, and F of the Ironshore Formation are located at depths greater than 25.8 m bsl (Fig. 3-1E). For Unit D (base is up to 41.0 m bsl) to be exposed, sea level would have had to

drop to 41.0 m bsl (Fig. 3-11). This situation contrasts strongly with the setting at Rogers Wreck Point where the base of Unit D is only 5 m bsl (Fig. 3-11). Thus, it is entirely possible that changing sea level may have led to the exposure of Unit D in the Rogers Wreck Point area but not in the offshore George Town area. Such differences are probably responsible for the differences in the diagenetic development of *Montastrea* and *Acropora* from the two areas.

Today, the freshwater lenses on Grand Cayman are of limited aerial extent and housed in the Tertiary carbonates of the Bluff Group (Rehman, 1992; Ng et al., 1992; Ng and Jones, 1995). As a result, most of the Ironshore Formation is currently bathed in seawater and only those parts of the Ironshore Formation exposed above sea level are prone to freshwater invasion following periods of rain. Climate conditions that existed during each lowstand period were critical because they controlled rainfall that, in turn, dictated the flow of freshwater through the limestones of the Ironshore Formation. As in Africa (deMenocal, 1995), tropical south America (Damuth and Fairbridge, 1970; Rull, 1996), and Europe and the Mediterranean (Bonatti and Gartner, 1973), the climate in the Caribbean region during the Pleistocene ice ages was more arid than during the highstand periods (Bonatti and Gartner, 1973). Low rainfalls during a particular lowstand meant that less freshwater flowed through the limestones and diagenesis was curtailed.

Theoretically, glacioeustatic sea-level fluctuations might lead to a paragenetic sequence wherein successive diagenetic events overprint older ones (Matthews and Frohlich, 1987; Whitaker et al., 1997). In most successions, such as the 700,000 year to Holocene sequence on the Great Barrier Reef (Braithwaite and Montaggioni, 2009) and the 355,840 year to Holocene sequence on Moruroa, French Polynesia (Braithwaite and Camoin, 2011), this has proved problematic because of the difficulties in related specific diagenetic signals to specific sea

levels. The same is true for the Ironshore Formation on Grand Cayman, where (1) there is no systematic decrease in the diversity or degree of diagenesis from the older to younger rocks, (2) the distribution of calcite in the corals is variable with no obvious correlation to individual depositional units (Figs. 3-3H, 3-6I), (3) the blocky calcite cements show no evidence of growth banding like that commonly seen in many ancient limestones (e.g., Kaufman et al., 1988), and (4) stable isotope compositions have only a poor correlation with the different diagenetic features. The degree of coral calcification decreases from Unit A to Unit C, but the stable isotope values for each unit are similar and provide no clear evidence of sequential overprinting. Although the degree of coral calcification in Unit D is much lower than that in Units A and B, the stable isotope values from the corals in Unit D are more negative than those from corals in Units A and B. This is somewhat surprising given that the maximum exposure time after deposition of Unit D was only 8 ka, the shortest duration of exposure that followed any depositional phase in the Ironshore Formation. The contrast between the corals in Unit D and those in Units A to C may be due to (1) the meteoric water that affected Unit D being more negative with respect to $\delta^{18}O$ than the waters that affected Units A to C, and/or (2) Unit D may have longer total subaerial exposure time than Units A to C.

The calcrete crust that caps Unit D in the Rogers Wreck Point area (Vézina, 1997) indicates exposure to the atmosphere following its deposition and prior to deposition of Unit E. Today, the upper part of Unit D lies above the saltwater phreatic zone and is thus prone to freshwater diagenesis and there is every reason to suspect that this has been the situation since deposition about 125,000 years ago. Although such considerations indicate that superimposed diagenetic fabrics should be expected in the corals of Unit D, it has not been possible to identify different cycles of diagenesis. In contrast, the diagenetic

fabrics and stable isotope signatures of the corals from Units E and F from offshore George Town largely reflect marine conditions.

The corals from the Ironshore Formation on Grand Cayman are petrographically and geochemically similar to Pleistocene corals from Barbados (Pingitore, 1976; Allan and Matthews, 1977; Fairbanks and Matthews, 1978; Dullo, 1987). As yet, however, the temporal changes in the diagenesis of the corals on Barbados are not known and it is therefore impossible to compare the corals from the two islands from this perspective. For Pleistocene corals from oceanic islands throughout the Caribbean Sea and the Pacific Ocean, various studies have investigated the relationship between Pleistocene sea-level change and reef diagenesis (Braithwaite and Montaggioni, 2009; Braithwaite and Camoin, 2011). On those islands, as on Grand Cayman, it has proved impossible to relate the specific diagenetic signatures in the corals with specific sea levels.

7. Conclusions

On Grand Cayman, the Ironshore Formation is composed of six unconformity-bounded depositional units that were deposited during different highstands during the Middle to Late Pleistocene. Detailed examination of the diagenetic alteration fabrics and stable isotopic compositions of *M. annularis* and *A. palmata* from these units has demonstrated the following points.

- *M. annularis* and *A. palmata* underwent similar marine and meteoric diagenetic processes.
- *M. annularis* and *A. palmata* are characterized by different degrees of calcification that can be attributed to differences in their skeletal structures.
- The degree of calcification of coral skeletons is stratigraphically variable.
- The degree of skeletal calcification is geographically variable.

- Based on their stable isotope signatures the corals belong to three diagenetic groups (I, II, III) that, in general, reflect the degree of meteoric diagenesis.
- The different diagenetic fabrics evident in the corals cannot be correlated with specific sea level lowstands.

References

Adey, W.H., Burke, R.B., 1977. Holocene bioherms of Lesser Antilles – geologic control of development. In: Frost, S.H., Weiss, M.P., Saunders, J.B. (Eds.), Reefs and Related Carbonates – Ecology and Sedimentology, volume 4. American Association of Petroleum Geologists Studies in Geology, Tulsa, Oklahoma, pp. 67-81.

Aissaoui, D.M., Purser, B.H., 1985. Reef diagenesis: cementation at Mururoa Atoll. Proceedings of the Fifth International Coral Reef Congress, Tahiti, pp. 257-262.

Allan, J.R., Matthews, R.K., 1977. Carbon and oxygen isotopes as diagenetic and stratigraphic tools: surface and subsurface data, Barbados, West Indies. Geology 5, 16-20.

Andersen, M.B., Stirling, C.H., Potter, E.K., Halliday, A.N., Blake, S.G., McCulloch, M.T., Ayling, B.F., O'Leary, M.J., 2010. The timing of sea-level high-stands during Marine Isotope Stages 7.5 and 9: constraints from the uranium-series dating of fossil corals from Henderson Island. Geochimica et Cosmochimica Acta 74, 3598-3620.

Bard, E., Hamelin, B., Arnold, M., Montaggioni, L.F., Cabioch, G., Faure, G., Rougerie, F., 1996. Deglacial sea level record from Tahiti corals and the timing of global meltwater discharge. Nature 382, 241-244.

Bar-Matthews, M., Wasserburg, G.J., Chen, J.H., 1993. Diagenesis of fossil coral skeletons: correlation between trace elements, textures, and $^{234}U/^{238}U$. Geochimica et Cosmochimica Acta 57, 257-276.

Blanchon, P., Jones, B., Ford, D.C., 2002. Discovery of a submerged relic reef and shoreline off Grand Cayman: further support for an early Holocene jump in sea level. Sedimentary Geology 147, 253-270.

Bonatti, E., Gartner, S., 1973. Caribbean climate during Pleistocene Ice Ages.

Nature 244, 563-565.

Braithwaite, C.J.R., Camoin, G.F., 2011. Diagenesis and sea-level change: lessons from Moruroa, French Polynesia. Sedimentology 58, 259-284.

Braithwaite, C.J.R., Montaggioni, L.F., 2009. The Great Barrier Reef: a 700,000 year diagenetic history. Sedimentology 56, 1591-1622.

Brunt, M.A., Giglioli, M.E.C., Mather, J.D., Piper, D.J.W., Richards, H.G., 1973. The Pleistocene rocks of the Cayman Islands. Geological Magazine 110, 209-304.

Buchbinder, B., 1977. Different responses to diagenesis of various coral groups in the Miocene Ziqlag Formation, Israel. Bureau Recherches Geologiques et Minieres, Mémoire 89, 26-32.

Constantz, B.R., 1986. The primary surface area of corals and variations in their susceptibility to diagenesis. In: Schroeder, J.H., Purser, B.H. (Eds.), Reef Diagenesis. Springer Verlag, Berlin, pp. 53-76.

Coyne, M.K., 2003. Transgressive-regressive cycles in the Ironshore Formation, Grand Cayman, British West Indies. Unpublished M. Sc. Thesis, University of Alberta, Edmonton, Canada, 98 pp.

Coyne, M.K., Jones, B., Ford, D., 2007. Highstands during Marine Isotope Stage 5: evidence from the Ironshore Formation of Grand Cayman, British West Indies. Quaternary Science Reviews 26, 536-559.

Cross, T.S., Cross, B.W., 1983. U, Sr, and Mg in Holocene and Pleistocene corals (*A. palmata* and *M. annularis*). Journal of Sedimentary Petrology 53, 587-594.

Damuth, J.E., Fairbridge, R.W., 1970. Equatorial Atlantic deep-sea arkosic sands and ice-age aridity in tropical South America. Geological Society of America Bulletin 81, 189-206.

Davies, P.S., 1980. Respiration in some Atlantic reef corals in relation to vertical distribution and growth form. The Biological Bulletin 158, 187-194.

deMenocal, P.B., 1995. Plio-Pleistocene African climate. Science 270, 53-59.

Dullo, W.C., 1986. Variation in diagenetic sequences: an example from Pleistocene coral reefs, Red Sea, Saudi Arabia. In: Schroeder, J.H., Purser, B.H. (Eds.), Reef Diagenesis. Springer-Verlag, Berlin, pp. 77-90.

Dullo, W.C., 1987. The role of microarchitecture and microstructure in the preservation of taxonomic closely related scleractinian. Facies 16, 11-22.

Emiliani, C., Hudson, J.H., Shinn, E.A., George, R.Y., 1978. Oxygen and carbon isotopic growth record in a reef coral from the Florida Keys and a deep-sea coral from Blake Plateau. Science 202, 627-629.

Epstein, S., Buchsbaum, R., Lowenstam, H.A., Urey, H.C., 1953. Revised carbonate-water isotopic temperature scale. Bulletin of the Geological Society of America 64, 1315-1326.

Fairbanks, R.G., Dodge, R.E., 1979. Annual periodicity of the $^{18}O/^{16}O$ and $^{13}C/^{12}C$ ratios in the coral *Montastrea annularis*. Geochimica et Cosmochimica Acta 43, 1009-1020.

Fairbanks, R.G., Matthews, R.K., 1978. Marine oxygen isotope record in Pleistocene coral, Barbados, West Indies. Quaternary Research 10, 181-196.

Fallon, S.W., McCulloch, M.T., Alibert, C., 2003. Examining water temperature proxies in *Porites* corals the Great Barrier Reef: a cross-shelf comparison. Coral Reefs 22, 389-404.

Geister, J., 1977. The influence of wave exposure on the ecological zonation of Caribbean coral reefs. In Taylor, D.L. (Ed.), Proceedings of the Third International Coral Reef Symposium, Volume 1 (Biology). University of Miami, Rosenstiel School of Marine and Atmospheric Science, University of Miami, Florida, pp. 23-29.

Gischler, E., Storz, D., 2009. High resolution windows into Holocene climate using proxy data from Belize corals (Central America). Palaeobiodiversity and

Palaeoenvironments 89, 211-221.

Goreau, T.J., 1959. The ecology of Jamaican coral reefs: I. Species composition and zonation. Ecology 40, 67-90.

Goreau, T.J., 1977. Coral skeletal chemistry: physiological and environmental regulation of stable isotopes and trace metals in *Montastrea annularis*. Proceedings of the Royal Society B: Biological Sciences 196, 291-315.

Gvirtzman, G., Friedman, G.D., 1977. Sequence of progressive diagenesis in coral reefs. American Association of Petroleum Geologists, Study in Geology 4, 357-380.

Hunter, I.G., 1994. Modern and ancient coral associations of the Cayman Islands. Unpublished Ph. D. Thesis, University of Alberta, Edmonton, Canada, 345 pp.

Hunter, I.G., Jones, B., 1996. Coral associations of the Pleistocene Ironshore Formation, Grand Cayman. Coral Reefs 15, 249-267.

James, N.P., 1974. Diagenesis of scleractinian corals in the subaerial vadose environment. Journal of Paleontology 48, 785-799.

Jones, B., 1994. Geology of the Cayman Islands. In: Brunt, M.A., Davies, J.E. (Eds.), The Cayman Islands: Natural History and Biogeography. Kluwer Academic Publishers, The Netherlands, pp. 13-49.

Jones, B., Hunter, I.G., 1990. Pleistocene paleogeography and sea levels on the Cayman Islands, British West Indies. Coral Reefs 9, 81-91.

Jones, B., Pemberton, S.P., 1989. Sedimentology and ichnology of a Pleistocene unconformity bounded, shallowing upward carbonate sequence: the Ironshore Formation, Salt Creek, Grand Cayman. Palaios 4, 343-355.

Jones, B., Ng, K.C., Hunter, I.G., 1997. Geology and hydrogeology of the Cayman Islands. In: Vacher, H.L., Quinn, T. (Eds.), Geology and Hydrogeology of Carbonate Islands. Elsevier, pp. 299-325.

Kaufman, J., Cander, H.S., Daniels, L.D., Meyers, W.J., 1988. Calcite cement

stratigraphy and cementation history of the Burlington-Keokuk Formation (Mississippian), Illinois and Missouri. Journal of Sedimentary Petrology 58, 312-326.

Lazar, B., Enmar, R., Scossberger, M., Bar-Matthews, M., Halicz, L., Stein, M., 2004. Diagenetic effect on the distribution of uranium in live Holocene corals from the Gulf of Aqaba. Geochimica et Cosmochimica Acta 68, 4583-4593.

Leder, J.J., Swart, P.K., Szmant, A.M., Dodge, R.E., 1996. The origin of variations in the isotopic record of scleractinian corals: I. Oxygen. Geochimica et Cosmochimica Acta 60, 2857-2870.

Lighty, R.G., Macintyre, I.G., Stuckenrath, R., 1982. *Acropora palmata* reef framework: a reliable indicator of sea level in the western Atlantic for the past 10,000 years. Coral Reefs 1, 125-130.

McCrea, J.M., 1950. On the isotopic chemistry of carbonates and a paleotemperature scale. The Journal of Chemical Physics 18, 849-857.

Matley, C.A., 1926. The geology of the Cayman Islands (British West Indies), and their relation to the Bartlett Trough. Quarterly Journal of the Geological Society 82, 352-387.

Matthews, R.K., Frohlich, C., 1987. Forward modeling of bank-margin carbonate diagenesis. Geology 15, 673-676.

McConnaughey, T., 1989. ^{13}C and ^{18}O isotopic disequilibrium in biological carbonates: I. Patterns. Geochimica et Cosmochimica Acta 53, 151-162.

McConnaughey, T.A., Burdett, J., Whelan, J.F., Paull, C.K., 1997. Carbon isotopes in biological carbonates: respiration and photosynthesis. Geochimica et Cosmochimica Acta 61, 611-622.

McGregor, H.V., Abram, N.J., 2008. Images of diagenetic textures in *Porites* corals from Papua New Guinea and Indonesia. Geochemistry, Geophysics, Geosystems 9, 1-17.

McGregor, H.V., Gagan, M.K., 2003. Diagenesis and geochemistry of *Porites* corals from Papua New Guinea: implications for paleoclimate reconstruction. Geochimica et Cosmochimica Acta 67, 2147-2156.

Mylroie, J.E., 2008. Late Quaternary sea-level position: evidence from Bahamian carbonate deposition and dissolution cycles. Quaternary International 183, 61-75.

Ng, K.C., Jones, B., 1995. Hydrogeochemistry of Grand Cayman, British West Indies: implications for carbonate diagenetic studies. Journal of Hydrology 164, 193-216.

Ng, K.C., Jones, B., Beswick, R., 1992. Hydrogeology of Grand Cayman, British West Indies: a karstic dolostone aquifer. Journal of Hydrology 134, 273-295.

Nothdurft, L.D., 2007. Microstructure and early diagenesis of recent reef building scleractinian corals, Heron Reef, Great Barrier Reef: implications for palaeoclimate analysis. Unpublished Ph. D. Thesis, Queensland University of Technology, Brisbane, Australia, 218 pp.

Nothdurft, L.D., Webb, G.E., 2009. Earliest diagenesis in scleractinian coral skeletons: implications for palaeoclimate-sensitive geochemical archives. Facies 55, 161-201

Perrin, C., 2003. Compositional heterogeneity and microstructural diversity of coral skeletons: implications for taxonomy and control on early diagenesis. Coral Reefs 22, 109-120.

Perrin, C., 2011. Diagenesis. In: Hopley, D. (Ed.), Enclyclopedia of Modern Coral Reefs: Structure, Form and Process. Springer, pp. 309-321.

Pingitore, N.E., 1970. Diagenesis and porosity modification in *Acropora palmata*, Pleistocene of Barbados, West Indies. Journal of Sedimentary Petrology 40, 712-721.

Pingitore, N.E., 1976. Vadose and phreatic diagenesis: processes, products and

their recognition in corals. Journal of Sedimentary Petrology 46, 985-1006.

Pingitore, N.E., Eastman, M.P., 1985. Barium partitioning during the transformation of corals from aragonite to calcite. Chemical Geology 48, 183-187.

Pingitore, N.E., Rangel, Y., Kwarteng, A., 1989. Barium variation in *Acropora palmata* and *Montastrea annularis*. Coral Reefs 8, 31-36.

Rabier, C., Anguy, Y., Cabioch, G., Genthon, P., 2008. Characterization of various stages of calcitization in *Porites* sp. corals from uplifted reefs - case studies from New Caledonia, Vanuatu, and Futuna (South-West Pacific). Sedimentary Geology 211, 73-86.

Rehman, J., 1992. Diagenetic alteration of *Strombus gigas*, *Siderastrea siderea* and *Montastrea annularis* from the Pleistocene Ironshore Formation of Grand Cayman. Unpublished M. Sc. Thesis, University of Alberta, Edmonton, Canada, 136 pp.

Rehman, J., Jones, B., Hagan, T.H., Coniglio, M., 1994. The Influence of sponge borings on aragonite-to-calcite inversion in Late Pleistocene *Strombus gigas* from Grand Cayman, British West Indies. Journal of Sedimentary Research 64, 174-179.

Ribaud-Laurenti, A., Hamelin, B., Montaggioni, L., Cardinal, D., 2001. Diagenesis and its impact on Sr/Ca ratio in Holocene *Acropora* corals. International Journal of Earth Sciences 90, 438-451.

Rigby, J.K., Roberts, H.H., 1976. Grand Cayman Island: geology, sediments and marine communities. Brigham Young University, Geology Studies, Special Publication No. 4. Department of Geology, Brigham Young University, Provo, USA, 122 pp.

Robinson, L.F., Henderson, G.M., Slowey, N.C., 2002. U-Th dating of marine isotope stage 7 in Bahamas slope sediments. Earth and Planetary Science Letters 196, 175-187.

Rull, V., 1996. Late Pleistocene and Holocene climates of Venezuela. Quaternary International 31, 85-94.

Sayani, H.R., Cobb, K.M., Cohen, A.L., Elliott, W.C., Nurhati, I.S., Dunbar, R.B., Rose, K.A., Zaunbrecher, L.K., 2011. Effects of diagenesis on paleoclimate reconstructions from modern and young fossil corals. Geochimica et Cosmochimica Acta 75, 6361-6373.

Schellmann, G., Radtke, U., Potter, E.K., Esat, T.M., McCulloch, M.T., 2004. Comparison of ESR and TIMS U/Th dating of marine isotope stage (MIS) 5e, 5c, and 5a coral from Barbados - implications for paleo sea-level change in the Caribbean. Quaternary International 120, 41-50.

Scherer, M., Seitz, H., 1980. Rare-earth element distribution in Holocene and Pleistocene corals and their redistribution during diagenesis. Chemical Geology 28, 279-289.

Schroeder, J.H., 1984. The petrogenetogram of corals: spatial variations in diagenetic sequences. Paleontographica Americana 54, 261-271.

Siddall, M., Chappell, J., Potter, E.-K., 2007. Eustatic sea level during past interglacials. Developments in Quaternary Science 7, 75-92.

Smith, J.M., 2006. Geochemical signatures in the coral *Montastraea*: modern and mid-Holocene perspectives. Unpublished Ph. D. Thesis, University of South Florida, Tampa, USA, 125 pp.

Spiro, B.F., 1971. Diagenesis of some scleractinian corals from the Gulf of Elat, Israel. Bulletin of the Geological Society of Denmark 21, 1-10.

Swart, P.K., 1983. Carbon and oxygen isotope fractionation in scleractinian corals: a review. Earth Science Reviews 19, 51-80.

Swart, P.K., Leder, J.J., Szmant, A.M., Dodge, R.E., 1996. The origin of variations in the isotopic record of scleractinian corals: II. Carbon. Geochimica et Cosmochimica Acta 60, 2871-2885.

Vézina, J.L., 1997. Stratigraphy and sedimentology of the Pleistocene Ironshore Formation at Rogers Wreck Point, Grand Cayman: a 400 ka record of sea-level highstands. Unpublished M. Sc. Thesis, University of Alberta, Edmonton, Canada, 131 pp.

Vézina, J.L., Jones, B., Ford, D., 1999. Sea level highstands over the last 500,000 years: evidence from the Ironshore Formation on Grand Cayman, British West Indies. Journal of Sedimentary Research 69, 317-327.

Webb, G.E., Nothdurft, L.D., Kamber, B.S., Kloprogge, J.T., Zhao, J.X., 2009. Rare earth element geochemistry of scleractinian coral skeleton during meteoric diagenesis: a sequence through neomorphism of aragonite to calcite. Sedimentology 56, 1433-1463.

Weber, J.N., Woodhead, P.M.J., 1970. Carbon and oxygen isotope fractionation in the skeletal carbonate of reef-building corals. Chemical Geology 6, 93-117.

Whitaker, F., Smart, P., Hague, Y., Waltham, D., Bosence, D., 1997. Coupled two-dimensional diagenetic and sedimentological modeling of carbonate platform evolution. Geology 25, 175-178.

Woodroffe, C.D., Stoddart, D.R., Giglioli, M.E.C., 1980. Pleistocene patch reefs and Holocene swamp morphology, Grand Cayman Island, West Indies. Journal of Biogeography 7, 103-113.

CHAPTER 4: CALCAREOUS CRUSTS ON EXPOSED PLEISTOCENE LIMESTONES: A CASE STUDY FROM GRAND CAYMAN, BRITISH WEST INDIES[1]

1. Introduction

Calcareous crusts that cap limestone bedrock are of great interest to sedimentologists because exposure surfaces covered by such crusts commonly highlight unconformities in marine carbonate sequences (Multer and Hoffmeister, 1968; Coniglio and Harrison, 1983; Wright, 1994), and can provide insights into climatic changes that took place during sea level lowstands when the surfaces were exposed (Cerling, 1984; Cerling and Hay, 1986; Tanner, 2010). Various studies of calcareous crusts associated with Carboniferous to Quaternary strata have focused on their classification (Netterberg, 1980; Netterberg and Caiger, 1983; Wright, 1990); stages of morphological development (Gile et al., 1966; Esteban and Klappa, 1983; Machette, 1985); mineralogy (Watts, 1980); diagenetic fabrics (James, 1972; Braithwaite, 1975; Alonso-Zarza and Jones, 2007; Zhou and Chafetz, 2009a); geochemistry (Talma and Netterberg, 1983; Cerling, 1984; Cerling and Hay, 1986; Salomons and Mook, 1986; Rossinsky and Swart, 1993); and genetic development (Gile et al., 1961; Multer and Hoffmeister, 1968; James, 1972; Harrison, 1977; Robbin and Stipp, 1979; Arakel, 1982; Coniglio and Harrison, 1983; Wright et al., 1988, 1995). Although the processes responsible for their formation are broadly understood (Wright and Tucker, 1991; Alonso-Zarza, 2003; Wright, 2008; Alonso-Zarza and Wright, 2010), many aspects of their physical and chemical evolution remain open to debate.

This paper examines the calcareous crusts that cap limestone sequences in

1 This chapter was published as: Li., R., Jones, B., 2014. Calcareous crusts on exposed Pleistocene limestones: A case study from Grand Cayman, British West Indies. Sedimentary Geology 299, 88-105.

the Pleistocene Ironshore Formation on Grand Cayman (Fig. 4-1). By integrating the mineralogy, petrography, and geochemical signatures of the calcareous crusts, this study identifies two different types of calcareous crusts, focuses on the processes involved in their development, and considers the paleoclimate conditions and vegetation cover that governed their development. Critically, this study shows that formation of calcareous crusts takes place in response to interactions between substrate, soil cover, climate, and biological influences that operate during lowstand regimes and highlights exposure unconformities that are critical for establishing the lowstand-highstand cycles in carbonate successions.

2. Terminology

Calcareous crusts that develop on the surfaces of exposed limestones (James, 1972; Walls et al., 1975; Kahle, 1977) have also been referred to subaerial laminated crusts (Multer and Hoffmeister, 1968; Harrison, 1977). Calcareous crusts with well-defined laminae have been referred to as laminar calcretes (Wright et al., 1988, 1995; Verrecchia et al., 1995; Freytet et al., 1997; Alonso-Zarza, 1999; Alonso-Zarza and Wright, 2010). Although calcrete commonly implies a pedogenic origin (Goudie, 1973; Watts, 1980), the term calcrete, as used herein, follows Wright and Tucker (1991) who applied it in a broader sense to include non-pedogenic authigenic carbonate bodies that form as a result of precipitation in the shallow phreatic zone.

Herein, "calcareous crust" is applied to calcareous crusts found on the top of bedrock following the usage of James (1972) and Kahle (1977). For the Cayman calcareous crusts, "laminar calcrete" refer to the laminated crusts following the usage of Alonso-Zarza and Wright (2010), whereas the "non-laminar calcrete" refer to those crusts that are not laminated.

3. Geological Setting

Grand Cayman, the largest of the Cayman Islands (Fig. 4-1A), is mostly less than 6 m above sea level (Jones et al., 1997). Today, the island enjoys a subhumid, tropical climate, with temperatures of 25-29°C (Blanchon et al., 1997). Rainfall averages ~1513 mm per year, with the highest intensity from May to October (Ng et al., 1992). Rainfall is, however, uneven with the eastern part of island having the lowest rainfall and highest evaporation rates (Ng et al., 1992).

On Grand Cayman, the Pleistocene Ironshore Formation (Matley, 1926; Jones et al., 1994) unconformably overlies the Tertiary limestones and dolostones of the Bluff Group (Fig. 4-1B). The Ironshore Formation comprises six unconformity-bounded units (A to F), each formed of poorly lithified limestones that originated in various shallow water environments and display various diagenetic fabrics (Brunt et al., 1973; Jones and Hunter, 1990; Vézina, 1997; Vézina et al., 1999; Coyne, 2003; Coyne et al., 2007; Li and Jones, 2013a; Li and Jones, 2013b). Calcareous crusts commonly mark the unconformities between the

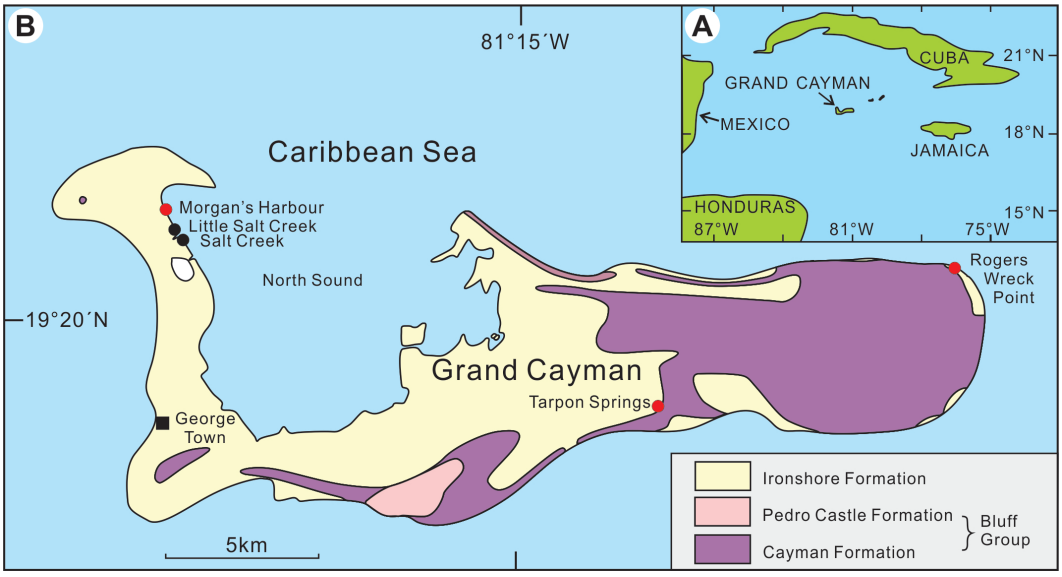

Fig. 4-1. (A) Location of Grand Cayman. (B) Geological map of Grand Cayman (modified from Jones, 1994) showing locations of Morgan's Harbour, Tarpon Springs, Rogers Wreck Point, Little Salt Creek, and Salt Creek.

units with those at the top of Unit D (125,000 years BP) especially well developed and exposed in many different areas on the island.

This paper focuses on laminar and non-laminar calcretes that are found on top of Unit D at (1) Rogers Wreck Point area, (2) Tarpon Springs, and (3) Morgan's Harbour (Fig. 4-1B).

4. Methods

The study is based on 27 samples collected from calcareous crusts at Rogers Wreck Point (6 samples), Tarpon Springs (5 samples), and Morgan's Harbour (16 samples). Each sample included both the calcareous crust and the underlying bedrock.

The mineralogy of the bedrock and the calcareous crusts was determined by X-ray diffraction (XRD) analysis. Powdered samples, each weighing about 1 g, were analyzed on a Rigaku Ultima IV Powder XRD system that was run at 38 kV and 38 mA using an Ultima IV X-ray generator with a Co tube. All scans were run from 5° to 90° 2θ at a speed of 2°θ/min. The aragonite and calcite weight percentages were calculated from the intensities of the d_{110}, d_{021}, and d_{104} peaks using an aragonite-calcite calibration curve derived from the analyses of artificial samples with known calcite:aragonite ratios. The values obtained using this method are accurate at ±2 wt%.

The microscopic features of the bedrock and the calcareous crusts were determined from standard optical microscopy and scanning electron microscope (SEM) analyses. Images of thin sections were obtained using a Polaroid DMC digital camera that is mounted on a Leica petrographic microscope. Small fractured samples (~1 cm^3) were mounted on SEM stubs using conductive glue, sputter coated with gold, and examined on a JEOL 6301 Field Emission SEM using an accelerating voltage of 5 kV. The elemental compositions of selected

spots on these samples were determined with an energy dispersive X-ray (EDX) analyzer that is attached to the SEM and operated at an accelerating voltage of 20 kV.

Stable oxygen and carbon isotopic compositions were determined for the bedrock and calcareous crusts. Where possible, individual laminae in the laminar calcrete were analyzed separately. Powder samples were dissolved in H_3PO_4 at 25°C in a constant temperature water bath for 60 minutes following the protocol outlined by McCrea (1950). The evolved gases were analyzed on a Finnigan MAT 251 mass spectrometer. The isotope values are calibrated relative to the Vienna Peedee Belemnite using the NBS 19 ($\delta^{18}O$ = –2.20‰, $\delta^{13}C$ = +1.95‰) and NBS 18 ($\delta^{18}O$ = –23.00‰, $\delta^{13}C$ = –5.00‰) standards. The accuracy is better than 0.2‰ for $\delta^{13}C$, and better than 0.6‰ for $\delta^{18}O$.

5. Results

5.1. Geomorphic setting

At Rogers Wreck Point, the calcareous crust at the top of Unit D is exposed on a coastal platform that is frequently swept by waves, especially during windy weather. As a result, there is no soil or vegetation covering the crust (Fig. 4-2A). There, the reddish-brown, non-laminar calcrete contains numerous white fragments of corals and shells (Fig. 4-2B-D).

In the Tarpon Springs area, the laminar calcrete on top of Unit D is exposed (Fig. 4-2E, 4-2F), covered with soil, or submerged beneath shallow pools (Fig. 4-2E). Where soil is present, the vegetation in this area is dominated by buttonwood (*Conocarpus erecta*) and various grasses (Brunt and Davies, 1994, their Map 1). The laminar calcrete, present over a wide area (Montpetit, 1998), has an undulatory surface with a relief of up to 6 cm (Fig. 4-2F).

In the area south of Morgan's Harbour, the laminar calcrete on top of

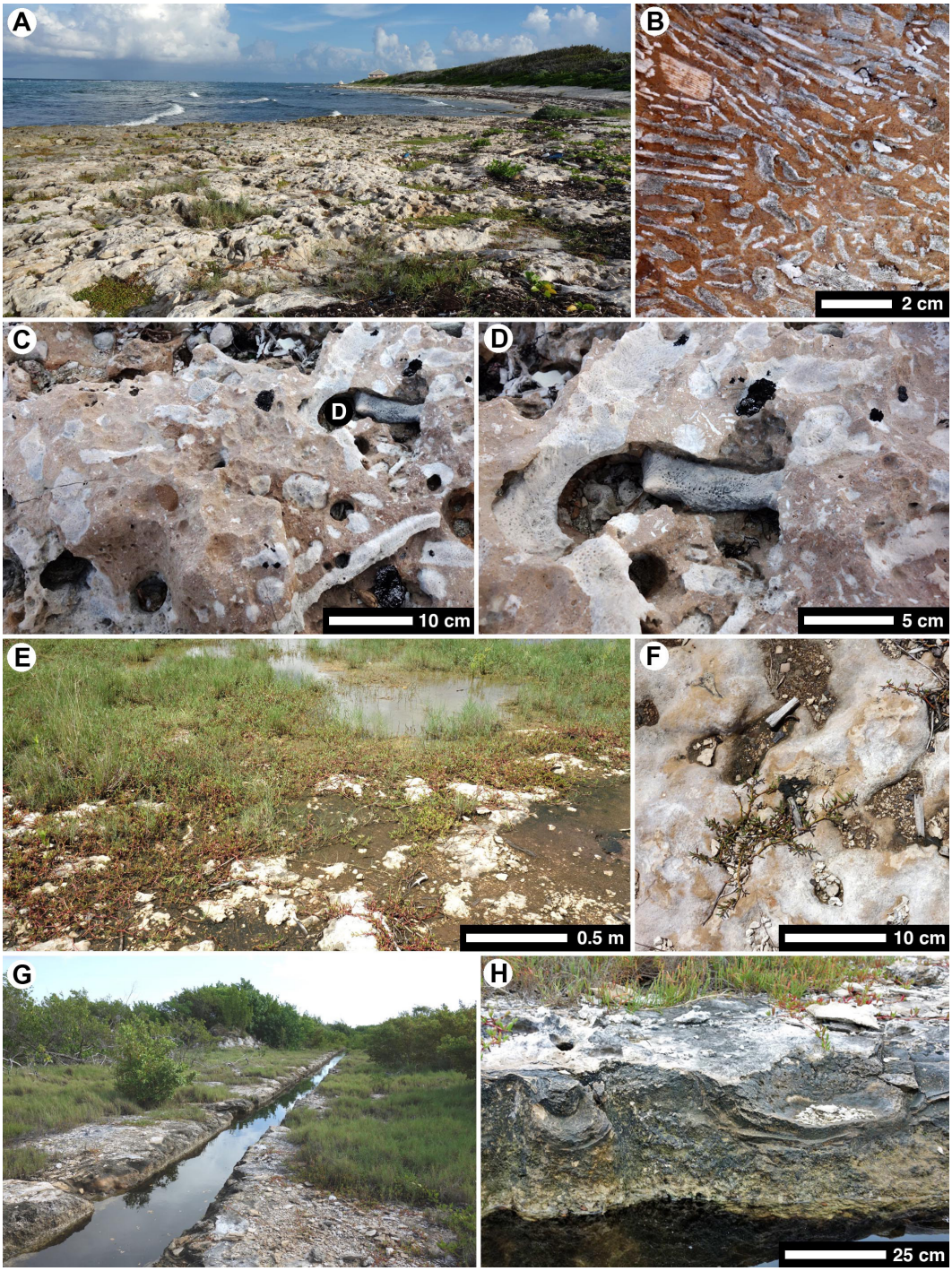

Fig. 4-2. Field photographs of calcareous crusts on exposed limestones of the Pleistocene Ironshore Formation, Grand Cayman. (A) Non-laminar calcrete with no vegetation or soil cover, Rogers Wreck Point. (B-D) White coral fragments and skeletal grains in non-laminar calcrete, Rogers Wreck Point area. Circled D in Panel C indicates location of Panel D. (E) Laminar calcrete at Tarpon Springs that is exposed to the atmosphere, covered by soil

and grass, or covered with shallow water. (F) Laminar calcrete with irregular surface, Tarpon Springs. (G) Laminar calcrete largely covered by trees and grasses, Morgan's Harbour area. Canal in centre of image is man-made. (H) Shallow and dish-like depressions in laminar calcrete, Morgan's Harbour area. Note vertical sections through dishes and lamination parallel to the original dish margins.

Unit D is areally extensive (Brunt and Davies, 1994). Throughout this area, the laminar calcrete is covered by a thin layer of soil that supports a vegetation dominated by black mangrove (*Avicennia germinans*), white mangrove (*Laguncularia racemosa*), and pickleweed (*Batis maritima*) (Fig. 4-2G; Brunt and Davies, 1994, their Map 1). The surface of the laminar calcrete is irregular, commonly with shallow channels and dish-like depressions with up to 10 cm relief (Fig. 4-2H). In nearby coastal exposures near Little Salt Creek and Salt Creek (Fig. 4-1B), Unit F unconformably overlies Unit D (Jones and Pemberton, 1989; Coyne et al., 2007), but there is no evidence of a calcareous crust at the top of Unit D (Jones and Pemberton, 1989, their Fig. 5; Coyne et al., 2007, their Fig. 8). Instead, the boundary between the units is marked by an uneven marine erosion surface (Fig. 4-3) that commonly has large, tabular lithoclasts resting on its surface (Jones and Pemberton, 1989; Coyne et al., 2007).

5.2. Stratigraphic succession

Samples capped by laminar calcrete can generally be divided into (1) unaltered host rock, (2) a transition zone in the bedrock, 0 to 6 cm thick (Fig. 4-4A-D), and (3) the laminar calcrete that is up to 6 cm thick (Fig. 4-4E, 4-4F). The transitional zone, however, is commonly absent (Fig. 4-5).

5.2.1. Host rock

At Rogers Wreck Point, the host rock is a skeletal wacke/pack/grain/floatstone containing scattered corals (Fig. 4-5B) that are commonly at or close

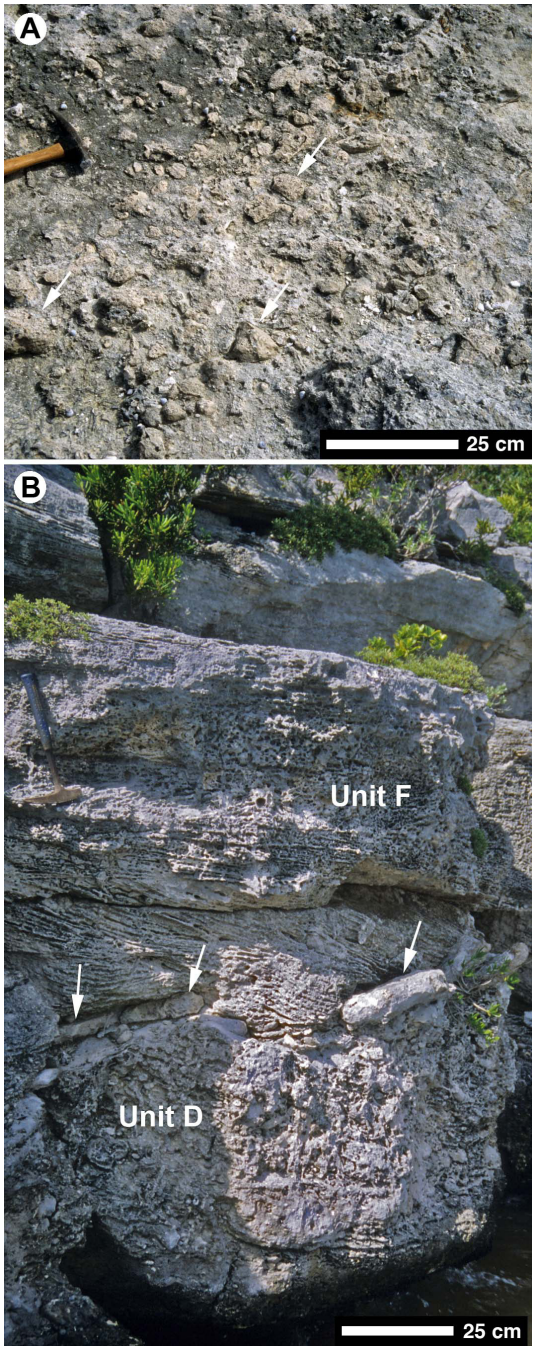

Fig. 4-3. Field photographs showing unconformity between units D and F of the Ironshore Formation, without any calcareous crust, west coast of North Sound just north of Little Salt Creek (Fig. 4-1B). (A) Lithoclasts (indicated by arrows) on the top of Unit D, but with no trace of calcareous crust. (B) Vertical section showing unconformity at top of Unit D with large lithoclasts resting on it (indicated by arrows), overlain by unit F. No calcareous crust is present.

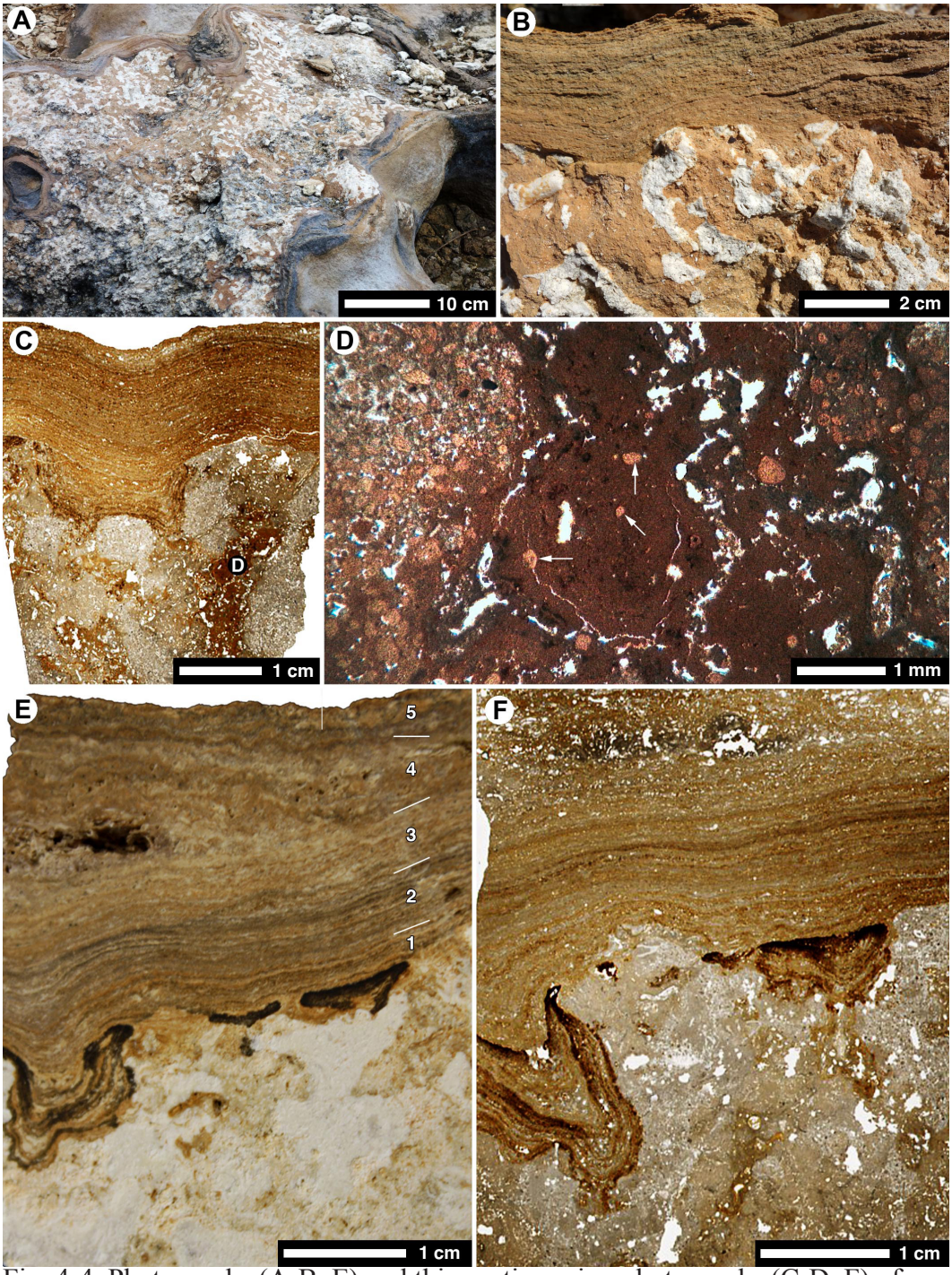

Fig. 4-4. Photographs (A-B, E) and thin section microphotographs (C-D, F) of laminar calcretes, Morgan's Harbour area. (A, B) Laminar calcrete and alteration zone with mottled fabric composed of patchy reddish calcrete and white unaltered host rock on top of oolitic limestone. (C) Laminar calcrete on top of alteration zone with diffuse boundaries between the reddish calcrete and unaltered oolitic host rock. Circled D in panel C indicates location of

panel D. (D) Calcrete patches in alteration zone containing ooid remnants (indicated by arrows). (E) Thick laminar calcrete with five distinct packages of laminae (1 to 5). (F) Laminar calcrete on top of alteration zone.

to life position. XRD analyses show that the host rock has 44 - 100 (average 81) wt% calcite (n = 45), whereas the coral skeletons contain less than 15 wt% calcite. These rocks are characterized by various marine (e.g., bioerosion, isopachous calcite cements) and vadose (e.g., dissolution and neomorphism of skeletal fragments, calcite cements) diagenetic fabrics (Li and Jones, 2013b).

At Tarpon Springs, the bedrock is a skeletal pack/grain/floatstone with foraminifera, bivalves, and conch being common (Fig. 4-5A). The host rock contains 33 - 55 (average 44) wt% calcite. As with the limestones from Rogers Wreck Point, common fabrics include (1) micritic envelopes around skeletal fragments, (2) small molluscan shell fragments (<2 mm), foraminifera, and *Halimeda* that have been partly dissolved and/or neomorphosed, and (3) meteoric calcite cements.

In the Morgan's Harbour area, the host rock is largely an ooid grainstone characterized by extensive *Ophiomorpha* burrow systems (Brunt et al., 1973; Woodroffe et al., 1980; Jones and Goodbody, 1984; Jones and Pemberton, 1989; Jones and Hunter, 1990; Shourie, 1993; Hunter and Jones, 1996; Coyne, 2003; Coyne et al., 2007). XRD analyses show that these grainstones contain 25 - 60 (average 40) wt% calcite (Li and Jones, 2013b). In these rocks, the aragonitic ooids are cemented by vadose meniscus calcite cement and phreatic blocky intergranular calcite cements (Li and Jones, 2013b).

5.2.2. Transition zone

There is no evidence of a transition zone in the Rogers Wreck Point area, where the reddish-brown non-laminar calcrete rests directly on the host limestone (Fig. 4-5B). Similarly, in the Tarpon Springs area, the boundary between the

laminar calcrete and the host rock is sharply defined (Fig. 4-5A) with no transition zone being present.

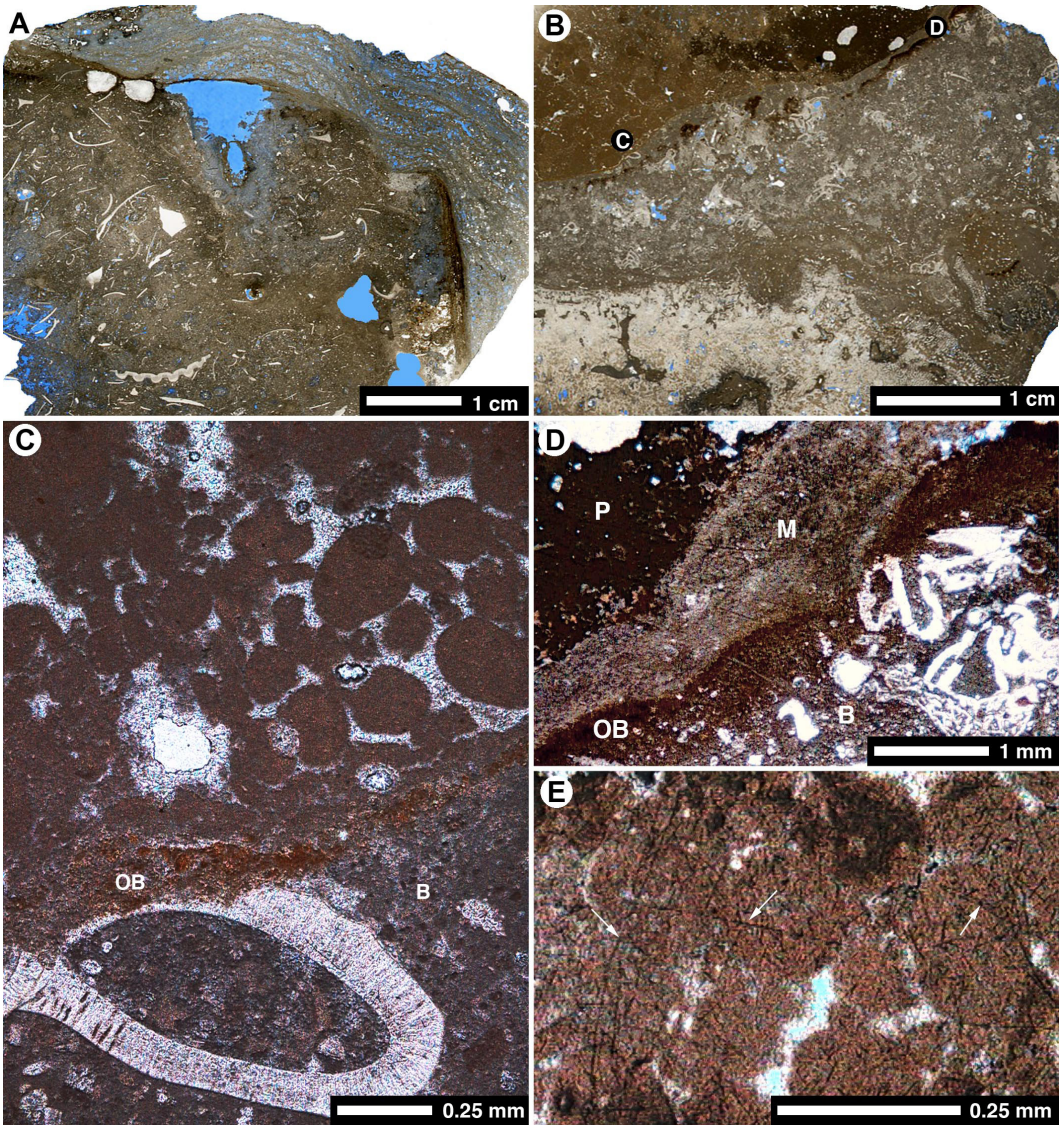

Fig. 4-5. Thin section microphotographs of laminar calcrete from Tarpon Springs (A) and non-laminar calcrete from Rogers Wreck Point (B-E). (A) Laminar calcrete on top of skeletal limestone. (B) Non-laminar calcrete and lithoclasts derived from underlying host rock. Circled C and D indicate location of panels C and D. (C) Bedrock (B) truncated by calcareous crust with organic-rich band (OB) at base overlain by peloidal zone. (D) Micritic grey band (M) with organic-rich band (OB) at bottom separating bedrock (B) from peloidal zone (P) of non-laminar calcrete. (E) Peloids with microborings (indicated by arrows).

In the Morgan's Harbour area, the transition zone between the host rock and the laminar calcrete, up to 6 cm thick, is mottled with irregular reddish-brown patches that contrast with the white host rock (Fig. 4-4A, 4-4B). These patches, up to 2.5 cm in diameter, have diffuse boundaries (Fig. 4-4C, 4-4D). XRD analyses show that the transitional zone as a whole contains about 33 - 58 (average of 47) wt% calcite, generally 10% more than in the host limestone. The altered bedrock in the transition zone (Fig. 4-6) is composed largely of dense

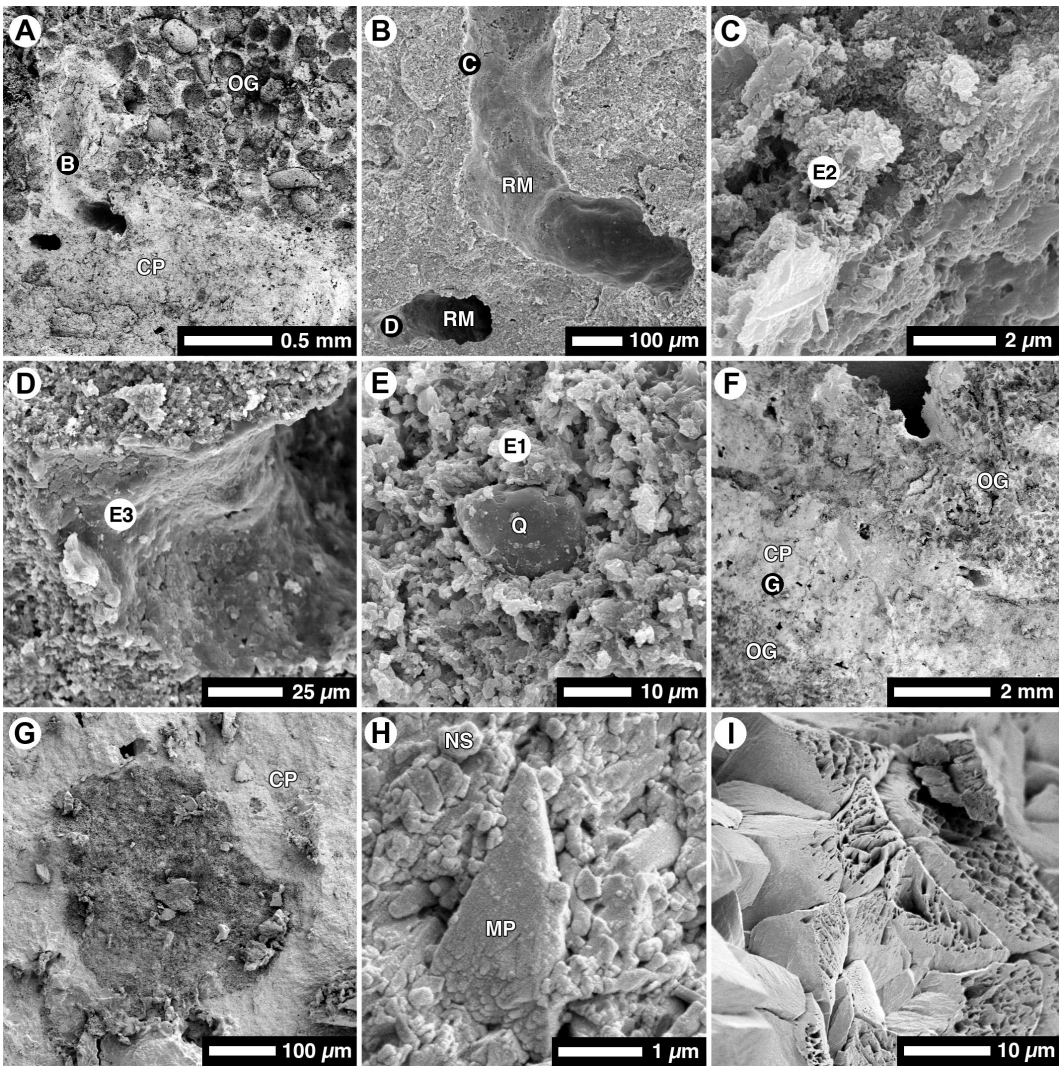

Fig. 4-6. SEM microphotographs showing microfabrics in alteration zone below laminar calcrete at Morgan's Harbour. (A) Calcrete patch (CP) with root molds in ooid grainstone (OG). Circled B indicates location of panel B. (B) Root molds (RM) in calcrete patch. Circled C and D indicate location of

panels C and D. (C, D) Coatings in the root molds. E2 and E3 indicate the positions of EDX analysis shown in Fig. 4-7B and 4-7C, respectively. (E) Micrite groundmass in calcrete patch with quartz (Q) grain. E1 indicates spot for EDX analysis shown in Fig. 4-7A. (F) Calcrete patch (CP) with cavities in ooid grainstones (OG). Circled G indicates location of panel G. (G) Aragonitic grain (ooid?) in calcrete patch (CP). (H) The groundmass of calcrete patch composed of varied micrite forms, including nano-spheres (NS), micro-rods, and micro-plates (MP). (I) Blocky microspars lining cavity in calcrete patch.

to porous micrite that is typically formed of nano-spheres, micro-rods, or platy micro-plates that are <1 μm long (Fig. 4-6H). Common features include (1) altered ooids that retain traces of their original internal fabrics (Fig. 4-6G), (2) minor amounts of quartz (Fig. 4-6E), and (3) root moulds, which are tubular voids left after decay of the roots (Fig. 4-6A, 4-6B; cf., Klappa, 1980), and cavities (Fig. 4-6F) that are up to 200 μm in diameter. EDX analyses of the micrite indicate that it contains Mg, Al, Si, and Fe (Fig. 4-7A). Many of the voids are coated with a film of Fe-Mn oxide-hydroxides (Figs. 4-6C, 4-7B), micrite (Figs. 4-6D, 4-7C), or blocky microspar (Fig. 4-6I).

5.2.3. Non-laminar and laminar calcrete

Non-laminar calcretes are found in the Rogers Wreck Point area (Figs. 4-2B-D, 4-5B) whereas laminar calcretes are found at Tarpon Springs (Fig. 4-5A) and Morgan's Harbour (Fig. 4-4). XRD analyses show that, irrespective of location, these calcareous crusts consist of 100% low Mg calcite (LMC) along with trace amounts of quartz. EDX analyses indicate that the groundmass and void fillings contain various combinations of Al, Mg, Si, Fe, Mn, Ti, Na, S, and K, albeit in trace amounts.

At Rogers Wreck Point, the reddish brown, non-laminar calcretes contain white biofragments (Fig. 4-2B-D) and lithoclasts derived from the host limestone

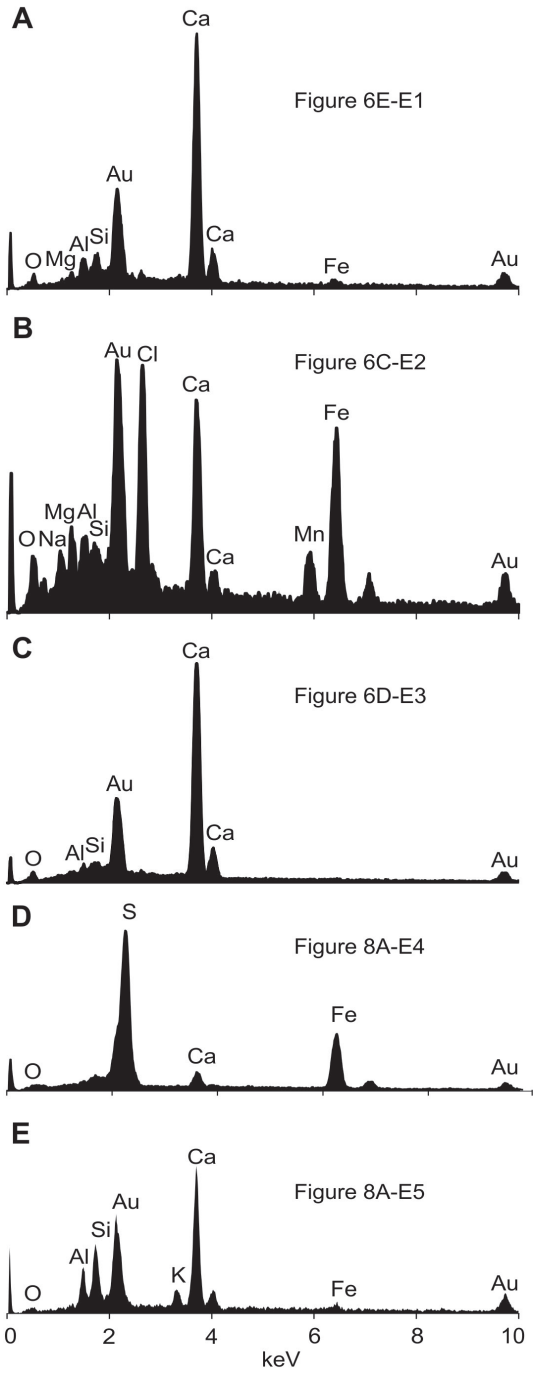

Fig. 4-7. EDX analyses for micrite groundmass (A, D-E) and various coatings (B-C) in alteration zone from the Morgan's Harbour area. Positions of EDX analyses are shown on Figs. 4-6C, 4-6D, 4-6E, and 4-8A.

(Fig. 4-5B). The boundary between the calcrete and the skeletal fragment/host limestone is sharp and, in some cases, highlighted by a discontinuous black,

organic-rich band (Fig. 4-5B). Skeletal fragments in the host limestone are truncated by the organic-rich black band (Fig. 4-5C). Peloids (Fig. 4-5C, 4-5D) are present in the basal part of the calcrete, and dark coloured peloids rich in organic matter are associated with the root moulds (Fig. 4-5B).

At Tarpon Springs area, the laminar calcrete is 0.5 - 3 cm thick (average 1 cm), whereas in the Morgan's Harbour area the laminar calcretes are 1 - 6 cm thick (average 4 cm). The thickness of the laminar calcrete is uneven, with local thickening and thinning being common (Figs, 4-2H, 4-4E, 4-4F). Individual laminae are recognizable by the following:

- Colors that include light yellow, light brown, grey, dark grey, orange, reddish-brown, and black (Fig. 4-4).
- Porosity contrasts that discriminate porous and non-porous laminae. Porous laminae (1) are >1 mm thick, (2) contain numerous pores up to 1 mm in diameter, and (3) have poorly defined boundaries. In contrast, the non-porous laminae (1) are <1 mm thick, (2) contain few pores, and (3) have sharp boundaries.

Laminar calcretes can commonly be divided into packages of laminae (0.2 to 2.3 cm thick) that are defined by their colour and porosity. In one sample collected from Morgan's Harbour, for example, the crust is divided into five packages that are, in ascending stratigraphic order, (1) low porosity, mostly light coloured laminae but with some discrete black laminae, (2) low porosity, alternating light and dark coloured laminae, (3) low porosity, dominantly light laminae, (4) high porosity, vaguely laminated, and (5) low porosity, alternating light and dark coloured laminae (Fig. 4-4E). The packages, however, are laterally discontinuous over distances of as little as 25 cm (Fig. 4-2H) and vary from sample to sample. Even individual package at the scale of hand sample are characterized by laterally discontinuous laminae that develop or pinch out at

random.

5.3. Components of calcareous crusts

The calcareous crusts are characterized by variable assemblages of micrite, calcified roots, peloids, needle fibre calcite, alveolar septal structures, calcified filaments and extracellular polymeric substances (EPS), microborings, and various void fillings.

5.3.1. Micrite

All of the calcareous crusts are composed largely of micrite, with grains <1 μm long (Fig. 4-8A, 4-8B). Particles range from nanospheres, to nodular clusters of smaller crystals (Fig. 4-8A), to elongate micro-rods (Fig. 4-8A), to sub-euhedral blocks (Fig. 4-8B). EDX analyses show that the micrite commonly contains trace amounts of Al, K, Si, Fe, and Cl. Pyrite (Fig. 4-7D) and clay minerals (Fig. 4-7E) occur locally.

5.3.2. Calcified roots

Root structures, up to 7 mm long and 2 mm in diameter, are present in both the laminar and non-laminar calcretes. In general, however, they are most common and best preserved in the laminar calcretes, and especially in the porous laminae. In the laminar calcretes from Morgan's Harbour and Tarpon Springs, variably preserved calcified roots are common (Figs. 4-8C-I, 4-9). The cells of the epidermis (or rhizoderm remnants) are partially preserved (Fig. 4-8C, 4-8D) or completely lost (Fig. 4-8E). Root cortices are commonly calcified and the central vascular systems of roots are missing. Rootlets, about 200 μm in diameter, are associated with most of the root structures (Fig. 4-8E). Preservation is locally good with calcified cell walls (Fig. 4-8F, 4-8G), calcified plasmodesmata (Fig. 4-8H), and other perforations (Fig. 4-8I) being evident. The prismatic,

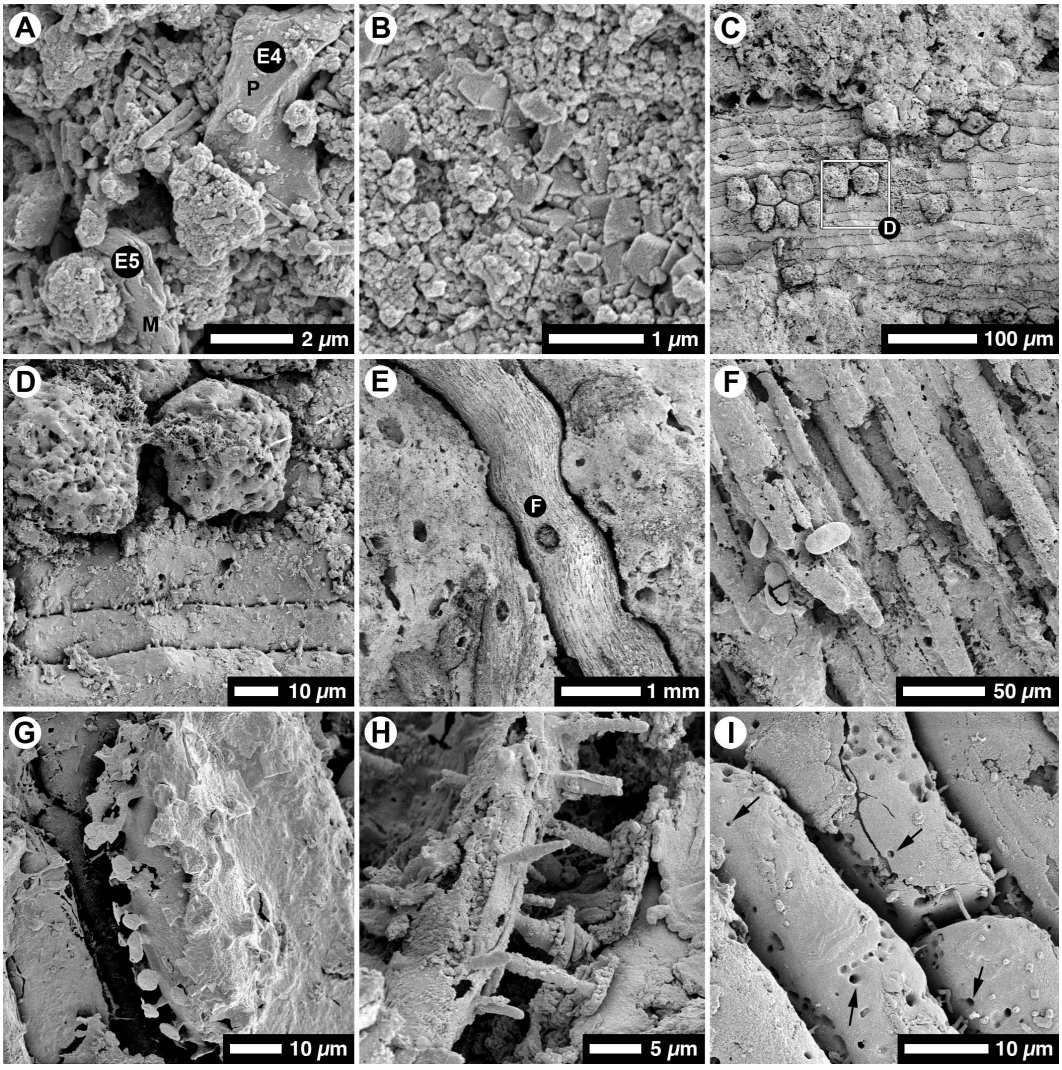

Fig. 4-8. SEM microphotographs of micrite (A-B) and calcified root structures (C-I) in calcareous crusts. (A) Nodular cluster of smaller grains and micro-rods, with pyrite (P) and clay minerals (M) being present. Morgan's Harbour. E4 and E5 indicate spots of EDX analyses shown in Fig. 4-7D and 4-7E. (B) Sub-euhedral to euhedral calcite in micrite groundmass of non-laminar calcrete, Rogers Wreck Point. (C, D) Calcified root partially coated by rhizoderm remnants. Morgan's Harbour. Box in panel C indicates location of panel D. (E) Calcified root with rootlet but no epidermal cells. Morgan's Harbour. Circled F indicates location of panel F. (F, G) Calcified root cells with cell walls preserved. Morgan's Harbour. (H) Calcified plasmodesmata between calcified root cells. Morgan's Harbour. (I) Calcified root cells with pits (indicated by arrows) on cells and some plasmodesmata remnants. Morgan's Harbour.

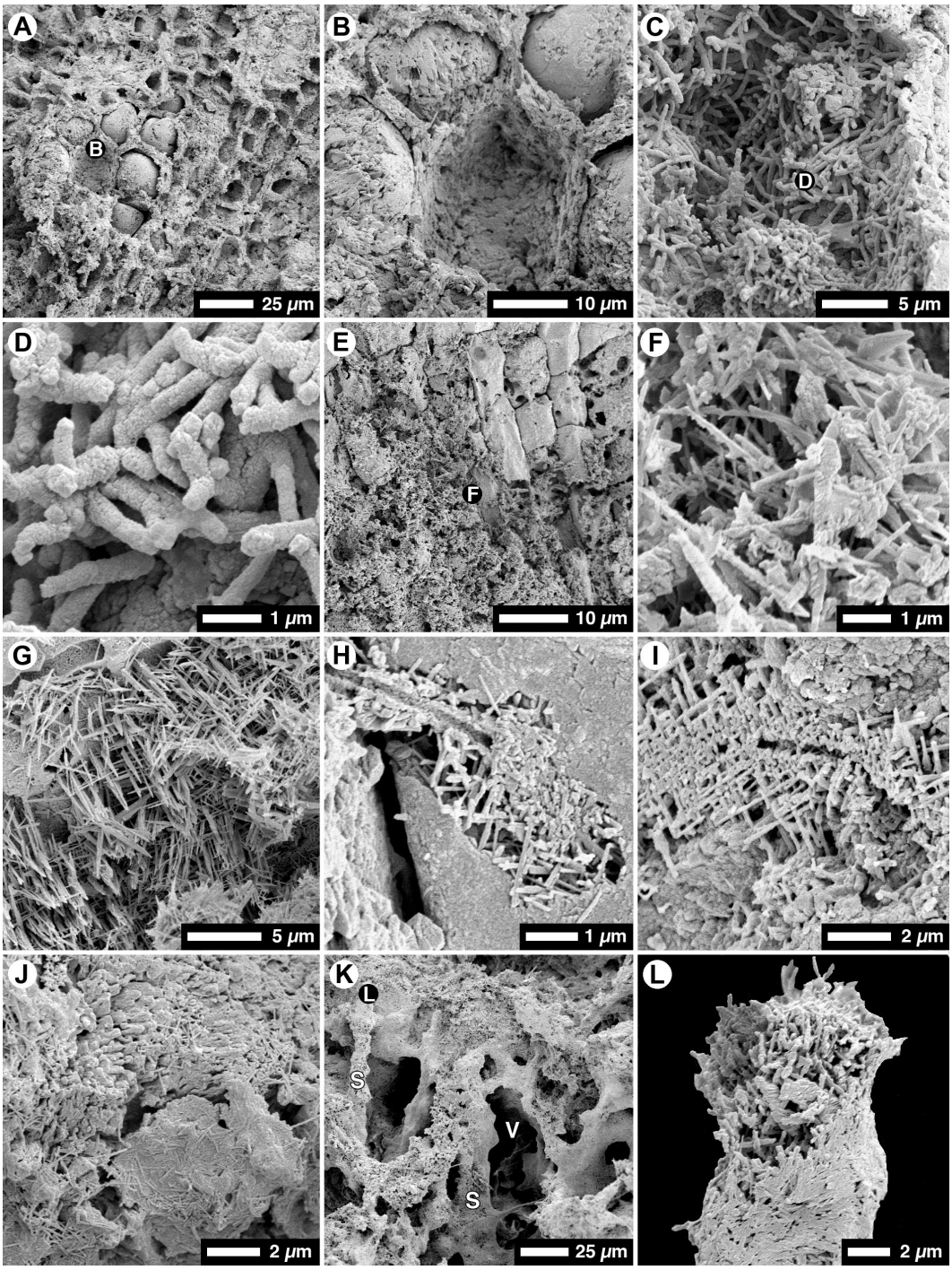

Fig. 4-9. SEM microphotographs showing poorly preserved root structures (A-F) and needle fibre calcite crystal fabrics (G-L). (A, B) Calcified root cells with poorly preserved internal structures. Tarpon Springs. Circled B in panel A indicates location of panel B. (C, D) Empty root cell voids filled with calcified filaments. Circled D in panel C indicates location of panel D. Morgan's Harbour. (E) Poorly preserved root cell structure. Circled F

indicates location of panel F. Tarpon Springs. (F) Root cells partly filled with needle fibre calcite crystals. Tarpon Springs. (G) Interwoven needle fibre calcite crystals coating wall of void. Tarpon Springs. (H) Interwoven needle fibre calcite crystals coating tubular filament penetrating calcified root cells. Tarpon Springs. (I) Interwoven needle fibre calcite crystals coating voids. Tarpon Springs. (J) Needle fibre calcite crystals coating substrate. Morgan's Harbour. (K) Alveolar septal structure with voids (V) surrounded by anastomosing septa (S). Circled L indicates location of panel L. Morgan's Harbour. (L) Septa composed of micrite with an outer layer of needle fibre calcite crystals. Morgan's Harbour.

polyhedral, and spherical calcified root cells are about 20 μm wide. Sections through the calcified cells reveal central crystalline parts encased by a thin, poorly crystallized outer layer. Borings, 1-2 μm in diameter, are present locally.

In some root cells, the cell walls have been calcified whereas the interiors have been lost (Fig. 4-9A, 4-9B). In many cases, these voids have been partially filled with calcified filaments that are 0.5 μm in diameter and 1-2 μm long (Fig. 4-9C, 4-9D). When both the cells walls and internal cells are destroyed (Fig. 4-9E), however, the voids are usually occupied by needle fibre calcite crystals (Fig. 4-9F).

In the non-laminar calcretes from Rogers Wreck Point, root cells are rare and poorly preserved. In most cases, the roots have been lost and root moulds, about 100 μm in diameter, are all that remain.

5.3.3. Peloids

Spherical to elliptical micritic peloids, 100-500 μm long, associated with root moulds (Fig. 4-5B) were found only in the non-laminar calcretes from Rogers Wreck Point. In thin section, a dark coloured peloidal zone is separated from the underlying host rock by a gray band with irregular thickness of up to 3 mm (Fig. 4-5D). The gray band is composed of micrite that contains trace amounts of Mg. In contrast, the light coloured peloidal zones display no gray band below, and they

are separated from underlying host only by the black band rich in organic matter (Fig. 4-5C). The skeletal fragments in the host limestone are usually truncated by the black band above (Fig. 4-5C). The boundary between dark coloured peloids and light coloured peloids is diffuse (Fig. 4-5B). Even in a single peloid, both dark and light color could be present. Some peloids contain remnants of skeletal fragments. Microborings, about 2 μm in diameter and up to 100 μm long, are present in many peloids (Fig. 4-5E).

5.3.4. Needle fibre calcite

Needle fibre calcite crystals, found mostly in the laminar calcretes from Tarpon Springs and Morgan's Harbour, are 1-5 μm long and 0.1-0.5 μm wide (Fig. 4-9G-J). In some areas, these crystals form a dense interwoven mesh (Type I) whereas in other areas the crystals are widely scattered (Type II). Type I crystals usually line voids (Fig. 4-9G) and filaments (Fig. 4-9H, 4-9I), whereas Type II crystals usually randomly fill in the voids and/or coat the substrate (Fig. 4-9J).

5.3.5. Alveolar septal structures

Well-developed alveolar-septal structures, found only in the laminar calcretes and commonly associated with root structures, consist of spheroidal and irregular voids that are segmented by anastomosing septa (Fig. 4-9K). The septa, about 10 μm thick, consist of micritic cores that are coated by needle fibre calcite crystals (Fig. 4-9L).

5.3.6. Calcified filaments/EPS

Solid and tubular calcified filaments, 0.5 - 20 μm in diameter and 1 - 200 μm long, are typically found in voids in the calcareous crusts. They are variously coated with micrite (Fig. 4-10A), needle fibre calcite (Fig. 4-10B), and/or microspar.

Strands and sheets of EPS are found throughout the calcareous crusts (Fig. 4-10C-E). The walls of many cavities are coated with thin (~5 µm), smooth, and dense micritic films (Fig. 4-10E), may represent calcified EPS.

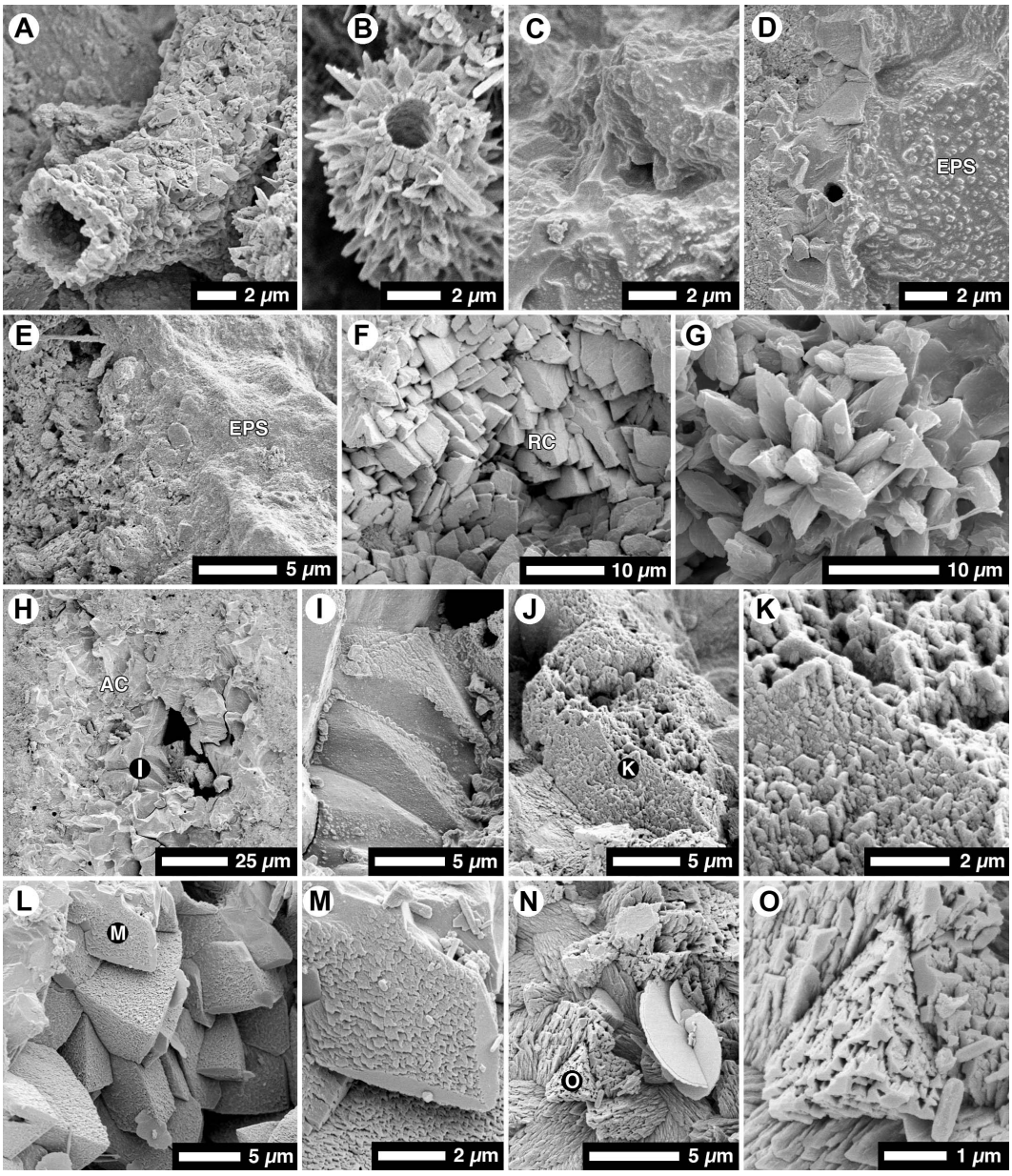

Fig. 4-10. SEM microphotographs of calcified filaments (A-B), EPS (C-E), and various spar and microspar cements (F-O). (A) Tubular filament composed of micrite. Tarpon Springs. (B) Tubular filament coated with needle fibre calcite crystals. Tarpon Springs. (C) Strands of EPS in calcrete crust. Rogers Wreck Point. (D, E) Sheets of EPS coating calcareous crusts groundmass. D is from Rogers Wreck Point, and E is from Morgan's Harbour. (F)

Rhombohedral calcite crystals (RC). Morgan's Harbour. (G) Rosette of calcite crystals. Morgan's Harbour. (H, I) Anhedral calcite crystals (AC) with overgrowths of euhedral calcite crystals. Rogers Wreck Point. Circled I indicates location of panel I. (J, K) Incomplete growth of composite trigonal crystals formed of numerous subcrystals. Rogers Wreck Point. Circled K in panel J indicates location of panel K. (L-O) Composite trigonal crystals formed of numerous trigonal subcrystals. Tarpon Springs. Circled M and O in panels L and N indicate location of panels M and O, respectively.

5.3.7. Microborings

Endolithic microborings, typically about 1 μm in diameter, are found in the calcareous crusts at all localities. They are empty, coated with EPS, or lined with micrite and/or spores. The microborings penetrate all substrates, including the peloids (Fig. 4-5E), calcified root structures (Fig. 4-9H), cements in void, and the micritic groundmass.

5.3.8. Microspar in voids

Microspar, formed of crystals 4 - 30 μm long (cf., Folk, 1959), includes rhombohedral crystals (Fig. 4-10F), rosettes of trigonal prisms (Fig. 4-10G), anhedral crystals (Fig. 4-10H), and composite trigonal crystals (cf., Binkley et al., 1980, their Fig. 2; Jones and Renaut, 1996, their Fig. 3) (Fig. 4-10I-O). Many of the anhedral microspar crystals are coated with syntaxial overgrowths of trigonal calcite crystals (Fig. 4-10H, 4-10I). The composite trigonal crystals, each formed of numerous trigonal subcrystals, are characterized by incomplete crystal walls and cores (Fig. 4-10J-O). The rhombohedral crystals and rosettes of trigonal prisms are found only in the laminar calcretes from the Morgan's Harbour area, whereas the anhedral and composite trigonal crystals are common in all three localities.

5.3.9. Other components

Other components scattered throughout the calcareous crusts include

spores, Fe and/or Mn precipitates, gypsum, halite, and pyrite.

Calcified and broken spherical spores, ~1 μm in diameter (Fig. 4-11A), occur alone or in clusters lining microborings and sitting on the surfaces of void cements. Although present in the calcareous crusts from all three localities, they are most common in the laminar calcretes from Morgan's Harbour and Tarpon Springs.

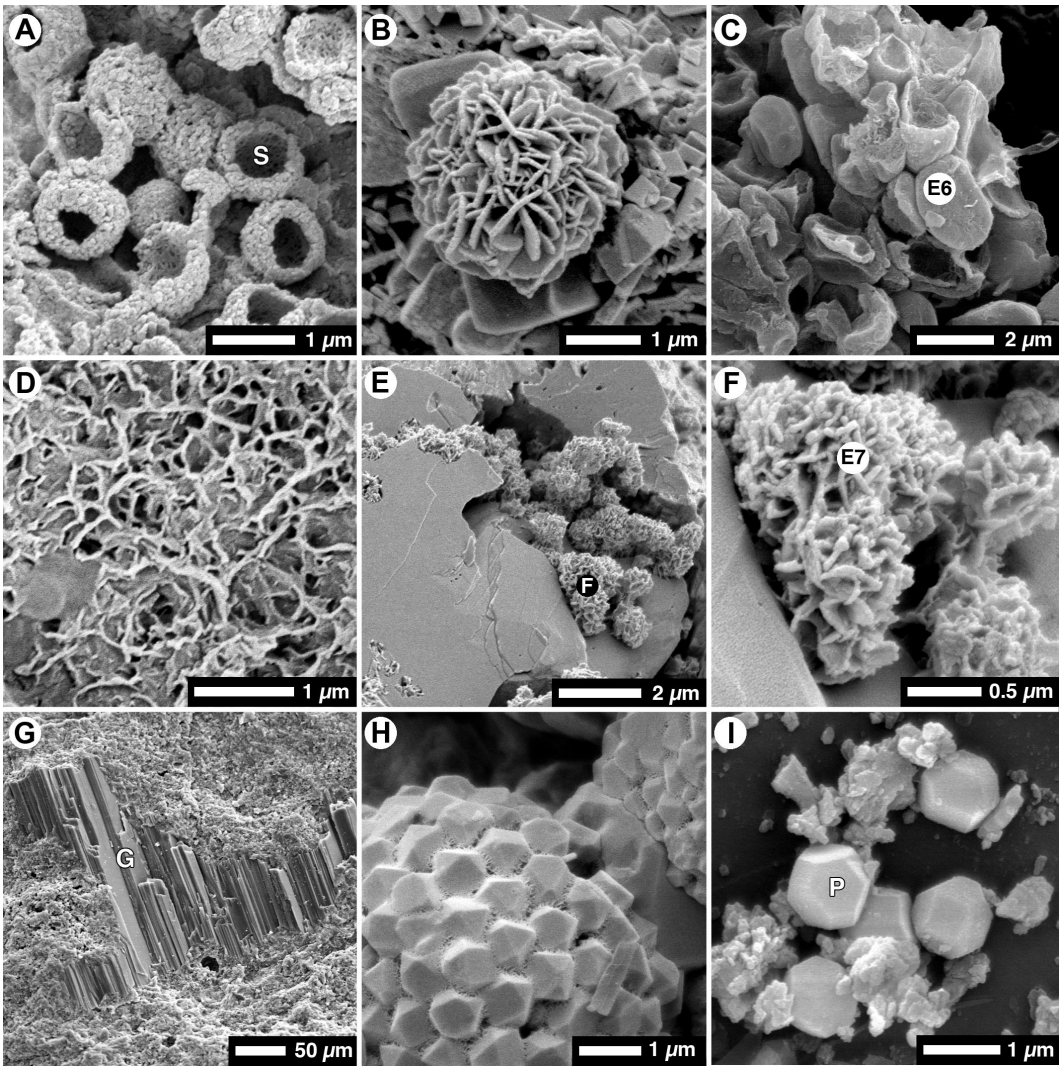

Fig. 4-11. SEM microphotographs showing spores, various Fe-Mn oxides/hydroxides, gypsum, and pyrite in calcareous crusts. (A) Calcified spores (S) in laminar calcrete groundmass. Tarpon Springs. (B) Rosette of bladed Fe-Mn precipitates. Morgan's Harbour. (C-F) Reticulate Fe-Mn precipitate coatings. C, E, and F are from Morgan's Harbour; D is from Tarpon Springs. Circled F in panel E indicates location of panel F. E6 and E7 indicate spots for

EDX analyses shown in Fig. 4-12. (G) Gypsum (G) filling void in laminar calcrete. Morgan's Harbour. (H) Framboidal pyrites associated with voids in root structures. Morgan's Harbour. (I) Dodecahedron pyrite crystals (P) on surface of gypsum. Morgan's Harbour.

The morphologically variable Mn-Fe precipitates, and/or Fe precipitates, coat void surfaces and grains as rosettes of bladed crystals (Fig. 4-11B), reticulate coatings (Fig. 4-11C-F), and fuzzy coating (Fig. 4-6C) in all the three localities. Along with Mn precipitates, trace amounts of Fe are usually detected by EDX analyzer (Fig. 4-12). Fe precipitates, however, can occur without Mn being present. Some Fe precipitates appear inside or on the surface of gypsum (Fig. 4-11E, 4-11F).

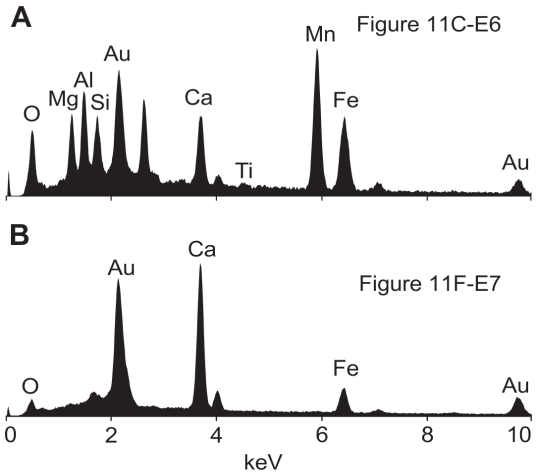

Fig. 4-12. EDX analyses of coatings in laminar calcrete from the Morgan's Harbour area. Positions of analyses are shown on Fig. 4-11C and 4-11F, respectively.

Gypsum (Fig. 4-11G) and halite are found in some of the cavities and desiccation cracks in the calcareous crusts from all three localities. In the laminar calcretes from Morgan's Harbour, framboidal and dodecahedron pyrite crystals are found in some root cavities (Fig. 4-11H, 4-11I).

5.4. Stable isotope composition

5.4.1. Host rock

Eight samples from Unit D in the Rogers Wreck Point area (97 - 100 wt% calcite) yielded an average $\delta^{18}O$ value of -5.91‰ and an average $\delta^{13}C$ value of -5.95‰ (Li and Jones, 2013b). One sample of skeletal floatstone from the Tarpon Springs area, with 55 wt% calcite, yielded a $\delta^{18}O$ value of -3.33‰ and a $\delta^{13}C$ value of -3.73‰.

In the Morgan's Harbour area, two ooid grainstones, both with 46% wt% calcite, yielded $\delta^{18}O$ values of -3.35‰ and -3.16‰ (average -3.25‰), and $\delta^{13}C$ values of +0.60‰ and +1.14‰ (average 0.87‰).

These stable isotope values, like the isotopic compositions of corals and

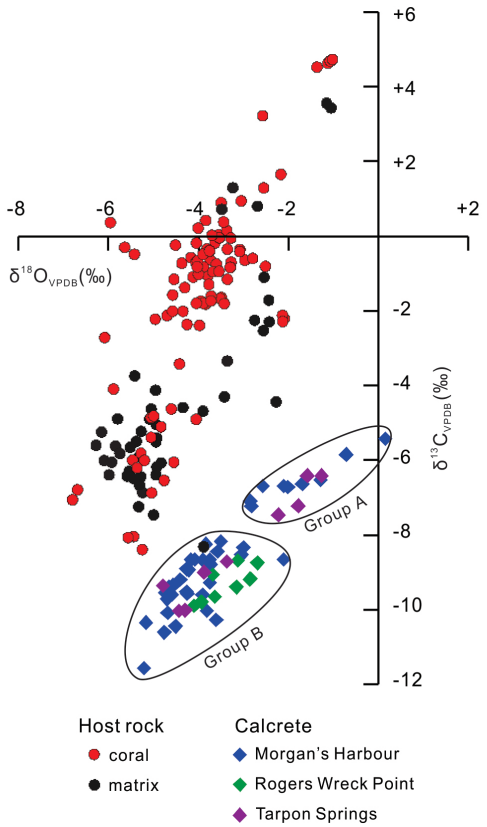

Fig. 4-13. Cross-plot of δ13C versus δ18O for calcareous crusts, and matrix and coral fragments in host rocks.

matrices derived from the Pleistocene Ironshore Formation (Li and Jones, 2013b), plot along the same trend line (Fig. 4-13).

5.4.2. Calcareous crust

The oxygen isotopic compositions of the calcareous crusts are similar to those of the host rocks, whereas the stable carbon isotopic compositions are significantly different (Fig. 4-13). In the Rogers Wreck Point area, the $\delta^{18}O$ and $\delta^{13}C$ values of the non-laminar calcretes are -4.09‰ to -2.69‰ and -9.89‰ to -8.68‰, respectively (Table 4-1). In the Tarpon Spring area, the $\delta^{18}O$ and $\delta^{13}C$ values of the laminar calcretes are -4.44‰ to -1.26‰, and -10.03‰ to -6.41‰, respectively (Table 4-1). In the Morgan's Harbour area, laminar calcretes yielded $\delta^{18}O$ and $\delta^{13}C$ values of -5.22‰ to +0.16‰, and -11.57‰ to -5.43‰, respectively (Table 4-1). Such data show that the isotopic signatures of the laminar calcretes are more variable than those from the non-laminar calcretes.

Table 4-1. Stable oxygen and carbon isotopic compositions of calcareous crusts developed on exposed limestones of Pleistocene Ironshore Formation. Total sample size is 58.

Morgan's Harbour (N=39)		$\delta^{18}O_{VPDB}$ (‰)	$\delta^{13}C_{VPDB}$ (‰)	Group
MH-1 top	porous	-3.83	-8.25	B
MH-1 middle	dense	-4.40	-9.21	B
MH-1 bottom	dense	-2.10	-8.66	B
MH-2 top	dense	0.16	-5.43	A
MH-2 upper middle	porous	-0.71	-5.84	A
MH-2 lower middle	dense	-3.73	-8.78	B
MH-2 bottom	dense	-2.85	-7.09	A

MH-3 bottom	dense	-3.58	-8.45	B
MH-4 top	dense	-4.09	-8.66	B
MH-4 upper middle	dense	-4.21	-8.94	B
MH-4 lower middle	dense	-4.75	-9.54	B
MH-4 bottom	dense	-3.60	-10.27	B
MH-5 middle	dense	-4.65	-9.38	B
MH-6 top	porous	-5.16	-10.35	B
MH-6 bottom	dense	-5.22	-11.57	B
MH-7_top	dense	-4.26	-8.91	B
MH-7_upper middle	dense	-4.17	-8.67	B
MH-7_middle	dense	-4.66	-9.52	B
MH-7_lower middle	dense	-4.56	-9.35	B
MH-7_bottom	dense	-4.70	-9.72	B
MH-8 top	dense	-3.75	-8.67	B
MH-8 upper middle	dense	-3.75	-9.27	B
MH-8 lower middle	dense	-4.51	-10.45	B
MH-8 bottom	dense	-4.76	-10.61	B
MH-9 top	dense	-2.01	-6.72	A
MH-9 top	dense	-2.10	-6.70	A
MH-9 middle	porous	-2.56	-6.69	A

MH-9 bottom	dense	-1.28	-6.52	A
MH-10 top	dense	-2.82	-7.24	A
MH-10 middle	dense	-3.50	-8.17	B
MH-10 bottom	dense	-3.05	-8.54	B
MH-13 top	dense	-4.26	-9.52	B
MH-13 middle	dense	-4.68	-10.09	B
MH-13 bottom	porous	-4.60	-9.61	B
MH-14 top	dense	-1.69	-6.63	A
MH-14 upper middle	dense	-3.00	-8.34	B
MH-14 middle	dense	-4.25	-9.58	B
MH-14 lower middle	dense	-3.91	-9.60	B
MH-14 bottom	dense	-3.82	-10.03	B

Rogers Wreck Point (N=10)		$\delta^{18}O_{VPDB}$ (‰)	$\delta^{13}C_{VPDB}$ (‰)	Group
RWP-1	Non-laminar	-2.69	-8.75	B
RWP-3 brown	Non-laminar	-4.09	-9.89	B
RWP-3 dark brown	Non-laminar	-2.86	-9.19	B
RWP-3 light brown	Non-laminar	-3.64	-9.66	B
RWP-3 light brown	Non-laminar	-3.93	-9.80	B
RWP-3 dark brown	Non-laminar	-2.84	-9.17	B
RWP-3 light brown	Non-laminar	-3.94	-9.78	B

RWP-4 brown matrix between coral	Non-laminar	-3.12	-8.68	B
RWP-5	Non-laminar	-3.68	-9.06	B
RWP-5	Non-laminar	-3.15	-9.40	B
Tarpon Springs (N=9)		$\delta^{18}O_{VPDB}$ (‰)	$\delta^{13}C_{VPDB}$ (‰)	Group
TSS-1 top	porous	-1.58	-6.41	A
TSS-2 middle	porous	-3.37	-8.71	B
TSS-2 bottom	dense	-3.87	-9.00	B
TSS-3 top layer	dense	-1.78	-7.22	A
TSS-3 bottom	dense	-4.44	-10.03	B
TSS-4 top	porous	-2.22	-7.46	A
TSS-4 middle	porous	-4.80	-9.36	B
TSS-4 bottom	porous	-4.29	-10.02	B
TSS-5	porous	-1.26	-6.42	A

In the laminar calcretes, the isotopic compositions of the dense laminae are essentially the same as those from the porous laminae (Table 4-1). A cross-plot of $\delta^{18}O$ against $\delta^{13}C$ shows that all of the isotope values for all the calcareous crusts plot along the same trend line (Fig. 4-13). Nevertheless, two groups can be distinguished, with Group A having more positive carbon values than Group B (Fig. 4-13). Laminar calcretes from Tarpon Springs and Morgan's Harbour belong to Groups A to B whereas the non-laminar calcretes from Rogers Wreck Point all belong to Group B. In general, all the samples that plot in Group A come from the uppermost (youngest) laminae of the laminar calcretes. The uppermost laminae tend to have more positive $\delta^{18}O$ and $\delta^{13}C$ values than those in the

lowermost part of the crusts (Fig. 4-14).

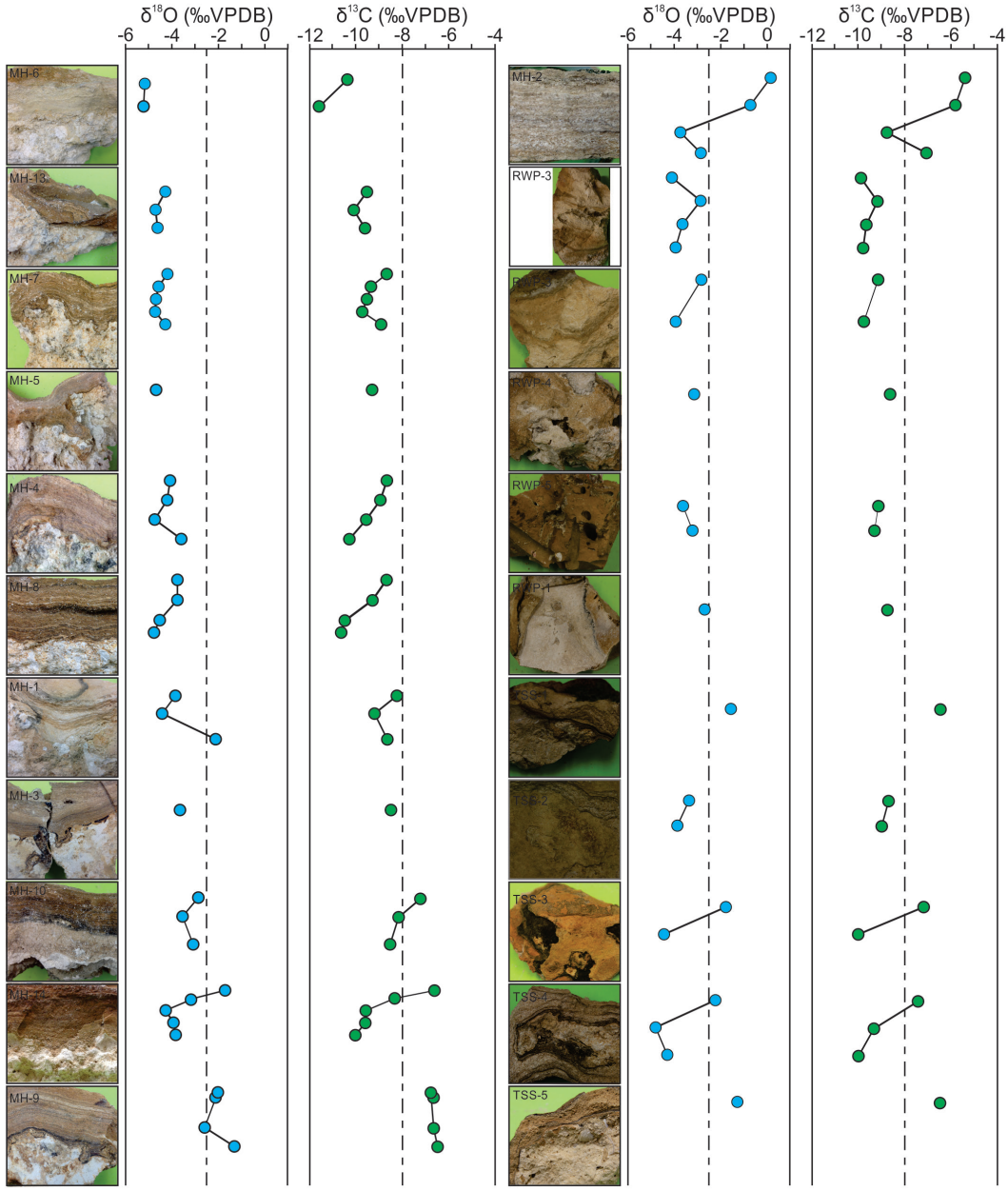

Fig. 4-14. Variation of δ13C and δ18O with depth in calcareous crusts collected from Rogers Wreck Point, Tarpon Springs, and Morgan's Harbour. Detailed information for each sample is given in Table 4-1.

6. Interpretation

The formation of calcareous crusts has been attributed to (1) surface accretionary build-up (e.g., Gile et al., 1966; Multer and Hoffmeister, 1968;

Robbin and Stipp, 1979; Coniglio and Harrison, 1983; Wright et al., 1988, 1995; Eren et al., 2008), or (2) *in situ* alteration of the bedrock (e.g., James, 1972; Goudie, 1973; Read, 1974; Harrison, 1977; Kahle, 1977; Knox, 1977; Watts, 1978; Arakel, 1982). The calcareous crusts associated with Unit D of the Ironshore Formation on Grand Cayman are characterized by a variety of petrographic and geochemical signatures that collectively reflect their genetic evolution (Table 4-2). Any model developed to explain their origin must account

Table 4-2. Features of microfabrics and stable isotope compositions in bedrock, transitional zone, and calcareous crusts. X = present, O = not observed in samples. VC = very common, C = common, R = rare.

	Laminar calcrete	Non-laminar calcrete	Transitional zone	Bedrock
Micrite	X (VC)	X (VC)	X (VC)	X (C)
Calcified root	X (VC)	(root mould only)	(root mould only)	O
Peloids	O	X (C)	O	O
NFC	X (VC)	X (R)	X (R)	X(R)
Alveolar septal	X (C)	O	O	O
Calcified filaments	X (VC)	X (R)	O	O
EPS	X (VC)	X (VC)	X (R)	X (R)
Microbor-ings	X (VC)	X (C)	X (C)	X (R)
Composite trigonal crystals	X (VC)	X (VC)	O	X (C)
Trigonal microspar	X (R)	O	X (R)	X (C)
Anhedral microspar	O	X (C)	X (C)	X (C)
Spores	X (VC)	X (C)	O	X (R)
Fe/Mn precipitate	X (VC)	X (C)	X (R)	O
Pyrite	X (R)	O	O	O

Gypsum	X (R)	O	O	O
Halite	X (VC)	X (C)	X (C)	X (C)
$\delta^{18}O$ (‰) range (average)	TS −4.44 to −1.26 (-3.07) MH −5.22 to +0.16 (-3.57)	RWP −4.09 to −2.69 (−3.39)	NA	RWP average -5.91 (100% calcite) TS -3.33 (55% calcite) MH -3.35 to -3.16 (-3.25) 46% calcite
$\delta^{13}C$ (‰) range (average)	TS −10.03 to −6.41 (-8.29) MH −11.57 to −5.43 (-8.71)	RWP −9.89 to −8.68 (-9.34)	NA	RWP average -5.95 (100% calcite) TS 3.73 (55% calcite) MH +0.60 to +1.14 (+0.87) 46% calcite

for the (1) stratigraphy of the calcareous crusts, (2) formation of non-laminar calcrete, (3) generation of porous and dense laminae in the laminar calcretes, (4) isotopic signatures of the calcareous crusts, and (5) age of the calcareous crusts.

6.1. Calcareous crust stratigraphy

At Rogers Wreck Point and Tarpon Springs, the calcareous crusts rest directly on the bedrock whereas those in the Morgan's Harbour area are separated from the bedrock by a transition zone (Fig. 4-4). Although the transition zone is critical to understanding the development of the calcareous crusts, its absence in some areas must also be explained.

That the transitional zone developed through localized diagenetic alteration of the host limestone is shown by (1) its mottled appearance (cf., Arakel, 1982), (2) its higher calcite content, and (3) the remnants of ooids, located in the reddish-brown patches, that have clearly undergone diagenetic alteration (Fig. 4-6G). The numerous microborings evident in the ooids, the intergranular sparry calcite cement of the host limestone, and micritization of the host limestone offer testimony to the importance of endolithic algae and fungi in the diagenetic

alteration of the host rock. Similar features are found in the alteration zone associated with Holocene calcrete crusts from the Florida Keys (Kahle, 1977; Tompkins, 1980; Coniglio and Harrison, 1983).

The calcareous crusts which all rest on limestones, are no more than 1 m above sea level (data from Vézina, 1997; Montpetit, 1998; Coyne, 2003). The local development of the transition zone in the Morgan's Harbour area, implies that the oolitic limestones are more susceptible to diagenetic alteration than the skeletal limestones found at Tarpon Springs and Rogers Wreck Point. Transformations in the transition zone involved micritization of the allochems and sparmicritization of the sparry calcite cements that can be attributed to concomitant dissolution-precipitation processes in a vadose environment (Kahle, 1977; Jones and Pemberton, 1986; Jones and Kahle, 1995). Given that the rate of dissolution in the vadose zone is largely diffusion-controlled (Constantz, 1986), the porosity and permeability of the host rock are crucial because they ultimately control the rate at which water moves through the limestone. The oolitic limestones from Morgan's Harbour have high porosity and permeability, are easily crushed, and water rapidly permeates through them. The presence of numerous open *Ophiomorpha* burrows also provides avenues by which groundwater can flow through the rocks. In contrast, the skeletal limestones found at Tarpon Springs and Rogers Wreck Point are less porous, less permeable, and lack *Ophiomorpha*.

6.2. Formation of non-laminar calcrete

The non-laminar calcretes at Rogers Wreck Point are characterized by a micritic groundmass that includes unaltered or altered grains derived from the parent rock, indicating that the crust formed through replacive and/or displacive diagenetic alteration of the host limestones (cf., Read, 1974; Braithwaite, 1975;

Watts, 1978; Arakel, 1982; Wright, 2008). Although these non-laminar calcretes consist largely of micrite, concentrations of peloids are locally present in their basal layers. These features, which are similar to the textural features found in caliche from Saldanha Bay in South Africa (Netterberg, 1969; Siesser, 1973; Knox, 1977), indicate that the micrite may have evolved from the peloids.

Peloids have been attributed to many different inorganic and organic processes, including micritization of skeletal grains (James, 1972; Harrison, 1977), precipitation (James, 1972), fecal pellets (Jones and Squair, 1989; Alonso-Zarza and Arenas, 2004), and substrate erosion and reworking (Alonso-Zarza and Jones, 2007). At Rogers Wreck Point, the peloids in the non-laminar calcretes are similar to the clotted "pelletoids" found in Quaternary calcareous crusts on Barbados (James, 1972, his Fig. 7a) and peloids found in Texan calcrete (Zhou and Chafetz, 2009a, their Fig. 8). That the host rock around the peloids has undergone dissolution and micritization is shown by corrosion of skeletal fragments (Fig. 4-5C), and the uppermost part of the bedrock (gray band, Fig. 4-5D) that is formed of featureless micrite. Most peloids in the non-laminar calcrete were probably formed by micritization of fragments derived from the host limestone, given that (1) the peloids are composed of micrite, (2) microborings are common in the peloids, and (3) remnants of unaltered skeletal grains are evident in some of the peloids.

The lack of microborings in the micrite that forms most of groundmass in the non-laminar calcrete crust at Rogers Wreck Point can probably be attributed to intensive micritization (Knox, 1977). The micrite groundmass, however, is characterized by microspar-filled voids, suggesting that initial desiccation was followed by precipitation in larger pores (Wright and Tucker, 1991).

6.3. Laminar calcrete

The laminar calcretes, formed of porous laminae and non-porous laminae, resemble calcareous crusts from the Florida Keys (Multer and Hoffmeister, 1968; Kahle, 1977; Robbin and Stipp, 1979) and Barbados (James, 1972; Harrison, 1977). Robbin and Stipp (1979) suggested that variations in rainfall and the length of the dry intervals may account for the variations in color and laminae thickness.

Porous laminae have been attributed to formation beneath a relatively thick, aggrading tropical forest cover (Multer and Hoffmeister, 1968). The widespread occurrence of calcified root structures in the porous laminae indicates that plant roots played a formative role in the development of these laminae (Jones and Ng, 1988; Jaillard et al., 1991; Wright et al., 1995; Alonso-Zarza and Jones, 2007). The vague laminations evident in some of the porous laminae may reflect the presence of calcified plant tissue (cf., Braithwaite, 1975). The variable preservation styles of the calcified roots indicate that many different factors, which operated on a microscale, were responsible for their preservation. Most of the diagenetic components in these laminae, including micrite, calcified EPS, calcified filaments, needle fibre calcite crystals, and alveolar septal structures were probably produced by biochemical processes that were influenced by the roots. Such processes were probably more important than the abiogenic processes.

The dense, non-porous laminae, composed largely of micrite and/or needle fibre calcite crystals associated with rare calcified root structures, probably developed during periods when root activity was reduced (Alonso-Zarza, 1999; Alonso-Zarza and Jones, 2007). Differences in the appearance of these laminae reflect (1) color variations associated with the presence or absence of organic matter and Mn/Fe precipitates, and (2) microfabric differences associated with

the variations in the relative proportion of micrite and needle fibre crystals, minor variations in porosity, and variations in the degree of cementation (Braithwaite, 1975; Alonso-Zarza, 1999; Zhou and Chafetz, 2009a; Durand et al., 2010). The dense laminae probably formed beneath thin azonal soils with frequent wetting and drying processes producing a denser crust (Multer and Hoffmeister, 1968).

6.4. Stable isotopes

6.4.1. Host rock

The $\delta^{18}O$ and $\delta^{13}C$ values from Rogers Wreck Point, Tarpon Springs, and Morgan's Harbour generally follow similar trends despite variations in the mineralogy of the host rocks (Fig. 4-13). This underlying pattern reflects variance in the influence of meteoric diagenesis on the host rocks (Li and Jones, 2013b, their Fig. 10). The $\delta^{18}O$ values indicate that the host limestones at Rogers Wreck Point underwent more meteoric diagenesis than the limestones at Tarpon Springs and Morgan's Harbour.

6.4.2. Calcareous crusts

The $\delta^{18}O$ and $\delta^{13}C$ values derived from the calcareous crusts, from -5.22‰ to +0.16‰ and from -11.57‰ to -5.43‰ respectively, are similar to those reported from calcretes elsewhere (Talma and Netterberg, 1983; Salomons and Mook, 1986). As in other situations, the variations in $\delta^{13}C$ are slightly higher than those in $\delta^{18}O$ (Talma and Netterberg, 1983; Khadkikar et al., 2000; Alonso-Zarza and Arenas, 2004).

If the $\delta^{18}O$ value of modern rainwater, on average -4.3 SMOW (Rehman et al., 1994) is used in the paleotemperature equation of Epstein et al. (1953) assuming an average water temperature of 27°C (Ng et al., 1992; Rehman et al., 1994), the calcite precipitated in equilibrium with meteoric water should have a

$\delta^{18}O$ value of -6.82‰$_{VPDB}$. This value, however, is lower than the values derived from the Cayman calcareous crusts. Thus, it appears that the meteoric waters involved in the development of the calcareous crusts probably underwent some evaporation that caused fractionation of the heavier ^{18}O (cf., Michel et al., 2013).

Carbon isotopic values have been used to infer the types of plants that lived at the surface while calcareous crusts were developing (Talma and Netterberg, 1983; Fox et al., 2012; Michel et al., 2013; Kaplan et al., 2013). In temperate areas, most trees, shrubs, and grasses use the C_3 photosynthetic pathway, whereas grasses in tropical and/or arid zones use the C_4 photosynthetic pathway (Talma and Netterberg, 1983). C_4 plants produce organic carbon that is isotopically heavier ($\delta^{13}C$ between -13 and -11‰) than that produced by C_3 plants ($\delta^{13}C$ between -30 and -24‰) (Tanner, 2010). Assuming a fractionation factor between soil organic matter and pedogenic calcite of 15.5‰ (Fox and Koch, 2003; Zhou and Chafetz, 2009b) and using the mean end-member values of -27‰ and -12‰ for C_3 and C_4 plants respectively, the percent C_3 biomass ($X_{percent\ of\ C3}$) can be estimated by the following mass balance equations.

$$\delta^{13}C_{soil\ organic\ matter} = \delta^{13}C_{C3}\, X_{percent\ of\ C3} + \delta^{13}C_{C4}\,(1\text{-}X_{percent\ of\ C3}) \quad (1)$$

$$\delta^{13}C_{soil\ organic\ matter} = \delta^{13}C_{pedogenic\ calcrete} - 15.5 \quad (2)$$

Equation (1) is modified from Gillson et al. (2004). This approach assumes negligible contribution to soil CO_2 from plants that employ crassulacean acid metabolism (CAM) as an adaptation to arid conditions (Talma and Netterberg, 1983) and from host carbonate and atmospheric CO_2. Based on the above equation, C_3 plants formed 81–89% of the vegetation in Rogers Wreck Point area. The largely abiogenic microfabric features and paucity of calcified root structures in the non-laminatar calcrete (Table 4-2), however, suggests that the impact of plant and soil CO_2 on the $\delta^{13}C$ values from the non-laminar calcrete was probably minimal. For the laminar calcretes from Tarpon

Springs and Morgan's Harbour, it appears that C_3 plants formed 90–100% of the vegetation when the lowermost laminae (Group B) formed, but only 60–66% of the vegetation when the uppermost laminae (Group A) developed. Given that C_4 plants mostly grow in tropical arid environments, the increase in the proportion of C_4 vegetation may reflect a change from cooler and potentially wetter conditions when the lower part of the crust developed to hotter and drier conditions while the upper part of the crusts formed. Today, the vegetation in the Morgan's Harbour and Tarpon Springs areas is dominated by mangroves, pickleweed and buttonwood, which belong to the C_3 plant consortium (Ball, 1986).

The positive covariance between $\delta^{18}O$ and $\delta^{13}C$ may reflect evaporation during the development of the calcareous crusts (Salomons et al., 1978; Rossinsky and Swart, 1993). The uppermost laminae tend to have more positive $\delta^{18}O$ and $\delta^{13}C$ values than those in the lowermost part of the crusts (Fig. 4-14), a trend similar to that in calcrete crusts from the Great Basin in the United States (Quade et al., 1989). The trend may be attributed to (1) isotopically heavier rains that preferentially infiltrate the ground (Quade et al., 1989), (2) different evaporation rates between the surface layers and deeper layers (Salomons et al., 1978), or (3) climatically induced changes from temperate and cool conditions to arid and warmer conditions (Bajnóczi et al., 2006).

6.5. Time of calcareous crust formation

Development of the Cayman calcareous crusts examined in this study followed deposition of Unit D in the Ironshore Formation ~125 ka ago (Vézina, 1997; Vézina et al., 1999; Coyne, 2003; Coyne et al., 2007) but before sedimentation associated with the Holocene mangrove swamp that started ~2100 years ago (Woodroffe, 1981). In the Morgan's Harbour area, the situation is more complex because the crusts found in the inland areas are absent between Unit

D and Unit F found in coastal exposures along North Sound only ~700 m away (Fig. 4-1B). This may be due to erosion of the calcareous crust from the top of Unit D before the deposition of Unit F, or formation of the calcareous crusts after deposition of Unit F, which took place ~84 ka ago (Coyne, 2003; Coyne et al., 2007).

7. Discussion

In marine limestone successions, calcareous crusts are important indicators of subaerial exposure surfaces (Multer and Hoffmeister, 1968) that form distinctive stratigraphic markers (unconformities) that can be used to divide successions and facilitate correlation between different areas (Coniglio and Harrison, 1983). Although non-laminar calcretes are rare in the Caribbean area, laminar calcretes developed on Pleistocene limestones have been reported from the Florida Keys (Multer and Hoffmeister, 1968; Kahle, 1977; Robbin and Stipp, 1979; Coniglio and Harrison, 1983; Rossinsky and Swart, 1993), Barbados (James, 1972; Harrison, 1977; Harrison and Steinen, 1978), Bermuda (Sayles, 1931; Ruhe et al., 1961; Land et al., 1967), Bahamas (Kornicker, 1958; Rossinsky and Swart, 1993), and the Turks and Caicos Islands (Rossinsky and Wanless, 1992; Rossinsky and Swart, 1993). Some of these have developed since the last glacial maximum (LGM), ~19,000 years ago. Robbin and Stipp (1979), for example, obtained radiocarbon dates from laminar calcretes on Key Largo (400 to 5680 years BP) and Big Pine Key (270 to 7800 years BP) and concluded that their formation occurred during the last 5000 to 6000 years. Shapiro et al. (1995) obtained an age of ~13 ka for calcrete on San Salvador (Bahama Platform) and concluded that the calcrete developed after the LGM. Calcareous crusts on the Turks and Caicos Islands are younger and may still be forming today (Rossinsky and Wanless, 1992; Rossinsky and Swart, 1993). The Cayman calcareous crusts

are perhaps most similar to those in the Florida Keys with common features being (1) development on ooid grainstones and/or skeletal limestones (Coniglio and Harrison, 1983), (2) similar bedrock ages of ~125 ka (Coniglio and Harrison, 1983; Hickey et al., 2010), (3) similar stratigraphic successions with an alteration zone overlain by an upward-accreted laminated calcareous crust (Coniglio and Harrison, 1983), (4) similar stable isotopic compositions (Robbin and Stipp, 1979; Rossinsky and Swart, 1993); and (5) similar modern vegetation cover dominated by mangroves (Lin and Sternberg, 1992; Ross et al., 1992). Such comparisons indicate that the Cayman and Florida calcareous crusts may be contemporaneous with their development being influenced by similar regional climate conditions.

Carbon isotopic values from the laminar calcretes from Tarpon Springs and Morgan's Harbour indicate that the basal parts of the laminar calcretes developed under the influence of a C_3 dominated vegetation that grew in a cool, wet climate whereas the upper parts of the crusts developed under a C_3/C_4 mixed plant vegetation that grew in a hotter, drier climate. This change is consistent with the trends in $\delta^{13}C$ value derived from the laminar calcretes from the Florida Keys (Robbin and Stipp, 1979). The exact time when that change in climate and vegetation took place is, however, difficult to estimate because the rate of growth of the crusts may vary and precise correlation between the $\delta^{13}C$ and lamination ages is questionable (Robbin and Stipp, 1979). In tropical Florida, there are few lakes and much of the landscape is covered by peat and swamps. No pollen and plant macrofossil records of vegetation change from LGM to early Holocene are available yet. Nevertheless, that change was important because it led to the development of different microfabrics in the laminar calcretes. The fact that needle fibre calcite crystals are more common in the upper part of the crusts, for example, may indicate that precipitation took place from supersaturated solutions that developed in response to evaporation (James, 1972; Knox, 1977).

The role of plant roots in the development of laminar calcretes is well-established (Wright et al., 1988, 1995; Alonso-Zarza, 1999; Alonso-Zarza and Jones, 2007) with laminar calcretes interpreted as rhizogenic calcretes (Wright et al., 1995). Given that calcified roots and related biogenic fabrics are common in the laminar calcretes from Tarpon Springs and Morgan's Harbour (Table 4-2), and contrast with the abiogenic fabrics and the rarity of calcified roots in the non-laminar calcrete from the Rogers Wreck Point area (Table 4-2), it can be argued that roots played an important role in the formation of the laminar calcretes but had little impact on the non-laminar calcretes. Generally, the microfabrics found in the laminae of the Cayman calcareous crusts are similar to those described by Alonso-Zarza (1999) in Neogene examples from Spain. In both cases, the complex arrays of microfabrics in the porous and non-porous laminae can be attributed to the interplay of plant roots and their associated microorganisms.

Soil is critical to calcrete formation because (1) it is a prerequisite for most plant growth, (2) it moderates the downward flow of meteoric water into the underlying bedrock (Harrison, 1977), and (3) the calcification of root mats in the soil may account for the formation of laminar calcrete (Wright et al., 1995). The hiatus between the lowermost laminae and the underlying bedrock/alteration zone implies, however, that a long period of emergence is required before plant growth is initiated and calcrete development begins (Robbin and Stipp, 1979; Braithwaite, 1983). During those periods, the role of meteoric diagenesis in reducing the porosity and permeability of substrates is critical because it leads to the generation of an impermeable foundation that is a prerequisite for the subsequent development of laminar calcrete (Gile et al., 1966). For the Cayman examples, however, there is no obvious correspondence between the type of calcareous crust and the underlying limestone because the laminar calcretes at Morgan's Harbour developed on an ooid grainstone whereas the laminar calcretes

at Tarpons Spring cap a skeletal floatstone.

Today, there is no soil cover on the non-laminar calcrete at Rogers Wreck Point, whereas the laminar calcretes in the Tarpon Springs and Morgan's Harbour are typically covered by soil, thin swamp deposits, and/or shallow ponds. In the Morgan's Harbour area, it appears that the porosity and permeability of the ooid grainstones was reduced by vadose diagenesis that promoted micritization and sparmicritization. Similarly, calcareous crusts found on Big Pine Key (Florida) developed on the Miami Limestone where the rocks became more impermeable as micritization progressed (Coniglio and Harrison, 1983). In the Tarpon Springs area, the relatively impermeable host limestones, the soil cover, and plants rooted in the soil collectively hold water close to the surface where evaporation leads to the formation of laminar calcretes. In the Rogers Wreck Point area, however, there is no soil cover or vegetation, and laminar calcretes did not form. Instead, substrate alteration led to the formation of a non-laminar calcretes.

8. Conclusions

Examination of laminar and non-laminar calcretes that developed on limestones in Unit D of the Pleistocene Ironshore Formation on Grand Cayman has led to the following important conclusions.

- Non-laminar calcretes from Rogers Wreck Point are dominated by abiogenic components, whereas laminar calcretes from Tarpon Springs and Morgan's Harbour are dominated by biogenic components.
- In the laminar calcretes, calcified root structures are common in porous laminae but rare in low-porosity laminae.
- Laminar calcretes are attributed to surface accretionary processes, whereas non-laminar calcretes are attributed to *in situ* alteration of the bedrock.
- The positive correlation between $\delta^{18}O$ and $\delta^{13}C$ values of the calcareous

crusts shows that evaporation played a role in the precipitation of $CaCO_3$ in the calcrete crusts.

- The range of $\delta^{13}C$ values in non-laminar calcretes is narrower than that in laminar calcretes.
- The $\delta^{13}C$ values of laminar calcrete crusts from Tarpon Springs and Morgan's Harbour record a vegetation change from C_3 dominated vegetation that grew in a cool, wet climate to a C_3/C_4 mixed plant vegetation that grew in a drier, hotter climate.

The similarities between the Cayman calcareous crusts found on the limestones in Unit D of the Ironshore Formation and the calcareous crusts in Florida that developed on the Pleistocene Miami Limestones may indicate that regional climate conditions played a critical role in their development. This also highlights the potential use of calcareous crusts for regional correlations.

References

Alonso-Zarza, A.M., 1999. Initial stages of laminar calcrete formation by roots: examples from the Neogene of central Spain. Sedimentary Geology 126, 177-191.

Alonso-Zarza, A.M., 2003. Palaeoenvironmental significance of palustrine carbonates and calcretes in the geological record. Earth Science Reviews 60, 261-298.

Alonso-Zarza, A.M., Arenas, C., 2004. Cenozoic calcretes from the Teruel Graben, Spain: microstructure, stable isotope geochemistry and environmental significance. Sedimentary Geology 167, 91-108.

Alonso-Zarza, A.M., Jones, B., 2007. Root calcrete formation on Quaternary karstic surfaces of Grand Cayman. Geologica Acta 5, 77-88.

Alonso-Zarza, A.M., Wright, V.P., 2010. Calcretes. In: Alonso-Zarza, A.M., Tanner, L.H. (Eds.), Carbonates in Continental Settings: Facies, Environments, and Processes. Developments in Sedimentology Volume 61, Elsevier, Amsterdam, pp. 225-267.

Arakel, A.V., 1982. Genesis of calcrete in Quaternary soil profiles, Hutt and Leeman Lagoons, Western Australia. Journal of Sedimentary Petrology 52, 109-125.

Bajnóczi, B., Horváth, Z., Demény, A., Mindszenty, A., 2006. Stable isotope geochemistry of calcrete nodules and septarian concretions in a Quaternary "red clay" paleovertisol from Hungary. Isotopes in Environmental and Health Studies 42, 335-350.

Ball, M.C., 1986. Photosynthesis in mangroves. Wetlands 6, 12-22.

Binkley, K.L., Wilkinson, B.H., Owen, R.M., 1980. Vadose beachrock cementation along a southeastern Michigan marl lake. Journal of Sedimentary Petrology 50, 953-962.

Blanchon, P., Jones, B., Kalbfleisch, W., 1997. Anatomy of a fringing reef around Grand Cayman: storm rubble, not coral framework. Journal of Sedimentary Research 67, 1-16.

Braithwaite, C.J.R., 1975. Petrology of palaeosols and other terrestrial sediments on Aldabra, Western Indian Ocean. Philosophical Transactions of the Royal Society of London, Series B, Biological Sciences 273, 1-32.

Braithwaite, C.J.R., 1983. Calcrete and other soils in Quaternary limestones: structures, processes and applications. Journal of the Geological Society of London 140, 351-363.

Brunt, M.A., Davies, J.E., 1994. The Cayman Islands: Natural History and Biogeography. Kluwer Academic Publishers, Dordrecht, the Netherlands, 576 pp.

Brunt, M.A., Giglioli, M.E.C., Mather, J.D., Piper, D.J.W., Richards, H.G., 1973. The Pleistocene rocks of the Cayman Islands. Geological Magazine 110, 209-304.

Cerling, T.E., 1984. The stable isotopic composition of modern soil carbonate and its relationship to climate. Earth and Planetary Science Letters 71, 229-240.

Cerling, T.E., Hay, R.L., 1986. An isotopic study of paleosol carbonates from Olduvai Gorge. Quaternary Research 25, 63-78.

Coniglio, M., Harrison, R.S., 1983. Holocene and Pleistocene caliche from Big Pine Key, Florida. Bulletin of Canadian Petroleum Geology 31, 3-13.

Constantz, B.R., 1986. The primary surface area of corals and variations in their susceptibility to diagenesis. In: Schroeder, J.H., Purser, B.H. (Eds.), Reef Diagenesis. Springer Verlag, Berlin, pp. 53-76.

Coyne, M.K., 2003. Transgressive-regressive cycles in the Ironshore Formation, Grand Cayman, British West Indies. Unpublished M.Sc. Thesis, University of Alberta, Edmonton, Canada, 98 pp.

Coyne, M.K., Jones, B., Ford, D., 2007. Highstands during Marine Isotope Stage

5: evidence from the Ironshore Formation of Grand Cayman, British West Indies. Quaternary Science Reviews 26, 536-559.

Durand, N., Monger, H.C., Canti, M.G., 2010. Calcium carbonate features. In: Stoops, G., Marcelino, V., Mees, F. (Eds.), Interpretation of Micromorphological Features of Soils and Regoliths. Elsevier, Amsterdam, pp. 149-194.

Epstein, S., Buchsbaum, R., Lowenstam, H.A., Urey, H.C., 1953. Revised carbonate-water isotopic temperature scale. Bulletin of the Geological Society of America 64, 1315-1326.

Eren, M., Kadir, S., Hatipoglu, Z., Gul, M., 2008. Quaternary calcrete development in the Mersin area, southern Turkey. Turkish Journal of Earth Sciences 17, 763-784.

Esteban, M., Klappa, C.F., 1983. Subaerial exposure environment. In: Scholle, P.A., Bebout, D.G., Moore, C.H. (Eds.), Carbonate Depositional Environments. American Association of Petroleum Geologists Memoir 33, Tulsa, Oklahoma, pp. 1-54.

Folk, R.L., 1959. Practical petrographic classification of limestones. Bulletin of the American Association of Petroleum Geologists 43, 1-38.

Fox, D.L., Honey, J.G., Martin, R.A., Peláez-Campomanes, P., 2012. Pedogenic carbonate stable isotope record of environmental change during the Neogene in the southern Great Plains, southwest Kansas, USA: carbon isotopes and the evolution of C_4-dominated grasslands. Geological Society of America Bulletin 124, 444-462.

Fox, D.L., Koch, P.L., 2003. Tertiary history of C_4 biomass in the Great Plains, USA. Geology 31, 809-812.

Freytet, P., Plaziat, J.C., Verrecchia, E.P., 1997. A classification of rhizogenic (root-formed) calcretes, with examples from the Upper Jurassic–Lower Cretaceous of Spain and Upper Cretaceous of France – discussion. Sedimentary

Geology 110, 299-303.

Gile, L.H., 1961. A classification of ca horizons in soils of a desert region, Dona Ana County, New Mexico. Soil Science Society Proceedings 25, 52-61.

Gile, L.H., Peterson, F.F., Grossman, R.B., 1966. Morphological and genetic sequences of carbonate accumulation in desert soils. Soil Science 101, 347-860.

Gillson, L., Waldron, S., Willis, K.J., 2004. Interpretation of soil $\delta^{13}C$ as an indicator of vegetation change in African savannas. Journal of Vegetation Science 15, 339-350.

Goudie, A., 1973. Duricrusts in Tropical and Subtropical Landscapes. Clarendon Press, Oxford, 174 pp.

Harrison, R.S., 1977. Caliche profiles: indicators of near-surface subaerial diagenesis, Barbados, West Indies. Bulletin of Canadian Petroleum Geology 25, 123-173.

Harrison, R.S., Steinen, R.P., 1978. Subaerial crusts, caliche profiles, and breccia horizons: comparison of some Holocene and Mississippian exposure surfaces, Barbados and Kentucky. Geological Society of America Bulletin 89, 385-396.

Hickey, T.D., Hine, A.C., Shinn, E.A., Kruse, S.E., Poore, R.Z., 2010. Pleistocene carbonate stratigraphy of South Florida: evidence for high-frequency sea-level cyclicity. Journal of Coastal Research 26, 605-614.

Hunter, I.G., Jones, B., 1996. Coral associations of the Pleistocene Ironshore Formation, Grand Cayman. Coral Reefs 15, 249-267.

Jaillard, B., Guyon, A., Maurin, A.F., 1991. Structure and composition of calcified roots, and their identification in calcareous soils. Geoderma 50, 197-210.

James, N.P., 1972. Holocene and Pleistocene calcareous crust (caliche) profiles: criteria for subaerial exposure. Journal of Sedimentary Petrology 42, 817-836.

Jones, B., 1994. Geology of the Cayman Islands. In: Brunt, M.A., Davies, J.E. (Eds.), The Cayman Islands: Natural History and Biogeography. Kluwer Aca-

demic Publishers, The Netherlands, pp. 13-49.

Jones, B., Goodbody, Q.H., 1984. Biological factors in the formation of quiet water ooids. Bulletin of Canadian Petroleum Geology 32, 190-200.

Jones, B., Hunter, I.G., 1990. Pleistocene paleogeography and sea levels on the Cayman Islands, British West Indies. Coral Reefs 9, 81-91.

Jones, B., Hunter, I.G., Kyser, K., 1994. Revised stratigraphic nomenclature for Tertiary strata of the Cayman Islands, British West Indies. Caribbean Journal of Science 30, 53-68.

Jones, B., Kahle, C.F., 1995. Origin of endogenetic micrite in karst terrains: a case study from the Cayman Islands. Journal of Sedimentary Research A65, 283-293.

Jones, B., Ng, K.C., 1988. The structure and diagenesis of rhizoliths from Cayman Brac, British West Indies. Journal of Sedimentary Petrology 58, 457-467.

Jones, B., Ng, K.C., Hunter, I.G., 1997. Geology and hydrogeology of the Cayman Islands. In: Vacher, H.L., Quinn, T. (Eds.), Geology and Hydrogeology of Carbonate Islands. Developments in Sedimentology Volume 54, Elsevier, Amsterdam, pp. 299-325.

Jones, B., Pemberton, S.G., 1986. The role of fungi in the diagenetic alteration of spar calcite. Canadian Journal of Earth Sciences 24, 903-914.

Jones, B., Pemberton, S.G., 1989. Sedimentology and ichnology of a Pleistocene unconformity-bounded, shallowing-upward carbonate sequence: the Ironshore Formation, Salt Creek, Grand Cayman. Palaios 4, 343-355.

Jones, B., Renaut, R.W., 1996. Skeletal crystals of calcite and trona from hot-spring deposits in Kenya and New Zealand. Journal of Sedimentary Research 66, 265-274.

Jones, B., Squair, C.A., 1989. Formation of peloids in plant rootlets, Grand Cayman, British West Indies. Journal of Sedimentary Petrology 59, 1002-1007.

Kahle, C.F., 1977. Origin of subaerial Holocene calcareous crusts: role of algae, fungi and sparmicritisation. Sedimentology 24, 413-435.

Kaplan, M.Y., Eren, M., Kapur, S., 2013. Mineralogical, geochemical and isotopic characteristics of Quaternary calcretes in the Adana region, southern Turkey: implications on their origin. Catena 101, 164-177.

Khadkikar, A.S., Chamyal, L.S., Ramesh, R., 2000. The character and genesis of calcrete in Late Quaternary alluvial deposits, Gujarat, western India, and its bearing on the interpretation of ancient climates. Palaeogeography Palaeoclimatology Palaeoecology 162, 239-261.

Klappa, C.F., 1980. Rhizoliths in terrestrial carbonates: classification, recognition, genesis and significance. Sedimentology 27, 613-629.

Knox, G.J., 1977. Caliche profile formation, Saldanha Bay (South Africa). Sedimentology 24, 657-674.

Kornicker, L.S., 1958. Bahamian limestone crusts. Gulf Coast Association of Geological Societies 8, 167-170.

Land, L.S., Mackenzie, F.T., Gould, S.J., 1967. Pleistocene history of Bermuda. Geological Society of America Bulletin 78, 993-1006.

Li, R., Jones, B., 2013a. Temporal and spatial variations in the diagenetic fabrics and stable isotopes of Pleistocene corals from the Ironshore Formation of Grand Cayman, British West Indies. Sedimentary Geology 286-287, 58-72.

Li, R., Jones, B., 2013b. Heterogeneous diagenetic patterns in the Pleistocene Ironshore Formation of Grand Cayman, British West Indies. Sedimentary Geology 294, 251-265.

Lin, G., Sternberg, L.S.L., 1992. Differences in morphology, carbon isotope ratios, and photosynthesis between scrub and fringe mangroves in Florida, USA. Aquatic Botany 42, 303-313.

Machette, M.N., 1985. Calcic soils of the southwestern United States. In: Weide,

D.L., Faber, M.L. (Eds.), Soils and Quaternary Geology of the Southwestern United States. Geological Society of America Special Paper 203, pp. 1-22.

Matley, C.A., 1926. The geology of the Cayman Islands (British West Indies), and their relation to the Bartlett Trough. Quarterly Journal of the Geological Society 82, 352-387.

McCrea, J.M., 1950. On the isotopic chemistry of carbonates and a paleotemperature scale. The Journal of Chemical Physics 18, 849-857.

Michel, L.A., Driese, S.G., Nordt, L.C., Breecker, D.O., Labotka, D.M., Dworkin, S.I., 2013. Stable-isotope geochemistry of vertisols formed on marine limestone and implications for deep-time paleoenvironmental reconstructions. Journal of Sedimentary Research 83, 300-308.

Montpetit, J.C., 1998. Sedimentology, depositional architecture, and diagenesis of the Cayman Formation at Tarpon Springs Estates, Grand Cayman, British West Indies. Unpublished M.Sc. Thesis, University of Alberta, Edmonton, Canada, 133 pp.

Multer, H.G., Hoffmeister, J.E., 1968. Subaerial laminated crusts of the Florida Keys. Geological Society of America Bulletin 79, 183-192.

Netterberg, F., 1969. The interpretation of some basic calcrete types. The South African Archaeological Bulletin 24, 117-122.

Netterberg, F., 1980. Geology of southern African calcretes: 1. Terminology, description, macrofeatures, and classification. Transactions of the Geological Society of South Africa 83, 255-283.

Netterberg, F., Caiger, J.H., 1983. A geotechnical classification of calcretes and other pedocretes. In: Wilson, R.C.L. (Ed.), Residual Deposits: Surface Related Weathering Processes and Materials. Geological Society of London Special Publication 11, Blackwell Scientific Publications, Oxford, pp. 235-243.

Ng, K.C., Jones, B., Beswick, R., 1992. Hydrogeology of Grand Cayman, British

West Indies: a karstic dolostone aquifer. Journal of Hydrology 134, 273-295.

Quade, J., Cerling, T.E., Bowman, J.R., 1989. Systematic variations in the carbon and oxygen isotopic composition of pedogenic carbonate along elevation transects in the southern Great Basin, United States. Geological Society of America Bulletin 101, 464-475.

Read, J.F., 1974. Calcrete deposits and Quaternary sediments, Edel Province, Shark Bay, Western Australia. In: Logan, B.W., Read, J.F., Hagan, G.M., Hoffman, P., Brown, R.G., Woods, P.J., Gebelein, A.D. (Eds.), Evolution and Diagenesis of Quaternary Carbonate Sequences, Shark Bay, Western Australia. American Association of Petroleum Geologists Memoir 22, Tulsa, Oklahoma, pp. 250-282.

Rehman, J., Jones, B., Hagan, T.H., Coniglio, M., 1994. The Influence of sponge borings on aragonite-to-calcite inversion in Late Pleistocene *Strombus gigas* from Grand Cayman, British West Indies. Journal of Sedimentary Research 64, 174-179.

Robbin, D.M., Stipp, J.J., 1979. Depositional rate of laminated soilstone crusts, Florida Keys. Journal of Sedimentary Petrology 49, 175-180.

Ross, M.S., O'brien, J.J., Flynn, L.J., 1992. Ecological site classification of Florida Keys terrestrial habitats. Biotropica 24, 488-502.

Rossinsky, V., Swart, P.K., 1993. Influence of climate on the formation and isotopic composition of calcretes. Geophysical Monograph 78, 67-75.

Rossinsky, V., Wanless, H.R., 1992. Topographic and vegetative controls on calcrete formation, Turks and Caicos Islands, British West Indies. Journal of Sedimentary Petrology 62, 84-98.

Ruhe, R.V., Cady, J.G., Gomez, R.S., 1961. Paleosols of Bermuda. Geological Society of America Bulletin 72, 1121-1142.

Salomons, W., Goudie, A., Mook, W.G., 1978. Isotopic composition of calcrete

deposits from Europe, Africa and India. Earth Surface Processes 3, 43-57.

Salomons, W., Mook, W.G., 1986. Isotope geochemistry of carbonates in the weathering zone. In: Fritz, P., Fontes, J.C. (Eds.), Handbook of Environmental Isotope Geochemistry Volume 2, Elsevier, Amsterdam, pp. 239-269.

Sayles, R.W., 1931. Bermuda during the ice age. Proceedings of the American Academy of Arts and Sciences 66, 381-468.

Siesser, W.G., 1973. Diagenetically formed ooids and intraclasts in South African calcretes. Sedimentology 20, 539-551.

Shapiro, R.S., Aalto, K.R., Dill, R.F., Kenny, R., 1995. Stratigraphic setting of a subtidal stromatolite field, Iguana Cay, Exumas, Bahamas. In: Curran, H.A., White, B. (Eds.), Terrestrial and Shallow Marine Geology of the Bahamas and Bermuda. Geological Society of America Special Paper 300, pp. 139-155.

Shourie, A., 1993. Depositional architecture of the Late Pleistocene Ironshore Formation, Grand Cayman, British West Indies. Unpublished M.Sc. Thesis, University of Alberta, Edmonton, Canada, 100 pp.

Talma, A.S., Netterberg, F., 1983. Stable isotope abundances in calcretes. In: Wilson, R.C.L. (Ed.), Residual Deposits: Surface Related Weathering Processes and Materials. Geological Society of London Special Publication 11, Blackwell Scientific Publications, Oxford, pp. 221-233.

Tanner, L.H., 2010. Continental carbonates as indicators of paleoclimate. In: Alonso-Zarza, A.M., Tanner, L.H. (Eds.), Carbonates in Continental Settings: Geochemistry, Diagenesis, and Applications. Developments in Sedimentology Volume 62, Elsevier, Amsterdam, pp. 179-214.

Tompkins, R.E., 1980. Origin and occurrence of selected worldwide calcrete deposits. Unpublished Ph.D. Thesis, Texas A&M University, USA, 142 pp.

Verrecchia, E.P., Freytet, P., Verrecchia, K.E., Dumont, J.L., 1995. Spherulites in

calcrete laminar crusts: biogenic $CaCO_3$ precipitation as a major contributor to crust formation. Journal of Sedimentary Research A65, 690-700.

Vézina, J.L., 1997. Stratigraphy and sedimentology of the Pleistocene Ironshore Formation at Rogers Wreck Point, Grand Cayman: a 400 ka record of sea-level highstands. Unpublished M.Sc. Thesis, University of Alberta, Edmonton, Canada, 131 pp.

Vézina, J.L., Jones, B., Ford, D., 1999. Sea level highstands over the last 500,000 years: evidence from the Ironshore Formation on Grand Cayman, British West Indies. Journal of Sedimentary Research 69, 317-327.

Walls, R.A., Harris, W.B., Nunan, W.E., 1975. Calcareous crust (caliche) profiles and early subaerial exposure of Carboniferous carbonates, northeastern Kentucky. Sedimentology 22, 417-440.

Watts, N.L., 1978. Displacive calcite: evidence from recent and ancient calcretes. Geology 6, 699-703.

Watts, N.L., 1980. Quaternary pedogenic calcretes from the Kalahari (southern Africa): mineralogy, genesis and diagenesis. Sedimentology 27, 661-686.

Woodroffe, C.D., 1981. Mangrove swamp stratigraphy and Holocene transgression, Grand Cayman Island, West Indies. Marine Geology 41, 271-294.

Woodroffe, C.D., Stoddart, D.R., Giglioli, M.E.C., 1980. Pleistocene patch reefs and Holocene swamp morphology, Grand Cayman Island, West Indies. Journal of Biogeography 7, 103-113.

Wright, V.P., 1990. A micromorphological classification of fossil and recent calcic and petrocalcic microstructures. In: Douglas, L.A. (Ed.), Soil Micromorphology: A Basic and Applied Science. Development in Soil Science 19, Elsevier, Amsterdam, pp. 401-407.

Wright, V.P., 1994. Paleosols in shallow marine carbonate sequences. Earth Science Reviews 35, 367-395.

Wright, V.P., 2008. Calcrete. In: Nash, D.J., McLaren, S.J. (Eds.), Geochemical Sediments and Landscapes. Blackwell Scientific Publications, Oxford, pp. 10-45.

Wright, V.P., Platt, N.H., Marriott, S.B., Beck, V.H., 1995. A classification of rhizogenic (root-formed) calcretes, with examples from the Upper Jurassic Lower Cretaceous of Spain and Upper Cretaceous of southern France. Sedimentary Geology 100, 143-158.

Wright, V.P., Platt, N.H., Wimbledon, W.A., 1988. Biogenic laminated calcretes: evidence of calcified root-mat horizons in paleosols. Sedimentology 35, 603-620.

Wright, V.P., Tucker, M.E., 1991. Calcretes. Reprint Series Volume 2 of the International Association of Sedimentologists. Blackwell Scientific Publications, Oxford, 352 pp.

Zhou, J., Chafetz, H.S., 2009a. Biogenic caliches in Texas: the role of organisms and effect of climate. Sedimentary Geology 222, 207-225.

Zhou, J., Chafetz, H.S., 2009b. The genesis of late Quaternary caliche nodules in Mission Bay, Texas: stable isotopic compositions and palaeoenvironmental interpretation. Sedimentology 56, 1392-1410.

CHAPTER 5: CONCLUSIONS

Like Pleistocene carbonate successions on other islands throughout the world, the Ironshore Formation on Grand Cayman displays complex diagenetic fabrics that reflect repeated episodes of exposure that became established during sea level lowstands. Comparison of diagenetic features associated with corals and coeval matrices in units A to F of the Ironshore Formation has produced the following important conclusions.

(1) The matrices have undergone more meteoric alteration than the corals, which can probably be attributed to the higher volumes of freshwater that flowed through the more permeable matrices.

(2) Although marine and meteoric diagenetic fabrics are evident in the corals and matrices of each unit, there is no systematic pattern to their distribution from unit A to F. Evidence of multiphase vadose diagenetic fabrics, such as multiple generations of calcite cements is rare despite the fact that some of the older units were repeatedly subject to the meteoric diagenesis. In unit A, for example, only two phases of calcite cement are evident.

(3) The diagenetic packages are not consistent with the depositional packages. Although there are six depositional units in Ironshore Formation, only three diagenetic packages are recognized. Maximum diagenesis took place during the lowstands (MIS 6, MIS 5d) that followed the deposition of units C and D, respectively. This can be attributed to the long durations of the lowstands and the wet climate with high rainfall associated with each lowstands.

(4) The fact that the $\delta^{18}O$-$\delta^{13}C$ values for the corals and matrices follow the same trend line indicates their genetic linkage. The aragonitic samples, which have largely retained their original marine signatures occupy

the upper to middle parts of the trend. In contrast, the calcitic samples which formed as freshwater mediated alteration of the original aragonitic components, occupy the lower part of the trend. Essentially, the trend line reflects the variation of isotopic compositions in response to mineralogy and diagenetic environment.

The heterogeneous diagenetic patterns evident in the Ironshore Formation reflect the complex interplay between many different intrinsic (e.g., rock components and compositions, porosity and permeability) and extrinsic factors (e.g., sea level position, climate, time). Thus, the diagenetic features evident in individual samples cannot be correlated with any of the unconformities that denote specific sea level lowstands. Detailed diagenetic examination of two coral genera (*Montastrea annularis* and *Acropora palmata*) from the Ironshore Formation also produced the same conclusions. During phases of subaerial exposure, scleractinian corals (100% aragonite skeletons) are subject to aragonite-to-calcite alteration. Using the aragonite to calcite ratio as a measure of the degree of calcification, it has been shown that the *M. annularis* and *A. palmata* are characterized by different degrees of calcification. The degree of coral skeletal calcification is also geographically variable. The variation in the degree of coral skeletal calcification with genera and geography can be attributed to differences in skeletal structures and diagenetic environments. The variable styles and degrees of diagenesis evident in the corals show that it is generally impossible to correlate specific diagenetic phases with specific sea level lowstands.

The comparative study of the non-laminar and laminar calcretes that developed on exposed surfaces of unit D of Ironshore Formation on Grand Cayman has demonstrated the following important points.

(1) Non-laminar and laminar calcretes formed through different processes.

Non-laminar calcretes developed through the in situ alteration of the

bedrock, whereas the laminar calcretes formed in response to surface accretionary processes.

(2) The formation of calcareous crusts is controlled by the interactions that take place between the substrate, soil cover, climate, and biological influences that are operative during lowstand regimes.

(3) Evaporation plays an important role in the formation of the Cayman calcareous crusts.

(4) The Cayman calcareous crusts record a vegetation change from C_3 dominated vegetation that grew in a cool, wet climate to a C_3/C_4 mixed plant vegetation that grew in a drier, hotter climate.

(5) The similarity between Cayman calcareous crusts and Florida crusts may indicate that regional climate conditions play a critical role in their development.

The study of diagenetic products in Pleistocene limestone succession on Grand Cayman reveals the complicated diagenetic response of carbonate successions to the ever-changing sea levels that characterized the Pleistocene. The variably altered corals and matrices in the limestones of Ironshore Formation show that the heterogeneous diagenetic patterns resulted from the interactions between many different intrinsic and extrinsic factors. The hypothesis that the distribution of diagenetic styles can be related to specific sea level lowstands and unconformities (Matthews and Frohlich, 1987; Whitaker et al., 1997; Braithwaite and Montaggioni, 2009; Braithwaite and Camoin, 2011) is not supported in this study. The two types of calcareous crusts in the Ironshore Formation emphasize the complex control factors that controlled their formation. Although the Cayman calcareous crusts resemble those found in Florida, the idea that they formed under the regional climate needs further investigation.

References

Braithwaite, C.J.R., Camoin, G.F., 2011. Diagenesis and sea-level change: lessons from Moruroa, French Polynesia. Sedimentology 58: 259-284.

Braithwaite, C.J.R., Montaggioni, L.F., 2009. The Great Barrier Reef: a 700,000 year diagenetic history. Sedimentology 56, 1591-1622.

Matthews, R.K., Frohlich, C., 1987. Forward modeling of bank-margin carbonate diagenesis. Geology 15, 673-676.

Whitaker, F., Smart, P., Hague, Y., Waltham, D., Bosence, D., 1997. Coupled two-dimensional diagenetic and sedimentological modeling of carbonate platform evolution. Geology 25, 175-178.